Development of Microfluidic Droptodes as a New Approach for Ionophore-Based Polyion Sensing

by

Nicholas Alexander Glenn

A dissertation submitted in partial fulfillment
of the requirements for the degree of
Doctor of Philosophy
(Chemistry)
in the University of Michigan
2023

Doctoral Committee:

Professor Ryan C. Bailey, Chair
Professor Andrew P. Ault
Professor Eric C. Martens
Professor Mark E. Meyerhoff

Nicholas A. Glenn

glennn@umich.edu

ORCID iD: 0000-0002-0771-1855

Dedication

To my fiancée, Sydney

Acknowledgements

I've been blessed to meet a number of great people dating back to as far as I can remember who've left a positive impression on me in my journey towards a higher education. I'd first like to acknowledge my 3rd and 4th grade teachers, Ms. Jackson, and Ms. Price. Even as a kid, I admired how passionate you both were about wanting your students to learn and succeed. In your classrooms is where I can distinctly remember developing my passion for learning.

I'd next like to acknowledge my general chemistry professor from college, Dr. Ibele for (unknowingly) giving me the confidence to change my major to chemistry. I started off in your class as an education major, intimidated by the general chemistry III course I heard everyone complain about. Though, while taking your class, it didn't take long for me to realize how much I enjoyed the problem-solving aspect of chemistry, using limited amounts of information to discover a solution that is not always immediately evident. I didn't know at the time, but this innate desire would be what led me to pursue a career as a research chemist. Thank you for patience in teaching and eagerness towards helping students learn.

I also have to mention my general chemistry II professor, Dr. Jia. When I was a sophomore, I remember asking you to write a recommendation letter for a scholarship I planned to use to help pay for a master's degree after I graduated. While agreeing to write the letter, you kindly let me know that I could actually pursue a PhD without any out-of-pocket costs through a fully funded program. Coming from a disadvantaged background, that little piece of information set me on a path that led me to where I am now, drastically changing the trajectory for my family and me.

To my Quantitative Analysis instructor, Professor Michael-Smith: thanks for providing a supportive learning environment within your classroom, a place where I discovered my interest in analytical chemistry. Before taking your course, most of my focus had been on the academic requirements (high GPA, performance on entry exams) needed to get into grad school. While these things were most definitely important, you encouraged me to pursue research opportunities outside of the classroom as a way to further explore my interests. This really pushed me to step out of my comfort zone considering many of the opportunities I came across were out of my home state of Missouri, a place which I rarely had traveled out of at that point in my life. It's safe to say that shifting my focus and moving out of state worked in my best interest.

My first undergraduate research experience was spent within the Ault lab at the University of Michigan. I'm grateful for the amount of training and guidance I received that summer from my mentor, Dr. Rebecca Craig, Professor Ault, and various other lab members. Additional thanks to Professor Schoenfisch and lab members at the University of North Carolina for welcoming me into their lab as a visiting research fellow the summer before my last year of college. I would especially like to thank Dr. Micah Brown for his valuable mentorship that summer as I began the process of applying to graduate programs. I'd also like to acknowledge my undergraduate research advisor at the University of Missouri - Saint Louis, Professor Keith Stine, for the opportunity to gain valuable research experience within his lab.

I'd like to acknowledge the University of Michigan chemistry department for giving me the opportunity to pursue a PhD. From the admissions committee to administration there is so much hard work that goes into making sure things run smoothly. A special thanks to Liz who gave me a much-needed pep talk after a challenging first semester in the program. Katie and

Emma for their support and responsiveness to various questions that came up throughout my time here.

As a member of the Bailey lab, I've had the honor to work with a number of talented scientists (and engineers) that enriched my experience in the department: Vishal, Mari, John, Emily, Cole, Steve, Colleen, Sara, Gloria, Krista, and Nico along with my cohort mates Claire and Marina. Special thanks to Shannon and Xuewei who I worked with frequently during the early stages of my PhD to get the newly introduced microfluidics project up and running. Leaving Michigan, I'm extremely excited about the future of the project which will be taken over by Ayush.

I'd like to thank Professor Meyerhoff whose decades of experience with polyion sensing was found to be very helpful at various points in my dissertation studies. Additional thanks to the rest of my committee for time spent investing into the success of my project through various meetings throughout the past years, along with recommendation letters for fellowships and grants.

To my advisor Ryan – thank you for the opportunity to complete my PhD in your lab. Being admitted to the chemistry doctoral program with the largest incoming class ever (73 students!), I wasn't always sure that I'd have the opportunity to work in your lab, which I was most interested in joining when I applied to Michigan. Ultimately, things worked out in the end. I leave here feeling very well prepared for the next step in my career. Thank you for all your support and providing a challenging environment that allowed me to grow as a scientist.

To my (future) in laws Veronica, Usha, Pierre, Carmen, Ronnie, Star, Nani, and Brandyn. Thank you for your warm welcomes to the East coast during my much-needed Christmas breaks

at the end of every year. I always came back to Michigan full of great food, recharged, and ready to start the new year.

I can't forget all the friends and amazing underrepresented scientists I met while at Michigan: James, Paulina, Lloyd, Rosalyn, Taylor, Wes, Matt, Keenan, and Faridat. Having a community is such an important part of graduate school and it was always great to have you guys to talk to and laugh with.

To my older sister Kellie, who put my very first book in my hands and always looked out for me growing up. My niece and nephew, Adele and Kendrick, two of the sweetest kids anyone will ever meet. I can't go without mentioning my little sister Darlena. I always enjoyed your random Facetime calls where we would sit on the phone cracking (years old) inside jokes that no one else could understand.

To my Grandma Sharon, a beautiful soul who left us way too soon. I remember all of our long conversations talking about any- and everything. Thank you for all your encouragement and pep talks along the way. I wouldn't be successful today without all that you taught me. I wish that you could be here for us to celebrate together but I know you're watching over me.

Last but not least, my wonderful fiancée Sydney. The first year of graduate school – we couldn't have met at a better time. Thank you for all your support and showing me the importance of taking breaks here and there. I couldn't imagine going through this PhD process with anyone else. Can't wait to celebrate all your accomplishments with you at your dissertation defense soon. And of course, all the other great adventures that lay ahead!

Table of Contents

List of Tables

List of Figures

Abstract

Negatively or positively charged macromolecular species – alternatively referred to as polyions – are key analytical targets found in several natural and synthetic forms. As the efficacy of these species in chemical and biological reactions is most often linked to their quantitative amount, methods capable of measuring polyion concentrations accurately and efficiently are essential. Herein, this dissertation presents the development of ionophore-based droplet microfluidics as a new analytical technique for polyion sensing.

Chapter 1 reviews several methods developed over the past several decades which have incorporated colorimetric and fluorescent molecules for chemical sensing of polyions. Subsequently – microfluidic droptodes derived from both droplet microfluidic and optical 'optode' sensing technologies – are detailed as a succeeding technology. Though to this point, a microfluidic droptode chemistry for fluorescent, biphasic sensing of polyanions does not exist, limiting the application of this method.

Chapter 2 entails the development, optimization, and application of a novel droptode sensing chemistry for the detection of polyanions using a familiar chromoionophore, ionophore, and ion exchanger format. Heparin – a molecule whose anticoagulative effects in blood are most commonly monitored using unstandardized clotting assays – is pursued as an initial target of interest. This chapter demonstrates polyanion-sensitive droptodes are responsive toward heparin at a wide range of concentrations (3 – 135 μg/mL) which can be fine-tuned based on the concentration of sensing reagents employed. Furthermore, heparin measurements in human plasma demonstrate how the intrinsic features of microfluidic droptodes allow for quantitative

polyanion measurements to be made in biologically complex and opaque matrices without optical interference from the sample.

Protamine, a positively charged protein, is primarily known as the only FDA-approved antidote for the reversal of heparin. Polycation-sensitive droptodes exist as an alternate method for biphasic protamine sensing, though they require usage of an organic solvent which has low compatibility with polydimethylsiloxane-fabricated microfluidic devices. This limits our ability to study the effects of several key parameters such as aqueous droplet volumes and segment spacing on overall response. Chapter 3 successfully implements a compatible, lipophilic fluorescein derivative-based chemistry to analyze the impact of reaction time, aqueous droplet volume, and segment spacing on response of protamine-sensitive microfluidic droptodes using both bulk (sub-mL volumes) and microfluidic (100s of pL) methods. Chapter 4 advances the utility of microfluidic droptodes beyond biomedical polyion sensing for the measurement of cationic, polymeric quaternary ammonium compounds (PQs). Three PQ species (PQ-2, PQ-6, PQ-10) are detected as targets of interest, each inducing a unique response within our droptode system.

Having developed and optimized a polyanion sensing chemistry, microfluidic droptodes are fully demonstrated in their ability to detect electrolytes, polycations, and polyanions. Though to this point, this method has only been demonstrated for single-plex sensing applications. Chapter 5 details the development and application of a droplet microfluidic "H-channel" device for spatial multiplexing of Na^+ and K^+ in individual samples. Lastly, Chapter 6 concludes this dissertation with an overview of the work presented in each chapter. Microfluidic droptodes are fully demonstrated for biphasic sensing of polyions and other targets in adjacent aqueous droplets. This method stands as a unique and novel variation of traditional droplet microfluidic

applications in which optical measurements (i.e., fluorescence, absorbance) are made in aqueous droplets. Additionally, suggested applications and alternative strategies for microfluidic droptodes as future work are provided to continue the advancement of this newly introduced category of droplet microfluidics.

Chapter 1 – Fluorescent and Colorimetric Methods for Optical Sensing of Polyions: A Framework for the Development of Polyion-Sensitive Droptodes

1.1 Introduction

Polyions – negative or positively charged macromolecules – are a diverse set of chemical compounds that are encountered in a wide range of settings including surgical procedures (heparin), male reproductive cells (protamine), cosmetic products (polyquaterniums), and pharmaceuticals (therapeutic antibody proteins). Despite their frequent usage, analytical characterization, and quantification of polyions in samples remains a significant challenge given that they are polydisperse (i.e., charge, size) and lack strong chromophoric or fluorescent signatures. Several analytical methods for polyion sensing have been developed to date, though they often require expensive instrumentation (10s to 100s of thousands of dollars) with limited configurability, large sample volumes, and/or extended analysis times (minutes to hours). Thus, the need for techniques which overcomes these challenges persists.

A number of optical methods have been developed throughout the past several decades to increase the accessibility and simplicity of techniques for polyion sensing. Most notably, the intrinsic ability of charged macromolecules to electrostatically interact with oppositely charged, polyionic species has allowed for a variety of chromophoric and fluorescent molecules to emerge as optical readout elements for target polyion measurements. Additionally, the pairing of lipophilic, chromophoric molecules and ionic compounds – a chemical combination commonly used in optical ‘optode’ sensors – has introduced an additional number of available polyion-

sensitive platforms. This chapter reviews several polyion-sensitive optical methods which have been developed over the past century. Furthermore, ionophore-based droplet microfluidics, or microfluidic droptodes, are discussed as an attractive and underutilized platform available to advance the field of optical polyion sensing.

1.2 Polyion-Sensitive, Charged Dyes

The electrostatic interaction of polyions with oppositely charged molecules whose UV-light absorbing properties are dependent on their degree of complexation is a fundamental chemical reaction which has been the core feature of several polyion-sensitive assays throughout the past decades. Some of the oldest works, dating back to nearly a century ago, have used cationic toluidine blue molecules for colorimetric sensing of polyanions.[1] Further application of charged molecular dyes for colorimetric polyion sensing continued in the following decades.[2,3] During the 1980s, an azure A molecule emerged as a novel charged dye for polyion sensing in biological samples. Formally used in an assay, changes in absorbance or color of azure A dye was found to track well with clinically relevant concentrations of heparin (U/mL) in both saline and plasma samples.[4] Subsequent to the development of the heparin-azure A assay, the idea of using azure A for indirect sensing of protamine, a cationic protein used to reverse the effects of heparin, was explored. In this case, protamine concentrations were found to be measurable based on a competitive binding displacement between protamine and heparin-azure A complex.[5] This results from dissociation of weakly interacting heparin-azure A complexes in samples upon addition of protamine – a consequence of favored heparin-protamine interactions. Similar to the original heparin-azure A assay, the protamine-heparin-azure A assay was successfully demonstrated for measurement of a target polyion (i.e. protamine) in plasma samples.[5] The direct

and indirect azure A methods in addition to early works with toluidine blue were pioneering in theory and application, providing a format for later-developed platforms.

Building upon the success of polyion-sensitive charged dyes in the 20th century, continued developments were made in the following decades. Fluorescein isothiocyanate-labeled protamine (F-protamine) was incorporated by Egawa et al. as a fluorescent dye which quenches, or decreases in fluorescence, upon electrostatic interaction with heparin.[6] Gao and coworkers developed a custom-synthesized, four-armed-amino-tailored tetraphenylethene molecule (TPE-NH_2) for fluorescent sensing of heparin and protamine.[7] For heparin, increases in fluorescence of TPE-NH_2 were dependent on the degree of interaction of negatively charged groups on heparin with positively charged amino groups on TPE-NH_2. The addition of protamine to solutions with heparin-TPE-NH_2 complexes was shown to generate decreases in fluorescence response. In this case, protamine and heparin react in a manner similar to a previously reported, competitive-binding displacement mechanism.[5] Pu and co-workers implemented a cationic polyfluorene derivative-2,1,3-benzothiadiazole dye which had measurable changes in photoluminescence upon interaction with polyanions (i.e. heparin).[8] Changes in fluorescence color of the cationic polyfluorene derivative-2,1,3-benzothiadiazole molecule in response to the degree of heparin-dye complexation in-tube were found to be highly visible, demonstrating the feasibility of using charged dyes for "naked eye detection" of polyions. Heparin Red – a polycationic fluorescent dye – is another notable molecule which has been employed as a readout element in commercially available assays which measure heparin in plasma samples.[9]

To this point, charged dyes have been primarily discussed for sensing of biomedical polyions, though the application of such dyes for measurement of non-biomedical polyions should not go without mention. A notable method involves the use of cationic *o*-toluidine blue in

solution with a target polycation.[10] This solution is titrated with a potassium salt of polyvinyl sulfate (PVSK) – a polyanionic molecule which can electrostatically interact with both *o*-toluidine blue and target polycation. Though, the target polycation is neutralized first in such a way that subsequent interactions result in the complexation of PVSK and *o*-toluidine blue molecules. The reaction of *o*-toluidine blue with PVSK is complete when a stable change in the color of the dye from blue to pink occurs. Based on the known charge density of PVSK (~6 mEq L^{-1}), the charge density of the target polycation in solution can effectively be calculated based on volume of PVSK titrant which was needed to reach the final end point of the titration. Previous works have used this method for characterization of polymeric quaternary ammonium compounds (PQs) – synthetic polycations commonly used in cosmetic[11] and industrial processes.[12]

The given examples of polyion-sensitive charged dyes provide an overview on how these molecules have been and continued to be used as optical readout elements for the measurement of polyions. Polyion-sensitive ion-selective optodes are next discussed as platforms which were developed contiguously to many of the previously described, charged-dye methods.

1.3 Polyion-Sensitive, Ion-Selective Optodes

In the context of this chapter a polyion-sensitive ion-selective optode (polyion-sensitive ISO) is an optical sensor which uses two separate molecules – a chromophoric dye and an ionic complexing agent – for polyion measurements. Though, most commonly, a polyion-sensitive ISO is simply considered as a derivation of ion-selective optode (ISO) technologies. Typically, ISOs consist of a surface coated with an ion-selective film or "organic phase" consisting of poly (vinyl chloride) (PVC), dioctyl sebacate (DOS), ionophore, pH-sensitive chromoionophore, and ion-exchanger. Optical properties of the film change as a result of analyte partitioning into the

film and binding to the ionophore inducing an ion charge-dependent protonation or deprotonation of the chromoionophore **(Figure 1.1)**.[13] This pioneering technology served as a model system for further developed ISOs[14–21] while concomitantly inspiring the discovery of polyion-sensitive ISOs.

Introduced in the mid 1990s, polyion-sensitive ISOs initially consisted of a glass slide coated with a polymeric film containing lipophilic ion-exchanger and chromoionophore. Polyion extraction from the aqueous sample induces changes in optical properties of the film as a result of protons partitioning into the aqueous matrix (polycations) or into the film (polyanions) **(Figure 1.1)**. Polyion-sensitive, polymeric films coated on glass surfaces in addition to other adaptations of polyion-sensitive ISOs such as microwell plates, cellulose filter papers, and emulsified nanospheres are discussed herein.

1.3.1 Polymeric Film-Coated, Glass Surfaces

The first polyion-sensitive ISO consisted of a glass slide coated with a polyanion-sensitive polymeric film formulaically derived from the film used on the surface of polyanion-sensitive, ion-selective electrodes (ISE). The sensing platform associated with the latter – demonstrated for potentiometric sensing of macromolecular heparin – consisted of respective amounts of weight percent (wt. %) PVC, DOS, and tridodecylmethylammmonium chloride (TDMACl), dissolved in tetrahydrofuran, and cast onto an electrode.[22] Polyanion-sensitive ISOs followed suit, incorporating a similar cocktail of wt. % PVC, DOS, TDMACl, and chromoionophore IV (CH IV), respectively, which was coated onto a glass surface (0.9x5 cm, 1 mm thickness).[23]

Pre-soaking glass slides in background solution at near neutral pH induced a co-expulsion of chloride ions from TDMACl and protons from CH IV from the polymeric film. Upon

interaction with heparin-concentrated samples, changes in absorbance of the polymeric membrane occurred as a result of polyanion and protons electrostatically interacting with respective cationic ($TDMA^+$) and anionic (C^-) sites. Notably, this was another demonstration of heparin's ability to electrostatically complex with lipophilic $TDMA^+$ within the organic polymeric film despite being an otherwise hydrophilic molecule.

Polycation-sensitive optical films were subsequently developed using protamine as a model polycation. Though in this case, a lipophilic fluorescein derivative was used as a three-in-one ionophore, chromoionophore, and ion-exchanger (polycation chromophore) in which cation exchange between the polycation and protons was shown to generate measurable changes in absorbance of the membrane film.[24] Though this sensing mechanism is unconventional to the traditional polyion-sensitive ISO format,[23] its sufficiency towards detection of protamine in calf serum proved as a promising step toward routinely applying these technologies for polyion sensing in biological samples. Overall, the successful implementation of polymeric films on glass slides for polyion sensing marked the beginning of a transformation towards miniaturization of polyion-sensitive ISOs.

1.3.2 Microwell Plates

Microwell or microtiter plate-based, polyion-sensitive ISOs were introduced as a means to increase the temporal throughput at which polyion concentrations could be measured in samples. Similar to the glass slide surface used in previous methods,[23,24] individual wells within a 96-well plate were coated with polymeric films containing amounts (wt. %) of lipophilic sensing components.[25] Though, in the latter case, only microliter-scale volumes of polyion-sensitive, cocktail solution were needed for film casting onto the bottom of individual wells. This provided a reagent-conservative alternative to film-coated glass slides which required mL-scale

volumes of sensing cocktail, magnitudes larger in volume. For polyanion sensing, the Nam group demonstrated the microtiter format for the detection of heparin in sample volumes no larger than a few hundred μL, a further demonstration of sample conservation relative to its previously developed polyanion-sensitive ISO counterpart.[25] Further applications of microtiter-formatted, polyion-sensitive ISOs followed thereafter. Having demonstrated lipophilic fluorescein derivatives as suitable reagents for polycation measurements,[24] the Meyerhoff group continued the use of such molecules for protamine sensing using microtiter plates. This method was shown as responsive toward a variety of protamine concentrations in both buffer and sheep plasma samples.[26] In the following years, respective polyanion- and polycation-sensitive, microtiter platforms found continued usage for measurement of other polyions including pentosan polysulfate, DNA, carrageenan (food additive), and heparin (in serum).[27,28]

1.3.3 Inkjet-Printed Cellulose Papers

After years of success with glass surface- and microtiter plate-based methods, polyion-sensitive ISOs which used filter paper as the substrate were introduced as an alternate platform. Using an inkjet printer, a polyion-sensitive cocktail of interest is printed onto a piece of filter paper. Final optode sizes, hole punched from the filter paper, are only a quarter inch in size. With this method, several polyions including heparin, protamine, and pentosan polysulfate were detected in samples only tens of μL in volume.[29] Notably, plasticizers traditionally included in polyion-sensitive cocktails (i.e. PVC, DOS)[23–28] were omitted from inkjet-printed polyion-sensitive ISOs, decreasing the complexity of the chemical composition of the sensing phase. Though, the main feature of cellulose filter paper-based polyion-sensitive ISOs is the usage of a smartphone camera as the detector which tracks changes in the color hue of individual optodes exposed to polyion concentrated samples.[29] This hand-held detector greatly reduced the

complexity of the analytical instrumentation needed for polyion-sensitive ISOs, a positive direction toward point-of-care analysis. Beyond biomedical polyion sensing, Ferguson et al. also found similar success in the use of the described inkjet-printed platform for the detection of several PQ species in both buffer and pool water samples.[30]

1.3.4 Nanospheres

Polyion-sensitive nanospheres were the first in the series of polyion-sensitive ISOs to incorporate (organic) sensing platforms only tens of nm in size. Notably, each polyion-sensitive nanosphere in solution has a diameter less than 100 nm. Considering that surface area mathematically scales with volume,[31] interactions between target polyions and nanospheres advantageously occur at a higher frequency relative to previously developed polyion-sensitive ISOs. For polycation-sensitive nanospheres, the sensing matrix consists of dinonylnaphthalene sulfonic acid, DOS, Pluronic F-127, and Ox Blue (chromoionophore) dissolved in tetrahydrofuran (THF).[32] An aliquot of the THF cocktail is placed into a fixed volume of water vortexed, and blown with compressed air, resulting in a suspension of polycation-sensitive nanospheres. Protamine was the initial target of interest for the aforementioned nanospheres, which were demonstrated to be responsive toward protamine at concentrations from 0 to 14 µg/mL. Polyion-sensitive nanospheres were further developed by Chen et al. for the measurement of heparin and protamine in both buffer and human serum.[33] For heparin measurements, polyanion-sensitive nanospheres (~50 nm in diameter) were functionalized by CH IV and TDMACl sensing components. Alternatively, to originally developed polycation-sensitive nanospheres, chromoionophore VI (CH VI) and sodium ion-exchanger were used as the sensing components of polycation-sensitive nanospheres developed by the Xie group. In this case, changes in the colorimetric properties of such nanospheres are dependent on degree of ion

exchange, or electrostatic interaction between deprotonated CH VI and protamine. This follows a similar format to classical polycation-sensitive ISOs previously described.[24,26] Polyion-sensitive nanospheres produced stable and measurable optical signal in under 10 seconds upon exposure to polyion-concentrated samples, a great improvement in response time (i.e. seconds vs minutes) relative to previously reported methods. Most notably, polyion-sensitive nanospheres were one of the first demonstrations of miniature and immobilized polyion-sensitive ISOs, a promising step away from classical or "bulk" methods.

1.4 Ionophore-Based Droplet Microfluidics

Several polyion sensing methods including charged-dye assays and polyion-sensitive ISOs have been discussed within this chapter. Optical sensing methods have found continued use in application due to their configurable nature, evidenced by continued improvements made in analytical response time, sensor size, and sample-reagent consumption over the past century. However, for polyion-sensitive ISOs, optical interference from sample color[29] **(Figure 1.2)** is a persistent limitation which has not been remedied in the many years since their initial development. In this case, high dilution factors are often required for measurements in biological samples.[33] Large sample volumes (milliliters), extended signal stabilization times (≥10 minutes), and/or irreversibility also remain as long-standing restraint(s) of polyion-sensitive ISOs as a collective.

Ionophore-based droplet microfluidics – a new development in the series of ISO technologies – offers the potential to mitigate many of the current problems with polyion-sensitive ISOs. As background, droplet microfluidics involves the manipulation of two immiscible liquids through micrometer-scale channels, in such a way that aqueous droplets (100s of picoliter) are formed in a continuous carrier (oil) phase, and has been utilized over the past

several decades to perform typical laboratory operations on a miniaturized chip.[34,35] Intrinsic features of droplet microfluidics such as low sample volumes[36] and high surface-area-to-volume ratios[37] allow for chemical analysis in a reagent conservative environment and enhanced mass charge transfer between phases. Traditionally, chemical sensing occurs in aqueous droplets, and the oil phase used to segment the aqueous stream is not chemically responsive.[38] This creates an analytical challenge for measurement of fluorescent and/or colorimetric signal from sensing reagents in aqueous samples which have an opaque nature such as serum, plasma, or blood. Ionophore-based droplet microfluidics, a method which inversely uses the oil phase as a chemical reporter for analyte sensing, thus remains as a technology which possesses the advantages of traditional droplet microfluidics without the associated limitations.

Herein, ionophore-based droplet microfluidics, a combination of droplet microfluidics and "optodes" are referred to as microfluidic droptodes. This specific technology utilizes a water-immiscible organic solvent concentrated with ionophore, ion-exchanger, and chromoionophore along with an intersected aqueous stream to generate a large number of segments that are individually analyzed.[39] Upon generation, each sub-nanoliter oil segment (per droplet) acts as an individual optical sensor, as the chromoionophore undergoes a change in fluorescence once the analyte migrates from the aqueous phase and binds to the ionophore in the organic phase **(Figure 1.3)**. In this way, the amount of fluorescence in oil segments tracks well with the concentration of analyte in aqueous samples. One of the major benefits of microfluidic droptodes is that the fluorescence is measured in the oil phase rather than the potentially complex, aqueous matrix. The selectivity of such sensors can also be tuned based on the number of ionophores available for target-selective binding of the analyte of interest. Lastly, oil-droplet

pairs are continuously generated at tens of Hz, eliminating the need to regenerate the oil phase for reuse.

To this point, microfluidic droptodes have been demonstrated for the detection of ions (K^+, Na^+, and Cl^-), and polycations in aqueous samples. For ion-selective droptodes, the fluorescence response toward the target ion of interest was found to be proportionally higher relative to the response toward other ions similar in charge and size – a demonstration of target specific binding.[39] Furthermore, potassium concentration of a half-fold diluted blood sample, measured with potassium-selective droptodes was found to be in good agreement with a commercial blood gas analyzer.[39] For polycation-sensitive droptodes, a dinonylnapthalene sulfonic acid and chromoionophore I sensing chemistry, as demonstrated in previous polyion-sensitive ISO works,[29] was found to be responsive toward a variety of protamine concentrations (1 – 100 µg/mL) further demonstrating the utility of microfluidic droptodes beyond single ion sensing. In this case, polycation-sensitive droptodes may find continued use for measurement of non-biomedical polyions such as PQs similarly to inkjet-printed, polycation-sensitive ISOs, demonstrated for both medical and non-biomedical polycation sensing.

Though microfluidic droptodes have been proven as an advancement to polycation-sensitive ISO methods, they remain undemonstrated as a feasible technique for measurement of polyanions. Given the response and reproducibility of polycation-sensitive droptodes, such may find use as an appropriate method for indirect polyanion sensing – a type of measurement which has been successfully implemented in previously developed polyanion-sensitive ISOs.[29] However, indirect sensing is not often preferred analytically, as it requires additional sample preparation steps with a oppositely-charged background polyion. Direct sensing using traditional TDMACl and CH IV polyanion-sensitive reagents[23] in the oil phase of microfluidic droptodes,

may be of interest. However, CH IV is not a fluorescent chromoionophore,[40] making it a poor candidate as an optical reporter in droptode systems. Extensive sample preparation associated with indirect sensing and the lack of fluorescence of the CH IV molecule used in standard polyanion-sensitive ISOs, highlight the need for the development of a fluorescent, polyanion-sensitive droptode chemistry for direct sensing of polyanions. In this way, polyion-sensitive droptodes may be considered as a more versatile method which can be used for both negatively and positively charged polyion sensing.

1.5 Conclusions

Several methods have been developed over the past century for colorimetric and fluorescent detection of polyions to reduce the complexity of analytical measurements. Polyion-sensitive, charged dyes – whose optical properties are dependent on their degree of electrostatic interaction with polyion amounts in a given sample – have found continued success in several analytical platforms over the past century. Furthermore, polyion-sensitive ISO-sensing chemistries have been continuously adapted into different platforms over the past several decades as a means to reduce sample volume, analysis time, reagent amounts, and size of analytical equipment needed for polyion measurements. Lastly, microfluidic droptodes are the latest advancement within a long series of ISO technologies. To achieve similar success to their single ion-sensing counterpart – applied for measurement of potassium in whole blood – polyion-sensitive droptodes must continue to be developed beyond single ion and polycation measurement applications. In this thesis, polyion-sensitive, microfluidic droptodes are further developed and applied for the measurement of additional polyions in both simple and complex matrices, advancing the fields of polyion-sensitive, optical methods and biphasic droplet microfluidics.

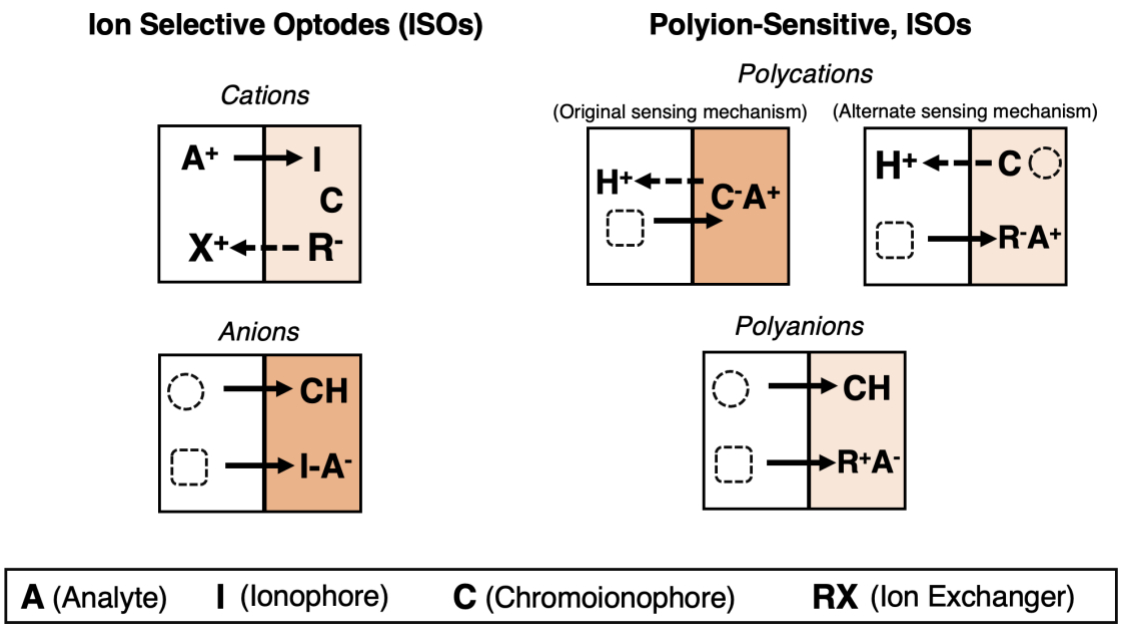

Figure 1.1. Common operation principle of single ion-selective optodes (ISOs) and polyion-sensitive, ISOs. Colorimetric changes of the organic phase are modulated by the chromoionophore's ability to accept (C) or donate (CH) a proton (H^+) in addition to the chemical properties of the analyte, ion-exchanger, and ionophore, respectively, in a given system.

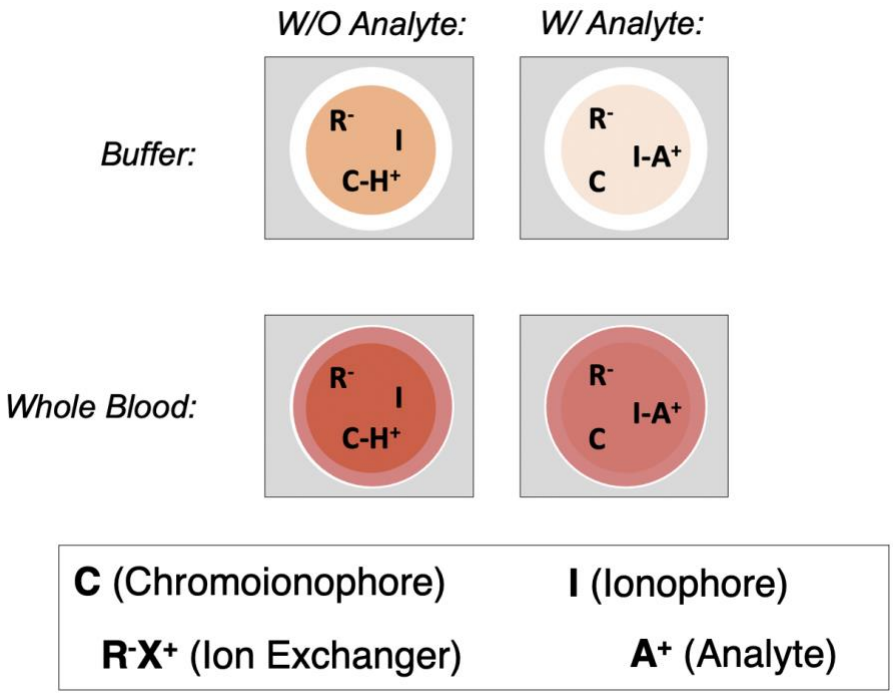

Figure 1.2. Schematic of analyte sensing using ionophore-based optodes in respective transparent and opaque matrices. The color of the biological sample suppresses the optical signal of the chromoionophore, limiting the differentiation between samples without and with the target analyte.

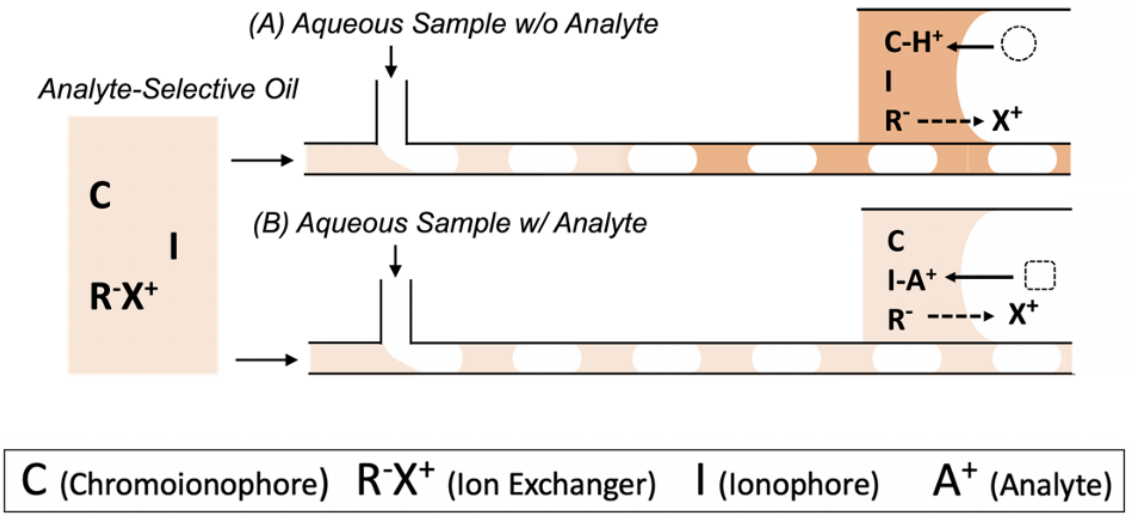

Figure 1.3. Schematic of ionophore-based biphasic sensing on a droplet microfluidic device for samples (A) without and (B) with the target analyte. Each individual segment per aqueous droplet is considered as an individual droptode. Local changes in pH are represented by migration of the proton (H^+) from the aqueous sample and into the droptode segment.

1.6 References

(1) MacIntosh, F. C. A Colorimetric Method for the Standardization of Heparin Preparations. *Biochem. J.* **1941**, *35* (7), 776–782. https://doi.org/10.1042/bj0350776.

(2) Smith, P. K.; Mallia, A. K.; Hermanson, G. T. Colorimetric Method for the Assay of Heparin Content in Immobilized Heparin Preparations. *Anal. Biochem.* **1980**, *109* (2), 466–473. https://doi.org/10.1016/0003-2697(80)90679-X.

(3) Young, M. D.; Balazs, E. A.; Phillips, G. Thermodynamic Studies of Heparin-Azure a Complexes in Solution. *Biochim. Biophys. Acta* **1967**, *141*, 374–381.

(4) Klein, M. D.; Drongowski, R. A.; Linhardt, R. J.; Langer, R. S. A Colorimetric Assay for Chemical Heparin in Plasma. *Anal. Biochem.* **1982**, *124*, 59–64.

(5) Yang, V. C.; Fu, Y. Y.; Teng, C. L. C.; Ma, S. C.; Shanberge, J. N. A Method for the Quantitation of Protamine in Plasma. *Thromb. Res.* **1994**, *74* (4), 427–434. https://doi.org/10.1016/0049-3848(94)90158-9.

(6) Egawa, Y.; Hayashida, R.; Seki, T.; Anzai, J. ichi. Fluorometric Determination of Heparin Based on Self-Quenching of Fluorescein-Labeled Protamine. *Talanta* **2008**, *76* (4), 736–741. https://doi.org/10.1016/j.talanta.2008.04.019.

(7) Gao, Y.; Wei, K.; Li, J.; Li, Y.; Hu, J. A Facile Four-Armed AIE Fluorescent Sensor for Heparin and Protamine. *Sensors Actuators, B Chem.* **2018**, *277* (August), 408–414. https://doi.org/10.1016/j.snb.2018.09.054.

(8) Pu, K. Y.; Liu, B. A Multicolor Cationic Conjugated Polymer for Naked-Eye Detection and Quantification of Heparin. *Macromolecules* **2008**, *41* (18), 6636–6640. https://doi.org/10.1021/ma801269n.

(9) Warttinger, U.; Giese, C.; Harenberg, J.; Holmer, E.; Krämer, R. A Fluorescent Probe Assay (Heparin Red) for Direct Detection of Heparins in Human Plasma. *Anal. Bioanal. Chem.* **2016**, *408* (28), 8241–8251. https://doi.org/10.1007/s00216-016-9940-y.

(10) Horn, D.; Heuck, C. C. Charge Determination of Proteins with Polyelectrolyte Titration. *J. Biol. Chem.* **1983**, *258* (3), 1665–1670. https://doi.org/10.1016/s0021-9258(18)33037-0.

(11) Nazir, H.; Zhang, W.; Liu, Y.; Chen, X.; Wang, L.; Naseer, M. M.; Ma, G. Silicone Oil Emulsions: Strategies to Improve Their Stability and Applications in Hair Care Products. *Int. J. Cosmet. Sci.* **2014**, *36* (2), 124–133. https://doi.org/10.1111/ics.12104.

(12) Hamad, M. J. A.; Chirwa, E. M. N. Forward Osmosis for Water Recovery Using Polyelectrolyte PolyDADMAC and DADMAC Draw Solutions as a Low Pressure Energy Saving Process. *Desalination* **2019**, *453* (May 2018), 89–101. https://doi.org/10.1016/j.desal.2018.11.016.

(13) Bakker, E.; Bühlmann, P.; Pretsch, E. Carrier-Based Ion-Selective Electrodes and Bulk

Optodes. 1. General Characteristics. *Chem. Rev.* **1997**, *97* (8), 3083–3132. https://doi.org/10.1021/cr940394a.

(14) Shortreed, M.; Bakker, E.; Kopelman, R. Miniature Sodium-Selective Ion-Exchange Optode with Fluorescent pH Chromoionophores and Tunable Dynamic Range. *Anal. Chem.* **1996**, *68* (15), 2656–2662. https://doi.org/10.1021/ac960035a.

(15) Wang, L.; Sadler, S.; Cao, T.; Xie, X.; Von Filseck, J. M.; Bakker, E. Simplified Fabrication for Ion-Selective Optical Emulsion Sensor with Hydrophobic Solvatochromic Dye Transducer: A Cautionary Tale. *Anal. Chem.* **2019**, *91* (14), 8973–8978. https://doi.org/10.1021/acs.analchem.9b01145.

(16) Apichai, S.; Wang, L.; Grudpan, K.; Bakker, E. Renewable Magnetic Ion-Selective Colorimetric Microsensors Based on Surface Modified Polystyrene Beads. *Anal. Chim. Acta* **2020**, *1094*, 136–141. https://doi.org/10.1016/j.aca.2019.10.011.

(17) Stelmach, E.; Nazaruk, E.; Maksymiuk, K.; Michalska, A. Cubosome Based Ion-Selective Optodes–Toward Tunable Biocompatible Sensors. *Anal. Chem.* **2021**. https://doi.org/10.1021/acs.analchem.1c01247.

(18) Xie, X.; Zhai, J.; Bakker, E. pH Independent Nano-Optode Sensors Based on Exhaustive Ion-Selective Nanospheres. *Anal. Chem.* **2014**, *86* (6), 2853–2856. https://doi.org/10.1021/ac403996s.

(19) Ortuño, J. A.; Albero, M. I.; García, M. S.; Sánchez-Pedreño, C.; García, M. I.; Expósito, R. Flow-through Bulk Optode for the Fluorimetric Determination of Perchlorate. *Talanta* **2003**, *60* (2–3), 563–569. https://doi.org/10.1016/S0039-9140(03)00189-9.

(20) Lee, J.; Hahn, Y. K.; Park, J. Y.; Seo, H.; Jung, J.; Cho, E.; Choi, Y. S.; Lee, S. S. An Integrated Ion-Selective Optode Sensor Cartridge for Directly Detecting Electrolyte Ions in Blood Plasma without Pretreatment to Adjust pH. *Sensors Actuators, B Chem.* **2019**, *280* (October 2018), 256–262. https://doi.org/10.1016/j.snb.2018.10.067.

(21) Brady, B.; Wang, R.; Cheong, R.; Wang, X. Digital Printing of Selective and Reversible Ion Optodes on Fabrics: Toward Smart Clothes for Epidermal Chemical Sensing. *Analyst* **2021**. https://doi.org/10.1039/d1an01349a.

(22) Ma, S. C.; Yang, V. C.; Meyerhoff, M. E. Heparin-Responsive Electrochemical Sensor: A Preliminary Study. *Anal. Chem.* **1992**, *64* (6), 694–697. https://doi.org/10.1021/ac00030a023.

(23) Wang, E.; Meyerhoff, M. E.; Yang, V. C. Optical Detection of Macromolecular Heparin Via Selective Coextraction into Thin Polymeric Films. *Anal. Chem.* **1995**, *67* (3), 522–527. https://doi.org/10.1021/ac00099a007.

(24) Wang, E.; Wang, G.; Ma, L.; Stivanello, C. M.; Lam, S.; Patel, H. Optical Films for Protamine Detection with Lipophilic Dichlorofluorescein Derivatives. *Anal. Chim. Acta* **1996**, *334* (1–2), 139–147. https://doi.org/10.1016/S0003-2670(96)00299-1.

(25) Kim, S. B.; Cho, H. C.; Cha, G. S.; Nam, H. Microtiter Plate-Format Optode. **1998**, *70* (22), 4860–4863.

(26) Dai, S.; Ye, Q.; Wang, E.; Meyerhoff, M. E. Optical Detection of Polycations via Polymer Film-Modified Microtiter Plates: Response Mechanism and Bioanalytical Applications. *Anal. Chem.* **2000**, *72* (14), 3142–3149. https://doi.org/10.1021/ac000060n.

(27) Dürüst, N.; Meyerhoff, M. E.; Ünal, N.; Naç, S. Spectrophotometric Determination of Various Polyanions with Polymeric Film Optodes Using Microtiter Plate Reader. *Anal. Chim. Acta* **2011**, *699* (1), 107–112. https://doi.org/10.1016/j.aca.2011.05.007.

(28) Kim, S. B.; Kang, T. Y.; Cha, G. S.; Nam, H. Quantitative Determination of Heparin Levels in Serum with Microtiter Plate-Format Optode. *Anal. Chim. Acta* **2006**, *557* (1–2), 117–122. https://doi.org/10.1016/j.aca.2005.10.053.

(29) Wang, X.; Mahoney, M.; Meyerhoff, M. E. Inkjet-Printed Paper-Based Colorimetric Polyion Sensor Using a Smartphone as a Detector. *Anal. Chem.* **2017**, *89* (22), 12334–12341. https://doi.org/10.1021/acs.analchem.7b03352.

(30) Ferguson, S. A.; Wang, X.; Mahoney, M.; Meyerhoff, M. E. Detection and Quantification of Polyquaterniums via Polyion- Sensitive Ion-Selective Optodes Inkjet Printed on Cellulose Paper. *Anal. Sci.* **2018**, *34* (1), 45–50. https://doi.org/10.2116/analsci.34.45.

(31) Harris, L. K.; Theriot, J. A. Surface Area to Volume Ratio: A Natural Variable for Bacterial Morphogenesis. *Trends Microbiol.* **2018**, *26* (10), 815–832. https://doi.org/10.1016/j.tim.2018.04.008.

(32) Xie, X.; Zhai, J.; Crespo, G. A.; Bakker, E. Ionophore-Based Ion-Selective Optical Nanosensors Operating in Exhaustive Sensing Mode. *Anal. Chem.* **2014**, *86* (17), 8770–8775. https://doi.org/10.1021/ac5019606.

(33) Chen, Q.; Li, X.; Wang, R.; Zeng, F.; Zhai, J.; Xie, X. Rapid Equilibrated Colorimetric Detection of Protamine and Heparin: Recognition at the Nanoscale Liquid-Liquid Interface. *Anal. Chem.* **2019**, *91* (16), 10390–10394. https://doi.org/10.1021/acs.analchem.9b01654.

(34) Whitesides, G. M. The Origins and the Future of Microfluidics. *Nature* **2006**, *442* (7101), 368–373. https://doi.org/10.1038/nature05058.

(35) Teh, S. Y.; Lin, R.; Hung, L. H.; Lee, A. P. Droplet Microfluidics. *Lab Chip* **2008**, *8* (2), 198–220. https://doi.org/10.1039/b715524g.

(36) Chou, W. L.; Lee, P. Y.; Yang, C. L.; Huang, W. Y.; Lin, Y. S. Recent Advances in Applications of Droplet Microfluidics. *Micromachines* **2015**, *6* (9), 1249–1271. https://doi.org/10.3390/mi6091249.

(37) Guo, M. T.; Rotem, A.; Heyman, J. A.; Weitz, D. A. Droplet Microfluidics for High-Throughput Biological Assays. *Lab Chip* **2012**, *12* (12), 2146–2155.

https://doi.org/10.1039/c2lc21147e.

(38) Joensson, H. N.; Andersson Svahn, H. Droplet Microfluidics-A Tool for Single-Cell Analysis. *Angew. Chemie - Int. Ed.* **2012**, *51* (49), 12176–12192. https://doi.org/10.1002/anie.201200460.

(39) Wang, X.; Sun, M.; Ferguson, S. A.; Hoff, J. D.; Qin, Y.; Bailey, R. C.; Meyerhoff, M. E. Ionophore-Based Biphasic Chemical Sensing in Droplet Microfluidics. *Angew. Chemie - Int. Ed.* **2019**, *58* (24), 8092–8096. https://doi.org/10.1002/anie.201902960.

(40) Xie, X.; Crespo, G. A.; Bakker, E. Oxazinoindolines as Fluorescent H+ Turn-on Chromoionophores for Optical and Electrochemical Ion Sensors. *Anal. Chem.* **2013**, *85* (15), 7434–7440. https://doi.org/10.1021/ac401367b.

Chapter 2 – Development of a Microfluidic Droptode Sensor for Heparin Detection in Human Citrated Plasma

Acknowledgments

This work was supported in part by the National Institute of Health Microfluidics in Biomedical Sciences Training Program (T32EB005582). Dr. Shannon Wetzler-Quevedo is thanked for providing basis for the macro code used for data analysis.

Abstract

Heparin, a large, negatively charged macromolecule, is widely used as an anticoagulant in extracorporeal procedures. Methods to quantitate the amount of heparin in blood are therefore essential to ensure correct dosing, thus avoiding unwanted side effects such as thrombosis and hemorrhaging. Electrochemical and optical methods have been developed for the detection of heparin in plasma and whole blood; however, deterioration of sensor response from matrix fouling and optical interference from sample color, respectively, are limitations of these technologies. Furthermore, methods that require minimal sample input are also desirable so as to limit consumption of blood during these procedures. Motivated by needs for a new, low volume and non-fouling clinical sensor, our group has developed a droplet microfluidic form of an ionophore-based optode. This method involves sub-nanoliter aqueous sample aliquots spaced by oil segments containing analyte-selective ionophore and pH-sensitive chromoionophore. Partitioning of the analyte from the aqueous droplet to the oil segment, facilitated by interactions with the ionophore, results in fluorescence changes that track with analyte concentration.

Fluorescence measurements are recorded from sub-nanoliter oil segments adjacent to aqueous droplets, therefore components of the sample do not interfere with the measurement. Here we report the application of this droplet optode (e.g., droptode) technology for the quantification of heparin in citrated human plasma samples over relevant clinical ranges.

2.1 Introduction

Heparin, a highly sulfated macromolecule with a molecular weight ranging from 3 – 30 kDa, is the oldest and most widely used anticoagulant in clinical medicine. With usage in extracorporeal processes such as kidney dialysis and open-heart surgeries, the availability of methods to monitor this biomolecule are essential as incorrect dosing can lead to serious medical complications including deep vein thrombosis[1] and excessive bleeding.[2] However, heparin is a challenging analytical target due to its polydispersity and chemical heterogeneity.[3] Most commonly, assays such as the activated partial thromboplastin time (APTT) – which compares the amount of time (i.e. tens of seconds) needed for visible clot formation in plasma samples relative to a control – is used by clinicians to make pivotal decisions on heparin treatment.[4] Though these assays are function based and relatively cheap, such remain unstandardized as over 300 variations of the APTT exist across clinical settings, differing in instrumentation and clot-initiating reagents employed.[5] Furthermore, the control sample used for the reference interval is based on clotting time of a pooled plasma sample from healthy adults, leaving several populations susceptible to misdiagnoses.

To address the shortage of heparin quantitation methods, polyanion-sensitive ion-selective electrodes (polyanion-sensitive ISEs) were developed in the early 1990s. Such sensors were functionalized by a plasticized poly-(vinyl chloride) (PVC) electrode membrane doped with lipophilic ion-exchanger tridodecylmethylammonium chloride (TDMACl), which provided

target specificity through ion-pairing interactions.[6] Using this technology, changes in the interfacial potential of the electrode were found to track with heparin concentration as the polyanion was extracted into the membrane. Despite its abilities to quantitate amounts of heparin in citrated plasma[6] and whole blood,[7] polyanion-sensitive ISEs can suffer from slow equilibrium response times,[8] and degradation of the sensing interface sample matrix artifacts (i.e. biofouling).[9]

Polyanion-sensitive, ion-selective optodes (polyanion-sensitive ISOs) were developed to mitigate challenges of their electrochemical counterparts. Initially, such sensors consisted of a glass substrate coated with a plasticized PVC film containing TDMACl and chromoionophore (i.e., hydrophobic fluorophore).[10] Upon interaction with sensing surface, polyanion and protons coextract from the aqueous sample and into the plasticized film based on cooperative ion pairing, inducing measurable changes in chromoionophore absorbance due to the local change in pH. Further developments allowed for the aforementioned sensing chemistry to be adapted to several configurations, including microtiter plates, emulsified nanospheres, and plasticizer-free cellulose papers.[11–14] These technologies have garnered attention due to their low cost and configurability, yet often require long signal stabilization times ($\geq$ 10 minutes), large sample volumes (mL-scale), sensor regeneration steps, and/or indirect sensing with oppositely charged macromolecules. Furthermore, application of ion-selective optodes in biological matrices such as plasma and whole blood presents an additional challenge as the optical properties of the sample can create further interferences in the measurement.

These examples highlight several general challenges in clinical sensing—interfacial biofouling, sample volume requirements, assay speed, and optical interference (for optical sensors). With all of these in mind, we have been exploring a new droplet-microfluidic optical

analog of ion-sensitive electrodes/optodes, which we have termed “droptodes”. Droplet microfluidic formats offer many potential benefits for chemical analysis as they utilize immiscible oil and aqueous phases to generate a large number of droplets that can be individually manipulated, mixed, and analyzed one-at-a-time.[15] Specific benefits include chemical analysis in a reagent conservative and high throughput fashion, efficient mass transfer, and often rapid analysis times. With applications ranging from single cell analysis[16–18] to point of care diagnostics[19,20], microfluidic technologies have been demonstrated suitable for rapid and sensitive analyte detection in biological environments.

For chemical analysis of samples, droplet microfluidics is often coupled with fluorescence-based read out strategies, as fluorescence is observable from a small number of dye molecules within sub-nanoliter droplets.[21–24] Though, most commonly, fluorescence is detected in the dispersed aqueous phase rendering such methods incompatible with sensing in opaque or otherwise non-transparent matrices, such as blood and plasma. To address this limitation, we recently have developed a droplet microfluidic form of an ion-selective optical sensor to detect ions (K^+, Na^+, and Cl^-) and protamine, a cationic protein, in buffer and whole blood.[25] This specific technology utilizes a water-immiscible oil containing both an analyte-selective ionophore and chromoionophore. An aqueous sample stream is intersected with this oil phase inducing the generation of a number of sub-nanoliter droplets at high frequency (~50 Hz). In this way, each aqueous droplet-oil segment pair can be thought of as separate reaction vessels with the only communication facilitated between these components being through interfacial, molecular transport. Ion-selective ionophores in the oil phase can interact with target species in the aqueous stream by sequestering them through the oil-water interface, resulting in modulation of chromoionophore fluorescence from proton transfer.

One of the major benefits of this overall approach is that the fluorescence is measured in the oil segments (i.e., readout segments) which do not suffer from optical interference of adjacent, aqueous droplets. Additionally, the selectivity of such sensors can be tuned with the incorporation of different ionophores, structurally modified to bind specific molecules over other analytes.[26] To date, the possibility of combing ionophore-based chemistries with droplet microfluidics for the detection of negatively charged macromolecules such as heparin has not been explored. Herein, for the first time, we demonstrate an ionophore-based, droplet microfluidic technology capable of detecting heparin in citrated human plasma.

2.2 Experimental Methods

2.2.1 Chemicals and Materials

Bis(2-ethylhexyl)-sebacate (DOS), tridodecylmethylammonium chloride (TDMACl), heparin from porcine intestinal mucosa (6 – 30 kDa; 180 USP/mg), enoxaparin sodium (low molecular weight heparin), diadenosine pentasodium polyphosphate, chondroitin sulfate (#C3788), and d-glucosamine 3-sulfate were purchased from Sigma Aldrich (St. Louis, MO). Fluorescein octadecyl ester, referred to as chromoionophore XI (CH XI), was purchased at the highest purity (≥97%) from both Sigma Aldrich and Abcam. Tris-HCl, Tris, 20 mL scintillation vials, and Haemonetics microaggregate filters were purchased from Fisher-Scientific. 30 AWG PTFE tubing was purchased from Cole-Palmer. Citrated human plasma (single donor) was obtained from Innovative Research (Novi, Michigan). Respective amounts of sensing reagents (mg) were measured in separate 20 mL scintillation vials, concentrated to 1000 µM with DOS as solvent, and sonicated for complete dissolution. Final readout phase employed in each experiment was created from sensing reagent stocks using DOS as diluent.

2.2.2 Device Fabrication

T junction devices were fabricated using a conventional photo and soft lithography method as described [25] in which polydimethylsiloxane (PDMS) devices are bound to PDMS coated glass slides. Droplet microfluidic channels were fabricated at a depth of 40 µm in which a 40 µm wide aqueous channel intersected perpendicularly (90º) with an 80 µm wide oil carrying channel, unless otherwise noted. All microfluidic channels were 35 mm in length from the junction to the waste port. Uncommon to traditional droplet microfluidic works, device channels were not treated with surfactants as such have been demonstrated to impact the sensitivity of ionophore based sensors.[27]

2.2.3 Preparation of Samples for Analysis

For polyanion experiments, compounds were weighed into vials and concentrated with 100 mM Tris-HCl/20 mM buffer (pH 7.4) as the solvent. Heparin solutions (USP/mL) were created from a 100 USP/mL stock, by dilution. Tested amounts in the polyanionic compound study were created from a 100 µg/mL solution which was ten-fold diluted from a 1000 µg/mL stock. For final experiments, white particulate matter ≥ 40 µm was removed from human citrated plasma samples using a Haemonetics microaggregate filter. Serial heparin dilutions were created in 100% plasma and diluted with buffer for measurements on device.

2.2.4 Droplet Generation, Imaging, and Fluorescence Quantitation

Segmented flow on the microfluidic device was generated by pressure using either a home-built pressure controller system as previously implemented by our group[21] or an Elveflow OB1 MK3+ flow controller connected to the described regulator. Aqueous droplet frequencies were maintained around 20 – 25 Hz throughout the experiments. A Phantom Miro eX2 high

speed camera attached to a Leica DMi8 fluorescence microscope was used to image segmented flow at 10× objective. For fluorescence stimulation, the device was exposed to filtered light from a Prior Lumen200 illumination system. Videos of generated segments in bright and dark field modes were collected at 100 frames per second. Fluorescent intensity within a 90x30, rectangular region of analysis generated from segments during a 1.0 second interval was quantified using a macro code custom written for Image J. Respective data points were obtained as an average of the peak values, or local maxima within fluorescence traces, which correspond to fluorescent readout segments at the distal end of the device (30 mm).

2.3 Heparin Sensing on a Droptode Device

In traditional heparin-sensing ISO works, TDMA (L^+) is incorporated into an organic sensing phase along with chromoionophore IV, as an optical readout element. In such systems, changes in absorbance of the organic sensing phase correspond to heparin concentration in the aqueous sample (Hep_{aq}^{z-}). To adapt this sensing mechanism for our fluorescence-based technology, CH IV was replaced with CH XI, a lipophilic derivative of fluorescein **(Figure 2.1)**. We hypothesize that CH XI's protonation chemistry is relatively similar to CH IV's, considering that both molecules have similar p*Ka* values[28] and structure **(Figure 2.2)**. Hence, we report a coextraction equilibrium for our system as previously described:[10]

$$zL_{oil}^{+} + zC_{oil}^{-} + zH_{aq}^{+} + \ Hep_{aq}^{z-} \rightleftharpoons \ L_zHep_{oil} + zCH_{oil}$$

where C_{oil}^{-} and CH_{oil} are representative of chromoionophore in its deprotonated and protonated states in the oil phase, respectively. The equilibrium constant ($K_{extraction}$) for this reaction can be written as such:

$$K_{extraction} = \frac{[L_zHep][CH]^z}{[L]^z[C^-]^z[H^+]^z[Hep^{z-}]}$$

Due to mass-charge balance, the ratio of deprotonated chromoionophore [C^-] to total chromoionophore concentration [CT] in the oil segments is dependent upon heparin concentration in the aqueous droplets. Furthermore, relative fluorescence (α) of the oil segments is plotted using the following equation:

$$\alpha = \frac{[C^-]}{[CT]} = \frac{\mathrm{F} - F_{min}}{F_{max} - F_{min}}$$

where F represents the average fluorescence of the readout segments interacting with heparin concentrated droplets. The fluorescence of the deprotonated (F_{max}) and protonated (F_{min}) are obtained when the chromoionophore in the oil segments is in its deprotonated and protonated state, respectively.

2.4 Results and Discussion

2.4.1 Preliminary Heparin Sensing

As the proposed polyanion sensing chemistry had not been tested in droptode systems, the ratio of sensing reagents used in chloride-selective droptodes[25] was used as a reference point for measuring negatively charged species. In this way, experiments for polyanion detection were conducted using TDMACl and CH XI in a 3:2 ratio. Herein, heparin concentration refers to United States Pharmacopoeia (USP) "U/mL" which correspond to mass values as provided by the manufacturer. Using a sensing phase concentrated with 400 µM CH XI and 600 µM TDMACl, heparin in buffer was detected with good agreement between fluorescence response and polyanion concentration (U/mL) (**Figure 2.3)**. As proposed, decreases in fluorescence of the readout segments occur with increasing amounts of heparin, demonstrating that these multiple negatively charged species are co-extracted with protons from the droplet and into readout

segments. Furthermore, a differentiable optical signal was obtained in the presence of physiological levels of chloride (~100 mM) demonstrating the readout phase's selectivity toward heparin over negatively charged ions. As heparin concentrations at 16 and 24 U/mL, respectively, are two and three times higher than the largest therapeutic dose amount used in treatments (8 U/mL)[29], further experiments were focused on optimization of sensor response within the 0 – 10 U/mL range.

2.4.2 Effect of Readout Phase Concentration on Sensor Response Toward Heparin

Further studies on varying sensing chemical concentrations at fixed heparin concentrations were conducted to identify trends with sensor response. **Table 2.1** and **Figure 2.4** demonstrate increasing concentrations of sensing components lead to a decreasing droptode response toward heparin**.** Such trends identify chromoionophore and TDMACl concentrations as impacting factors in the droptode's ability to make sensitive heparin measurements within and outside clinically relevant range of 0.2 – 8 U/mL.[29] Hence, further experiments were conducted using a readout phase concentrated with 200 µM CH XI and 300 µM TDMACl, the lowest concentrations of these components at which differentiable signal between the droplets and oil segments could be attained. Trends toward increased sensitivity at this specific oil phase composition continue as sensor response toward heparin at 10 U/mL is ~1.5 times larger than that of oil phase A **(Table 2.1)**. Furthermore, linear detection is achieved in the produced response curve at both low and high concentrations demonstrating the sensor's ability to detect heparin at a dynamic range of concentrations **(Figure 2.5b)**.

2.4.3 Analysis of Segmented Flow in Droplet Microfluidic Device

Analysis of segmented flow was conducted to further align sensing principle with observed optical trends. Obtained bright and dark field images of segmented flow (**Figure 2.5c)** demonstrate that fluorescence measurements are in fact being taken in the readout segments, as elliptical-shaped aqueous droplets generate a signal approximate to the device background. Additionally, peak heights from fluorescent oil segments **(Figure 2.5a)** decrease with increasing amounts of heparin as co-extracted protons saturate CH XI. Variations in background signal observed at the bottom of peaks in collected traces are likely due to the hydrophilic portion of CH XI from readout segments leaching into aqueous droplets which alternate through the small region of analysis used in the macro code. Yet, this further demonstrates how each readout segment functions as an individual (droptode) sensor allowing for n≥20 measurements to be made per heparin sample. Henceforth, the sensor is able to quantitate heparin concentrations in a 1.0 second time interval, which is a great improvement to recently reported polyanion-sensitive optodes.[13,14]

2.4.4 Droptode Response Toward Polyanions and Charged Fragments

Taking the cationic nature of $TDMA^+$ into consideration along with its steric accessibility to bind other negatively charged species, the specificity of the aforementioned sensing methodology toward heparin was of question. Hence, sensor response toward various other negatively charged macromolecules at fixed concentration was investigated. Samples containing heparin were found to generate the largest change in fluorescence relative to other listed compounds **(Table 2.2)**. Such a response is attributed to heparin's negative charge density, which is the highest relative to any other known biomolecule.[30] Notably, the sensor exhibits the same optical response to both heparin and low molecular weight (LMWH) heparin, indicating a full equilibrium response is not being obtained with the larger heparin fragments during the rapid

reaction period. Yet, error associated with sensor response toward LMWH is higher than that of UFH, as larger fragments are likely to form more stable complexes with $TDMA^+$.[31] Subsequently lower optical responses from chondroitin sulfate (porcine-derived)[32], glucosamine-3-sulfate (monosaccharide unit of heparin) and polyphosphate demonstrate that heparin's specific polymeric structure and sulfate content allow for it to be selectivity detected over other compounds. Furthermore, distinct optical responses of this sensor toward compounds of varying structural composition and charge state **(Figure 2.6)** further indicates polyanion-sensitive droptodes can be used to differentiate negatively charged macromolecules.

2.4.5 Heparin Detection in Human Citrated Plasma

To test the feasibility of measuring heparin in biomatrices in which it is commonly encountered, further studies were conducted in a citrated plasma background. In this case, heparin concentrations were able to be measured at concentrations within and outside clinically relevant ranges **(Figure 2.7a)**. Despite the reduced transparency of the plasma sample, readout segments possess a distinct fluorescent signal relative to the background signal of aqueous droplets (**Figure 2.7b**). Furthermore, generated segments maintain their structural integrity at the detection point, allowing for measurements to be made in complex matrices without chemical interference from surfactants. Variations, or associated uncertainties associated relative fluorescence measurements still exist at each data point, likely due to interference from negatively charged plasma proteins[33] and electrolytes[34] competing with heparin for the limited number of $TDMA^+$ sites in the readout segments.

2.5 Conclusions

An ionophore-based droptode sensor capable of heparin detection in backgrounds of both buffer and human citrated plasma has been demonstrated. Additional experiments demonstrate this sensor as most responsive toward heparin relative to other negatively charged macromolecules and fragments, an occurrence which can be attributed to heparin's high charge density and degree of sulfation. Furthermore, analysis of continuously generated, segmented flow demonstrates fluorescence measurements are being taken in readout segments adjacent to aqueous droplet in both cases where the sample matrix has a complete (i.e., 100% buffer) and reduced (i.e., human citrated plasma) transparency. This method is a major improvement relative to traditional electrochemical and optical heparin sensors which are susceptible to degradation from matrix artifacts and interference from sample color, respectively.

Further studies analyzing the effect of droplet size and oil segment spacing on droptode sensitivity toward polyanions are currently being conducted within our lab – parameters which have been demonstrated to impact the sensitivity of single ion-selective droptodes.[35] Upon optimization of the mentioned parameters, this technology can be further advanced toward heparin sensing in whole blood as previous and current work within our lab has demonstrated the color of the sample matrix does not affect fluorescence signal. Additionally, the development of glass material droptode devices to mitigate chromoionophore-PDMS interactions (**Figure 2.8**) in our current PDMS design is being explored. Henceforth, the detection of heparin and polyanionic molecules has further demonstrated the versatility of microfluidic droptodes beyond electrolyte and protein sensing, serving as a novel optical method for analyte detection in both opaque and transparent matrices.

Oil composition	[CH XI] (μM)	[TDMACl] (μM)	Δ Relative Fluorescence (α) (0 – 10 U/mL)
A	400	600	-0.39 (±0.01)
B	600	900	-0.17 (±0.05)
C	800	1200	-0.11 (±0.04)

Table 2.1. Readout phase concentration effect on droptode sensitivity toward heparin. Increasing concentrations of CH XI and TDMACl in the readout phase led to a decrease in polyanion-sensitive droptode response toward heparin. Response is represented by average relative fluorescence (α) ± standard deviation for n=3 trials.

Tested Compound (12 µg/mL[a])	Δ Relative Fluorescence (±S. D)	M_w average (kDa)	Sulfated Groups Per Monomer
Heparin (UFH)	-0.16 (±0.03)	18	3
Heparin (LMWH)	-0.16 (±0.04)	4.4	3
Chondroitin Sulfate	-0.10 (±0.06)	18	1
Glucosamine-3-Sulfate	-0.01 (±0.04)	0.26	1
Polyphosphate	+0.01 (±0.02)	1.0	0[b]

Table 2.2. Fluorescent response of droptode toward different polyanionic compounds. Response toward each compound is represented by average relative fluorescence (α) ± standard deviation for n=3 trials. [a]12 µg/mL of heparin corresponds approximately to 2.2 U/mL. [b]Compound has five negatively charged phosphate groups per molecule.

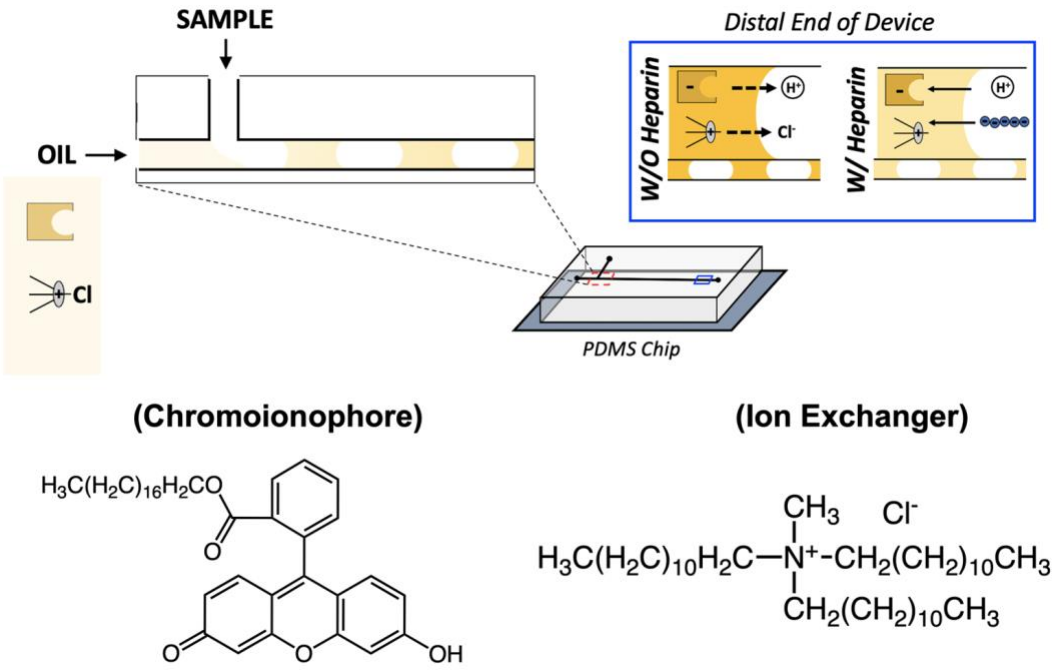

Figure 2.1. Schematic for heparin sensing. For samples without polyanion, protons and chloride ions co-expulse into the aqueous droplets. When aqueous droplets are concentrated with polyanion, the polyanion and protons migrate into the readout phase, binding to chromoionophore and $TDMA^+$, respectively.

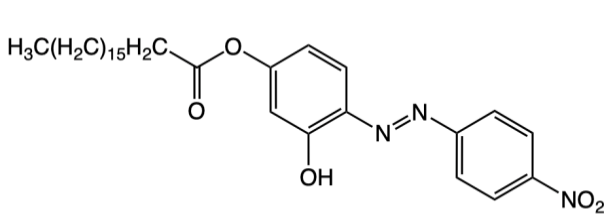

Chromoionophore IV

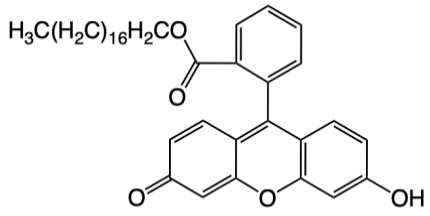

Chromoionophore XI

Figure 2.2. Chemical structures of chromoionophore IV and chromoionophore XI. Each molecule has a hydroxyl group which is expected to react similarly in respective colorimetric (CH IV) and fluorescence (CH XI) applications.

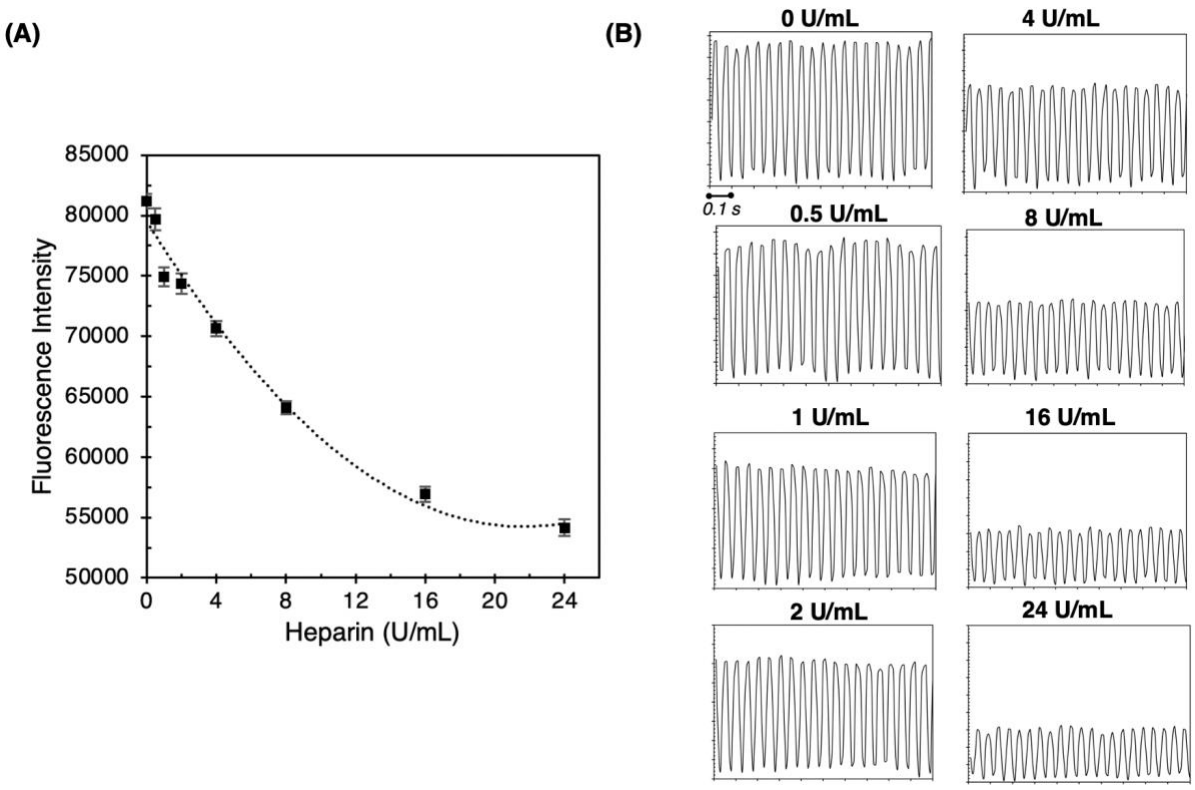

Figure 2.3. (A) Response of a 400 µM CH XI/600 µM TDMACl readout phase towards heparin in 100 mM Tris-HCl/20 mM Tris buffer (pH 7.4). Data points are representative of the average fluorescence intensity from n ≥ 19 readout segments ± standard deviation (B) Fluorescence traces of segmented flow during a 1.0 second interval (excitation: 470/40 nm; emission: 500 - 550 nm). Dimensions of the droplet microfluidic device used consist of an overall depth of 80 µm and a 64 µm width aqueous channel intersecting with an 80 µm width oil carry channel.

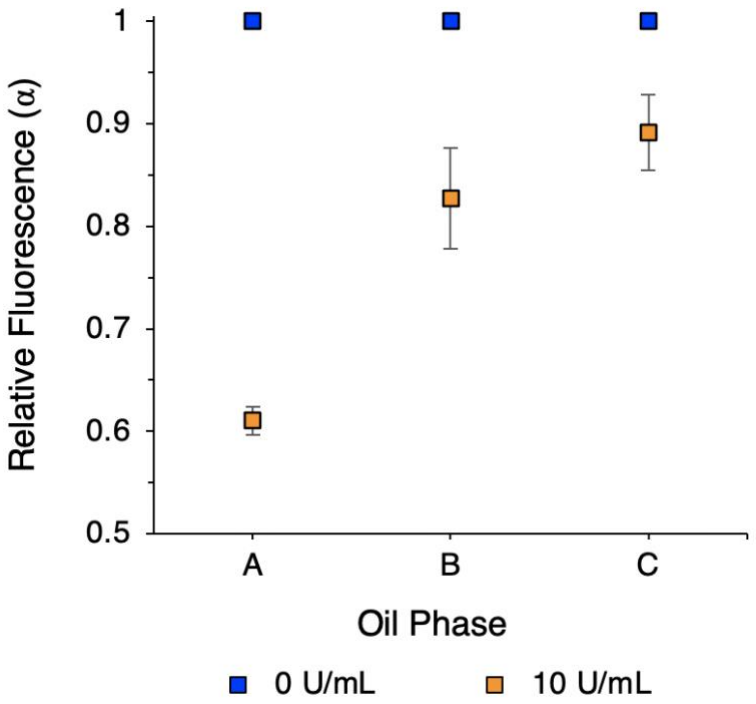

Figure 2.4. Changes in droptode response toward heparin in 100 mM Tris-HCl/20 mM Tris buffer (pH 7.4) based on concentration of CH XI and TDMACl sensing components in the readout phase. Oil phase A, B, and C are representative of 400 µM CH XI:600 µM TDMACl, 600 µM CH XI:900 µM TDMACl, and 800 µM CH XI:1200 TDMACl readout phases, respectively. Data points represent average relative fluorescence (α) of readout segments ± standard deviation for n=3 trials**.**

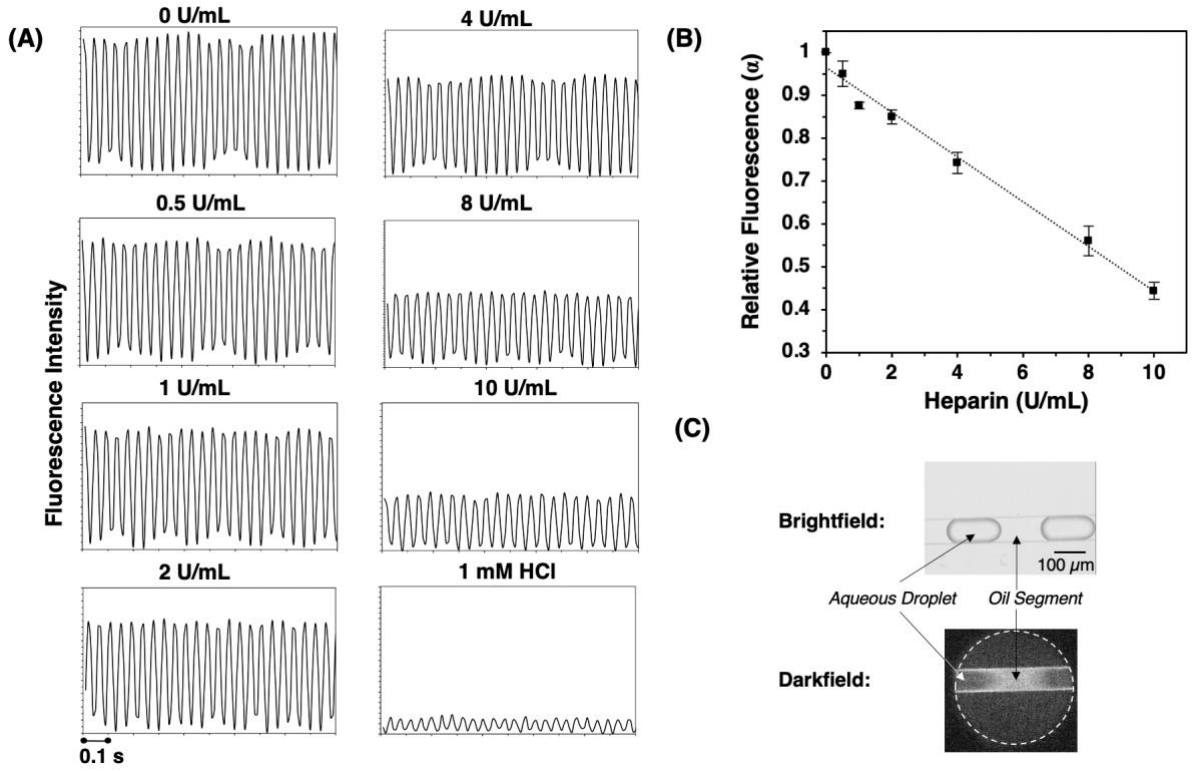

Figure 2.5. (A) Fluorescence traces of segmented flow during a 1.0 second interval (n=1) (excitation: 470/40 nm; emission: 500 - 550 nm) (B) Response curve of 200 µM CH XI/300 µM TDMACl readout phase toward heparin in 100 mM Tris-HCl/20 mM Tris buffer (pH = 7.4). Data points represent average relative fluorescence (α) ± standard deviation for n=3 trials (C) Bright and dark field images of segmented flow in a microfluidic device

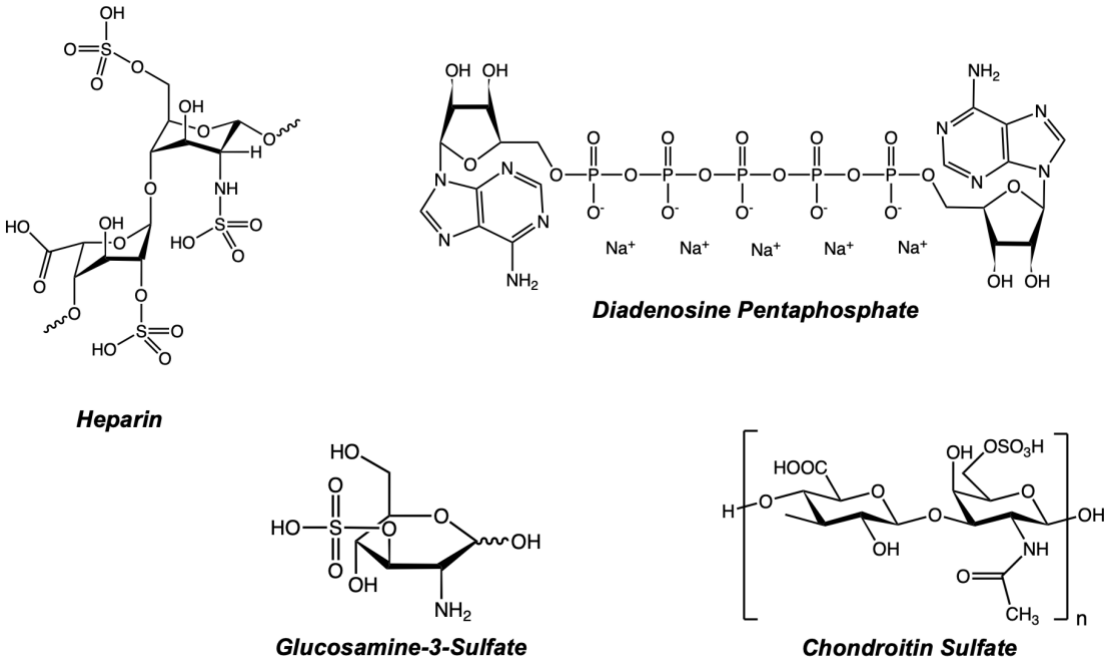

Figure 2.6. Chemical structures of polyanions and charged fragments measured in polyanionic compound study.

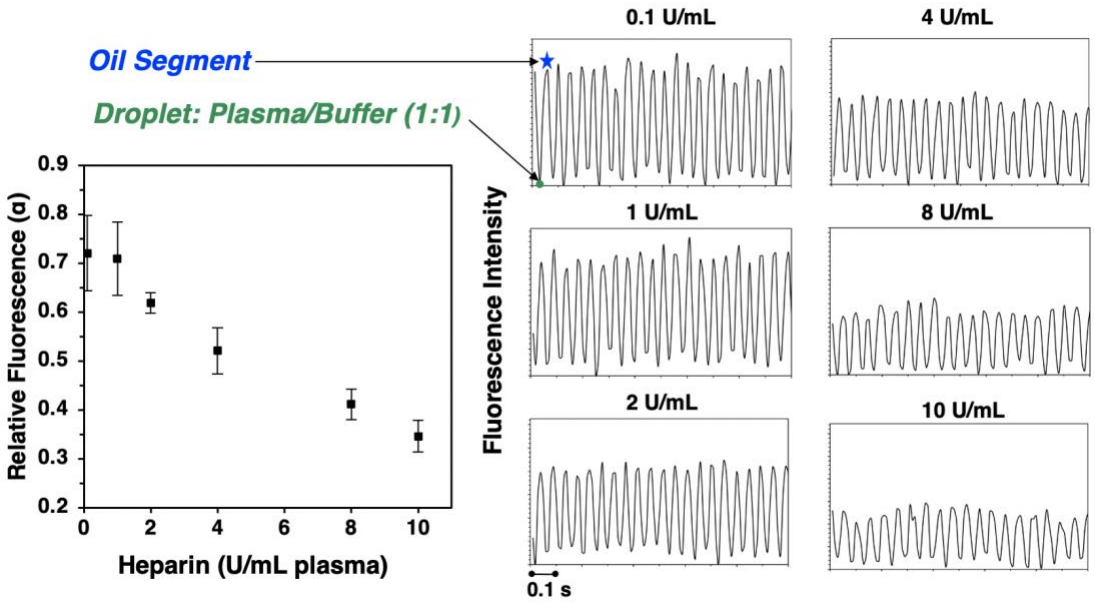

Figure 2.7. (A) Response curve of 200 µM CH XI/300µM TDMACl sensing oil phase towards heparin in half-fold diluted plasma samples. Data points represent average relative fluorescence (α) ± standard deviation for n=3 trials (B) Fluorescence traces of segmented flow at respective heparin concentration.

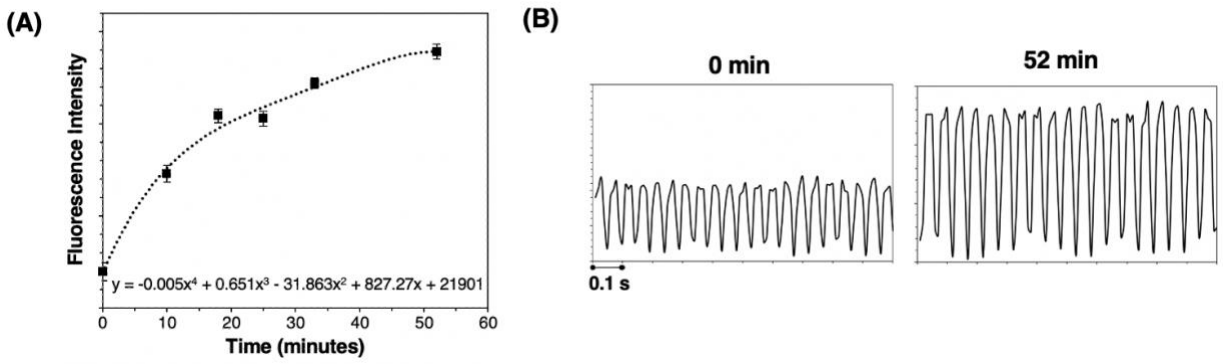

Figure 2.8. Analysis of chromoionophore-PDMS interactions respective to time. (A) Data points at each time point are an average fluorescence ± S.D for n ≥ 19 readout segments interacting with Tris-HCl/Tris buffer (pH=7.4) over a 1.0 second interval. (B) Fluorescence traces of segmented flow at initial and final time points. A distinct height difference exists between the fluorescence traces collected at the initial and final time points, indicating chemical interaction of CH XI with PDMS fabricated devices. Unused devices were first conditioned with segmented flow consisting of a heparin-less aqueous sample and readout phase for 45 minutes to minimize effects from PDMS-CH XI interactions.

2.6 References

(1) Kikkar, V. V.; Nicolaïdes, A. N.; Field, E. S.; Flute, P. T.; Wessler, S.; Yin, E. T. Low Doses of Heparin in Prevention of Deep-Vein Thrombosis. *Lancet* **1971**, *298* (7726), 669–671.

(2) Monagle, P.; Studdert, D. M.; Newall, F. Infant Deaths Due to Heparin Overdose: Time for a Concerted Action on Prevention. *J. Paediatr. Child Health* **2012**, *48* (5), 380–381. https://doi.org/10.1111/j.1440-1754.2011.02127.x.

(3) Liu, H.; Zhang, Z.; Linhardt, R. J. Lessons Learned from the Contamination of Heparin. *Nat. Prod. Rep.* **2009**, *26* (3), 313–321. https://doi.org/10.1039/b819896a.

(4) Kamal, A. H.; Tefferi, A.; Pruthi, R. K. How to Interpret and Pursue an Abnormal Prothrombin Time, Activated Partial Thromboplastin Time, and Bleeding Time in Adults. *Mayo Clin. Proc.* **2007**, *82* (7), 864–873. https://doi.org/10.4065/82.7.864.

(5) Hakim, N. S.; Canelo, R. *Haemostasis in Surgery*; **2007**. https://doi.org/10.1142/P467.

(6) Ma, S. C.; Yang, V. C.; Meyerhoff, M. E. Heparin-Responsive Electrochemical Sensor: A Preliminary Study. *Anal. Chem.* **1992**, *64* (6), 694–697. https://doi.org/10.1021/ac00030a023.

(7) Ma, S. C.; Yang, V. C.; Fu, B.; Meyerhoff, M. E. Electrochemical Sensor for Heparin: Further Characterization and Bioanalytical Applications. *Anal. Chem.* **1993**, *65* (15), 2078–2084. https://doi.org/10.1021/ac00063a024.

(8) Fu, B.; Bakker, E.; Yun, J. H.; Yang, V. C.; Meyerhoff, M. E. Response Mechanism of Polymer Membrane-Based Potentiometric Polyion Sensors. *Anal. Chem.* **1994**, *66* (14), 2250–2259. https://doi.org/10.1021/ac00086a009.

(9) Dybko, A. Errors in Chemical Sensor Measurements. *Sensors* **2001**, *1* (1), 29–37. https://doi.org/10.3390/s10100029.

(10) Wang, E.; Meyerhoff, M. E.; Yang, V. C. Optical Detection of Macromolecular Heparin Via Selective Coextraction into Thin Polymeric Films. *Anal. Chem.* **1995**, *67* (3), 522–527. https://doi.org/10.1021/ac00099a007.

(11) Kim, S. B.; Kang, T. Y.; Cha, G. S.; Nam, H. Quantitative Determination of Heparin Levels in Serum with Microtiter Plate-Format Optode. *Anal. Chim. Acta* **2006**, *557* (1–2), 117–122. https://doi.org/10.1016/j.aca.2005.10.053.

(12) Kim, S. B.; Cho, H. C.; Cha, G. S.; Nam, H. Microtiter Plate-Format Optode. **1998**, *70* (22), 4860–4863.

(13) Chen, Q.; Li, X.; Wang, R.; Zeng, F.; Zhai, J.; Xie, X. Rapid Equilibrated Colorimetric Detection of Protamine and Heparin: Recognition at the Nanoscale Liquid-Liquid Interface. *Anal. Chem.* **2019**, *91* (16), 10390–10394.

https://doi.org/10.1021/acs.analchem.9b01654.

(14) Wang, X.; Mahoney, M.; Meyerhoff, M. E. Inkjet-Printed Paper-Based Colorimetric Polyion Sensor Using a Smartphone as a Detector. *Anal. Chem.* **2017**, *89* (22), 12334–12341. https://doi.org/10.1021/acs.analchem.7b03352.

(15) Wheeler, A. R.; Throndset, W. R.; Whelan, R. J.; Leach, A. M.; Zare, R. N.; Liao, Y. H.; Farrell, K.; Manger, I. D.; Daridon, A. Microfluidic Device for Single-Cell Analysis. *Anal. Chem.* **2003**, *75* (14), 3581–3586. https://doi.org/10.1021/ac0340758.

(16) Joensson, H. N.; Andersson Svahn, H. Droplet Microfluidics-A Tool for Single-Cell Analysis. *Angew. Chemie - Int. Ed.* **2012**, *51* (49), 12176–12192. https://doi.org/10.1002/anie.201200460.

(17) Zilionis, R.; Nainys, J.; Veres, A.; Savova, V.; Zemmour, D.; Klein, A. M.; Mazutis, L. Single-Cell Barcoding and Sequencing Using Droplet Microfluidics. *Nat. Protoc.* **2017**, *12* (1), 44–73. https://doi.org/10.1038/nprot.2016.154.

(18) Kang, D. K.; Monsur Ali, M.; Zhang, K.; Pone, E. J.; Zhao, W. Droplet Microfluidics for Single-Molecule and Single-Cell Analysis in Cancer Research, Diagnosis and Therapy. *TrAC - Trends Anal. Chem.* **2014**, *58*, 145–153. https://doi.org/10.1016/j.trac.2014.03.006.

(19) Pandey, C. M.; Augustine, S.; Kumar, S.; Kumar, S.; Nara, S.; Srivastava, S.; Malhotra, B. D. Microfluidics Based Point-of-Care Diagnostics. *Biotechnol. J.* **2018**, *13* (1), 1–11. https://doi.org/10.1002/biot.201700047.

(20) Hassan, S. U.; Nightingale, A. M.; Niu, X. Continuous Measurement of Enzymatic Kinetics in Droplet Flow for Point-of-Care Monitoring. *Analyst* **2016**, *141* (11), 3266–3273. https://doi.org/10.1039/c6an00620e.

(21) Doonan, S. R.; Bailey, R. C. K-Channel: A Multifunctional Architecture for Dynamically Reconfigurable Sample Processing in Droplet Microfluidics. *Anal. Chem.* **2017**, *89* (7), 4091–4099. https://doi.org/10.1021/acs.analchem.6b05041.

(22) Baret, J. C.; Miller, O. J.; Taly, V.; Ryckelynck, M.; El-Harrak, A.; Frenz, L.; Rick, C.; Samuels, M. L.; Hutchison, J. B.; Agresti, J. J.; et al. Fluorescence-Activated Droplet Sorting (FADS): Efficient Microfluidic Cell Sorting Based on Enzymatic Activity. *Lab Chip* **2009**, *9* (13), 1850–1858. https://doi.org/10.1039/b902504a.

(23) Mazutis, L.; Gilbert, J.; Ung, W. L.; Weitz, D. A.; Griffiths, A. D.; Heyman, J. A. Single-Cell Analysis and Sorting Using Droplet-Based Microfluidics. *Nat. Protoc.* **2013**, *8* (5), 870–891. https://doi.org/10.1038/nprot.2013.046.

(24) Sjostrom, S. L.; Bai, Y.; Huang, M.; Liu, Z.; Nielsen, J.; Joensson, H. N.; Andersson Svahn, H. High-Throughput Screening for Industrial Enzyme Production Hosts by Droplet Microfluidics. *Lab Chip* **2014**, *14* (4), 806–813. https://doi.org/10.1039/c3lc51202a.

(25) Wang, X.; Sun, M.; Ferguson, S. A.; Hoff, J. D.; Qin, Y.; Bailey, R. C.; Meyerhoff, M. E.

Ionophore-Based Biphasic Chemical Sensing in Droplet Microfluidics. *Angew. Chemie - Int. Ed.* **2019**, *58* (24), 8092–8096. https://doi.org/10.1002/anie.201902960.

(26) Wang, X.; Zhang, Q.; Nam, C.; Hickner, M.; Mahoney, M.; Meyerhoff, M. E. An Ionophore-Based Anion-Selective Optode Printed on Cellulose Paper. *Angew. Chemie - Int. Ed.* **2017**, *56* (39), 11826–11830. https://doi.org/10.1002/anie.201706147.

(27) Malinowska, E.; Manzoni, A.; Meyerhoff, M. E. Potentiometric Response of Magnesium-Selective Membrane Electrode in the Presence of Nonionic Surfactants. *Anal. Chim. Acta* **1999**, *382* (3), 265–275. https://doi.org/10.1016/S0003-2670(98)00802-2.

(28) Qin, Y.; Bakker, E. Quantitive Binding Constants of H+-Selective Chromoionophores and Anion Ionophores in Solvent Polymeric Sensing Membranes. *Talanta* **2002**, *58* (5), 909–918. https://doi.org/10.1016/S0039-9140(02)00405-8.

(29) Qiao, M.; Lin, L.; Xia, K.; Li, J.; Zhang, X.; Linhardt, R. J. Recent Advances in Biotechnology for Heparin and Heparan Sulfate Analysis. *Talanta* **2020**, *219* (May), 121270. https://doi.org/10.1016/j.talanta.2020.121270.

(30) La, C. C.; Takeuchi, L. E.; Abbina, S.; Vappala, S.; Abbasi, U.; Kizhakkedathu, J. N. Targeting Biological Polyanions in Blood: Strategies toward the Design of Therapeutics. *Biomacromolecules* **2020**, *21* (7), 2595–2621. https://doi.org/10.1021/acs.biomac.0c00654.

(31) Fu, B.; Bakker, E.; Yang, V. C.; Meyerhoff, M. E. Extraction Thermodynamics of Polyanions into Plasticized Polymer Membranes Doped with Lipophilic Ion Exchangers: A Potentiometric Study. *Macromolecules* **1995**, *28* (17), 5834–5840. https://doi.org/10.1021/ma00121a021.

(32) Buzzega, D.; Maccari, F.; Volpi, N. Determination of Molecular Mass Values of Chondroitin Sulfates by Fluorophore-Assisted Carbohydrate Electrophoresis (FACE). *J. Pharm. Biomed. Anal.* **2010**, *51* (4), 969–972. https://doi.org/10.1016/j.jpba.2009.10.015.

(33) Hankins, J. The Role of Albumin in Fluid and Electrolyte Balance. *J. Infus. Nurs.* **2006**, *29* (5), 260–265. https://doi.org/10.1097/00129804-200609000-00004.

(34) Timerga, A.; Kelta, E.; Kenenisa, C.; Zawdie, B.; Habte, A.; Haile, K. Serum Electrolytes Disorder and Its Associated Factors among Adults Admitted with Metabolic Syndrome in Jimma Medical Center, South West Ethiopia: Facility Based Crossectional Study. *PLoS One* **2020**, *15* (11 November), 1–16. https://doi.org/10.1371/journal.pone.0241486.

(35) Wetzler-Quevedo, S. P.; Meyerhoff, M. E.; Bailey, R. C. Characterization of the Impact of Mixing and Droplet Volumes on the Behavior of Microfluidic Ion-Selective Droptodes. *Analyst* **2021**, *146* (16), 5095–5101. https://doi.org/10.1039/d1an00733e.

Chapter 3 – Implementation of a Lipophilic Fluorescein Derivate for Analysis on the Effects of Reaction Time and Phase Ratio on Response of Protamine-Sensitive Droptodes

Acknowledgments

This work was supported in part by the National Institute of Health Microfluidics in Biomedical Sciences Training Program (T32EB005582).

Abstract

Protamine – a polycationic molecule – has remained as one of the most commonly used and reliable antagonists to anticoagulative heparin for nearly a century. Having significant pharmaceutical relevance, several methods for protamine sensing have been developed including mass spectrometry, HPLC, electrodes, and optical sensors. Ionophore based droplet microfluidics or "microfluidic droptodes" have been implemented as an alternative method for quantitation of protamine amounts (µg/mL) in aqueous droplets (100s of pL) correspondent to fluorescence of neighboring readout segments. Despite their utility, sensing reagents have only been demonstrated to be responsive at low concentrations and when dissolved in dichloroethane, a toxic organic solvent that is incompatible with PDMS devices. This study incorporates a lipophilic fluorescein derivative (CH VI) as an alternative reagent for biphasic sensing of protamine via bulk and microfluidic methods. Concomitantly, the effects of aqueous to readout phase ratios and reaction time on droptode response are extensively studied by these macro- and micro- techniques, revealing intrinsic information on protamine-CH VI complex stability.

3.1 Introduction

Protamine, a polypeptide consisting of approximately 32 amino acids, is an electrostatic agent active in various biochemical and medicinal reactions. With involvement in several key processes including diabetes management[1,2] and stabilization of DNA in male reproductive cells[3,4], it is most known for its usage in clinical settings as the only U.S. FDA approved heparin reversal agent.[5] Blood clotting assays, such as the activated clotting time (ACT)[6] and activated partial thromboplastin time (aPTT)[7], exist as the gold standard for clinicians, yet they are dependent on time-based effects of heparin-protamine administration as the readout rather than quantitative amounts. This presents a significant analytical challenge as several technologies including electrochemical sensors[8,9], high performance liquid chromatography[10], and mass spectrometry[11] have been developed to address this limitation. Additionally, optical sensors functionalized by colorimetric[12–15] and fluorescent dyes[16–19] exist as an alternative method for user-friendly and configurable measurements.

Ionophore-based droplet microfluidics or "microfluidic droptodes" have emerged as a novel technique for both single ion and macromolecule sensing. This method utilizes multiple segments of organic solvent concentrated with various combinations of ionophore, ion-exchanger, and chromoionophore to fluorescently determine the concentration of target analyte per *adjacent*, aqueous droplet (sub nanoliter).[20] For protamine detection, fluorescent readout segments are functionalized by dinonylnaphthalene sulfonic acid as the ion-exchanger, which protonates the chromoionophore and complexes with protamine extracted from the aqueous droplet.[20] Protamine concentrations were detected within clinically relevant ranges (1 – 100 µg/mL) using this sensing mechanism, with selectivity over physiological concentrations of mono- and divalent electrolytes. Despite its sensitive response towards protamine, background

fluorescence is prevalent, likely due low concentration of chromoionophore (i.e., 5 μM) in adjacent readout segments. Additionally, incorporated reagents are dissolved in dichloroethane – a toxic, volatile solvent demonstrated to highly permeate the polydimethylsiloxane (PDMS) material in which microfluidic devices are fabricated.[21–24]

Alternatively, lipophilic fluorescein derivatives (LFDs) exist as fluorescent probes capable of analysis in environments of varying polarity. These molecules generally consist of a fluorescein-like compound attached to a long hydrocarbon chain ($CH_3(CH_2)_n$: $n \geq 10$) which allows for the molecule to be amphiphilic in its entirety.[25,26] Similar to their hydrophilic counterpart, the fluorescence of these molecules is directly correlated to their ionic states.[27] Initial polycation-sensitive, ion-selective optodes incorporated LFDs as a three-in-one ionophore, chromoionophore, and ion-exchanger in which cation exchange between protamine and protons from fluorescein was shown to generate measurable changes in absorbance of polymeric films.[28] Most recently, emulsified nanospheres containing LFDs were utilized for protamine sensing[29], a promising deviation from traditional bulk substrate sensors. However, the possibility of using LFDs for protamine sensing in droplet microfluidic, biphasic sensors has not yet been explored.

Individual microfluidic droptodes can most simply be characterized as miniaturized liquid-liquid extractions (LLEs), in which partitioning of analyte from the aqueous droplet induces a color change of an immiscible organic phase concentrated with chromoionophore molecules. While bulk aqueous-organic phase extractions operate on a similar principle as microfluidic droptodes, they have not been extensively explored as a contiguous method to such. Given their similarities, the utilization of bulk LLEs to investigate alternate protamine sensing chemistries such as the classical LFD mechanism previously described is of high interest. Herein, bulk LLEs are incorporated as a preliminary tool for implementation of an LFD-based,

protamine sensing chemistry into microfluidic droptodes. Furthermore, the effect of reaction time and aqueous-organic phase ratio on response toward protamine are separately explored in specified micro- and macro- systems.

3.2 Experimental Methods

3.2.1 Chemicals and Materials

Protamine sulfate salt from salmon (Grade X), bis(2-ethylhexyl) sebacate (DOS), and sodium tetrakis[3,5-bis(trifluoromethyl)phenyl]borate (NaBARF) were purchased from Sigma Aldrich. 4', 5' – Dibromo fluorescein octadecyl ester (CH VI) was purchased from CymitQuimica. 0.75 mm biopsy punches were purchased from World Precision Instruments Inc. and 30-gauge PTFE tubing from Cole-Parmer. Tris was purchased from Fisher Scientific. Devices were made using a microfabrication process consisting of photolithography and soft lithography with standard reagents and materials as previously described.[30] Inlet and outlets of fabricated T-Channel devices were punched using a 0.75 mm biopsy punch and bound to glass slide coated with a thin layer of PDMS. Channels were 80 µm in depth with a 64 µm width aqueous channel, intersecting perpendicularly with an 80 µm width oil carrying channel.

3.2.2 Bulk and Microfluidic Droptode Experiments

All protamine samples were diluted from a 1000 µg/mL protamine stock solution prepared in 10 mM Tris-HCl (pH 7.4) buffer. Respective amounts of CH VI and NaBARF were completely dissolved in DOS organic solvent via sonication to make 1000 µM stocks. For protamine measurements, a readout phase of 200 µM CH VI and 400 µM NaBARF was employed. For bulk droptode experiments, a 0.6-mL Eppendorf tube containing specified ratios of aqueous sample and protamine-sensitive readout phase, was vortexed at specified times at

3000 rpm using a Fisher Scientific Digital Vortex Mixer. Eppendorf tubes were centrifuged for 10 seconds by sets of six (i.e., per trial) to separate the aqueous and readout phases. A Tecan Infinite® F500 well plate reader was used to measure the fluorescence ($\lambda_{excitation}$= 485/10 nm, $\lambda_{emission}$= 522.5 – 547.5 nm) of 100 µL of the reacted readout phase, extracted from each respective Eppendorf tube.

A home-built pressure system as previously described[31] was used to generate segmented flow for on-device experiments. Readout and aqueous phase pressures were maintained around 75 kPa to manipulate droplet sizes relative to readout segments. A VEO 640L high speed camera (Vision Research Inc.) connected to a DMi8 light microscope (Leica Microsystems) was used to image the device and capture videos of segmented flow. For excitation of CH VI, the device was exposed to a light source (Lumen 200, Prior Scientific) passing through a GFP filter cube (excitation: 470/40 nm; emission: 500 – 550 nm). Videos of generated segments in bright and dark field modes were collected at 100 frames per second, with a 9.9 ms exposure time. Fluorescence intensity of segmented flow was measured 45 mm from the T-junction of the device, unless otherwise noted and quantitated using an Image J (NIH) macro code. Data points were calculated as average fluorescence intensity (± S.D) of local maxima corresponding to readout segments interacting with sample-containing droplets.

3.3 Results and Discussion

3.3.1 Lipophilic Fluorescein Derivative for Protamine Sensing

To quantitatively compare the effect of various parameters on readout phase (i.e., organic phase) sensitivity toward protamine, initial bulk experiments were conducted taking the ionic state of CH VI before and after polycation interaction into consideration:

$$C_n^- + Protamine^+ \rightarrow C_n - Protamine$$

(C_n^-) and (C_n) are representative of chromoionophore molecules in their deprotonated and complexed states, respectively. The reaction quotient (Q) results from this, in which:

$$(Q) = \frac{C_n - Protamine}{C_n^- + Protamine^+}$$

As protamine – chromoionophore complexes (C_n – Protamine) and deprotonated chromoionophore molecules are the primary species in the reaction:

$$Relative\ Degree\ of\ Complexation = 1 - \frac{C_n - Protamine}{Total\ C^-\ Sites} = 1 - \frac{F_{sample} - F_{100}}{F_0 - F_{100}}$$

where F_0 and F_{100} are representative of the maximum and minimum levels of fluorescence in the system, or buffer and 100 µg/mL sample, respectively. CH VI demonstrates surfactant-like behavior when complexed with protamine **(Figure 3.1)**, thus the following schematic in **Figure 3.2** was established as a fundamental sensing model.

3.3.2 Effect of Phase Ratio on Bulk Droptode Response

A unique feature of microfluidic droptodes lies within the ability of aqueous phase volumes to be adjusted relative to the adjacent readout segments in a high throughput manner. That is, the stochiometric ratio of target analyte to binding sites can be increased or decreased as a means to tune the linear response range.[30] Furthermore, previous works have demonstrated that the distance the readout segment has traversed on the device, or reacted with adjacent sample, can drastically alter response.[20,32] As the effects of aqueous to readout phase ratio and reaction time have only been studied for single-ion sensing in biphasic, droplet microfluidic systems, bulk LLEs were first implemented to study such towards macromolecular protamine.

Conditions were inferred for phase ratio studies based on the amount of aqueous volume relative to volume of readout phase. Aqueous volumes 1× and 3× relative in magnitude to readout segment volumes were considered as balanced and oversaturating conditions,

respectively, whereas under-saturating conditions were synonymous with aqueous volumes 4x smaller in size. Notably, each phase ratio revealed unique information on the stability and formation of protamine-CH VI complexation chemistry (**Table 3.1**). For protamine concentrations in the 0 – 10 µg/mL range, the largest change in response, and thus most sensitive, were observed for under saturating conditions. However, measurements at these conditions also produced the largest error, magnitudes higher than either other condition, indicating that protamine-chromoionophore complexes (protamine-CH VI) are weakly forming due to limited amounts of sample in the aqueous phase. The balanced phase ratio condition results in the lowest error, but it is slightly less sensitive than the under saturating condition. Thus, the formation of stable protamine-CH VI complexes at the balanced phase ratio was determined to be the most favorable.

The over saturating phase ratio produced the lowest sensitivity relative to the other listed conditions in the 0 – 10 µg/mL concentration range but the largest response at 50 µg/mL. Oversaturating the readout phase with 50 µg/mL protamine appeared to be the only case which aligned with expected trends. Overall, the bulk phase ratio study produced unique responses and variations at respective concentrations, though alignment with the expected trend of increase in readout response with aqueous to organic phase ratio was not observed in all cases. Results also demonstrate how aqueous sample volume relative to readout phase can drastically impact the formation of stable protamine-CH VI complexes which can be tied to the varying amount of error associated with each phase condition at different concentrations.

3.3.3 Analysis of Reaction Time on Bulk Droptode Response

Bulk droptodes were next employed to study the effects of reaction time on overall sensitivity. As the balanced condition produced the most stable protamine-CH VI complexes at

lower concentrations (0 – 10 µg/mL) with additional sensitivity at 50 µg/mL, it was implemented as a fixed condition for further bulk experiments. Unlike phase ratio experiments, increasing amounts of the independent variable (i.e., vortex time) produced a trend-following response (**Figure 3.3**). The most sensitivity was exhibited in the 0 – 10 µg/mL range for the 10 second vortex time, referenced from the balanced condition in **Table 3.1**, respective to the other two reaction times. At vortex times of 15 seconds, response within the same concentration range began to decrease, though a ~1.5× higher response occurred at 50 µg/mL. Notably, at both 10 and 15 second vortex times, large deviations (≥ ±16%) occurred at 50 µg/mL concentrated samples, indicating weak interactions between protamine and CH VI.

When phases were reacted for 30 seconds, further characteristics about the stability protamine-CH VI complexes were revealed. Fluorescence response towards samples in the 0 – 10 µg/mL range continued to decrease relative to both 10 and 15 second reaction times. This suggests that protamine-CH VI complexes may not be stable at low concentrations, though the low amount of error associated with measurements made at 1 and 10 µg/mL indicates weakly interacting complexes dissociate with longer reaction times. The latter is further evidenced by measurements made at 50 µg/mL, which possessed an error ~4x lower in magnitude relative to responses seen at the same concentration with shorter reaction times. Conclusively, for bulk droptodes, response in the 0 – 10 µg/mL range decreased with lengthened reaction times, though measurements are the most reproducible in this case. Such experiments reinforced our fundamental understanding of the response of the protamine-sensitive readout phase at several conditions, providing a basis for initial droplet microfluidic experiments.

3.3.4 Protamine-Sensitive Microfluidic Droptodes

Previous works have demonstrated microfluidic liquid-liquid extractions to be orders of magnitude faster than bulk extractions[33]. Thus, the fluorescence of protamine-sensitive readout segments was used to quantitatively compare the effects of phase ratio and reaction time on response. Though we expected the protamine-CH VI complexation chemistry from bulk experiments (**Figure 3.1**) to remain relatively similar to on-device experiments (**Figure 3.2**), we sought to compare the effects of such parameters separately from bulk droptode experiments, where phase volumes magnitudes (hundreds of thousands) larger than microfluidic droptodes. For reference, an increase in the amount of protamine-CH VI complex or deprotonated CH VI, produces decreases in fluorescence. Changing the size of the aqueous droplet relative to the readout segment led to distinct changes in the fluorescence signal intensity of adjacent readout segments and the overall sensitivity (**Figure 3.4**). As expected, increasing the aqueous to readout phase ratio led to decreases in fluorescence for each respective protamine concentration, a result of increasing amounts of deprotonated CH VI relative to larger sample volumes.

Using slope as reference for overall sensitivity, readout segments generated in the undersaturated system produced the lowest response towards aqueous droplets due to the limited amount of protamine in restricted sample volumes, while readout segments in the oversaturated system produced a much higher response towards increasing amounts of sample. Notably, readout segments in the balanced system were the most responsive towards protamine, a deviation from expected trends. Such could likely be due to the formation of protamine-CH VI complexes within the microfluidic channel (**Figure 3.6**) which appear to impact aqueous droplet frequencies (**Figures 3.7 and 3.8, Table 3.2)** of samples concentrated with ≥50 μg/mL protamine. CH VI molecules demonstrate surfactant-like behavior with protamine in bulk droptodes (**Figure 3.1**), so the accumulation of protamine-CH VI complexes along the interface

of the aqueous droplets, specifically in the oversaturating system, may be a contributing source of error to the observed deviation.

3.3.5 Droplet Microfluidic Distance Study

Lastly, to study the effects of reaction time on readout phase response for microfluidic experiments, a distance study using balanced phase ratios was employed. Five-millimeter increments marked on the device allowed for micro reactions to be monitored at ten different points for each respective protamine concentration (**Figure 3.5**). For 1 µg/mL samples, average fluorescence signal began to equilibrate after readout segments had traveled only a third of the total distance on the microfluidic device. However, the signal slightly fluctuated throughout the next several points indicating protamine-CH VI complexes are continuously forming and disassociating as segments traverse the channel. Similarly, the largest overall decrease in fluorescence in 50 µg/mL protamine-containing droplets occurred between distances of 0 and 15 mm. The signal appears to steadily decrease between 15 and 30 mm and steadily increase from 30 mm to the end of the device. Considering the larger amount of protamine encapsulated in aqueous droplets, achieving a stable signal may require extended reaction time. Furthermore, error associated with fluorescence measurements from readout segments interacting with 50 µg/mL samples is much lower, indicating a proportionally higher amount of tightly bound protamine-CH VI complexes.

3.4 Conclusions

In conclusion, bulk and microfluidic protamine-sensitive droptodes were incorporated to study the effects of phase ratios and reaction times on readout phase response. Though fundamentally the same, differences in parameters employed in each, such as volume (100s of

μL vs 100s of pL) and total reaction time (tens of seconds vs seconds), highlight how readout phase responsiveness changes on macro- and micro- scales. Notably, the surfactant-like interaction of CH VI with protamine was demonstrated in both methods indicating bulk droptodes as a useful tool for investigating chemistries previously untested on-device.

For bulk droptodes, changing the volume of readout phase relative to the aqueous phase volume caused drastic variations in the reproducibility of measurements at different protamine concentrations whereas lengthening reaction times lead to improvements in reproducibility. In microfluidic experiments, increasing aqueous to readout segment volume ratios allowed for fluorescence response toward protamine to be fine-tuned in the 0 – 100 μg/mL range based on calculated slope. Fluorescent measurements of readout segments interacting with protamine concentrated droplets at several distances on device show continuous fluctuation of protamine-CH VI complex formation with reaction time. For future work, protamine-sensitive readout phase should be implemented for detection of larger cationic molecules (i.e., > 5.1 kDa) as the higher amount of charged sites should increase the number of CH VI interactions. Furthermore, polycations of similar size with higher charge density may be considered suitable analytes of interest as well.

Aqueous: Readout Phase	Δ Relative D.O.C, Protamine (0 – 1 µg/mL)	Δ Relative D.O.C, Protamine (0 – 10 µg/mL)	Δ Relative D.O.C, Protamine (0 – 50 µg/mL)
0.25:1	0.06 (±0.10)	0.26 (±0.18)	0.75 (±0.11)
1:1	0.05 (±0.02)	0.17 (±0.05)	0.52 (±0.16)
3:1	-0.02 (±0.03)	0.13 (±0.08)	1.10 (±0.11)

Table 3.1. Effect of phase ratio on response of bulk LLE toward protamine. Response of bulk, protamine-sensitive droptode towards samples at various aqueous to readout phase volume ratios. Data points representative of average relative degree of complexation (D.O.C) ± standard deviation.

Aqueous: Readout Phase	Average Droplet Frequency (± S.D) (Hz)
Balanced	19 (±8)
Oversaturated	20 (±13)
Undersaturated	17 (±2)

Table 3.2. Average aqueous droplet frequency (Hz) for microfluidic phase ratio study. Stable droplet frequencies are most easily attained at undersaturated conditions whereas the largest variations occur at oversaturating conditions.

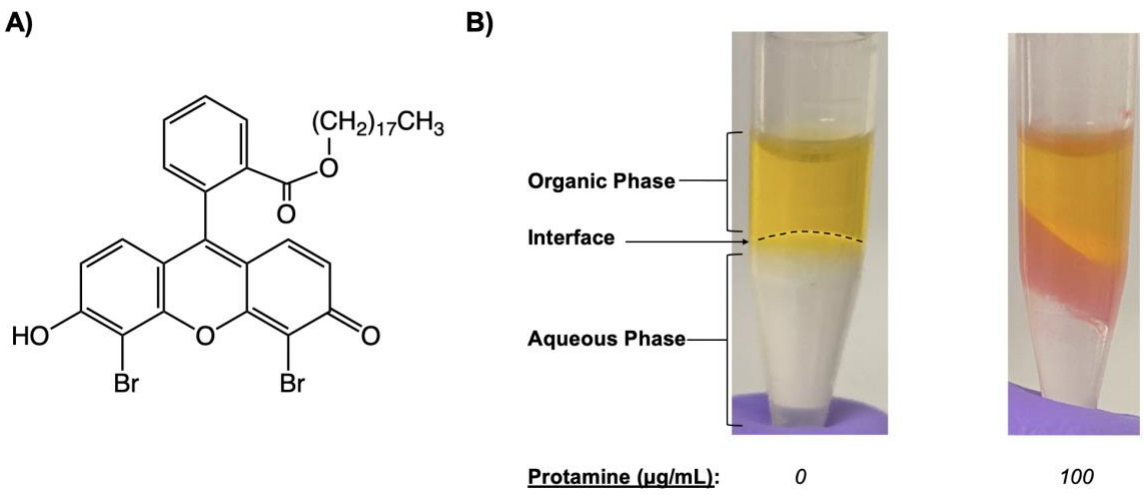

Figure 3.1. Overview of the interaction of lipophilic fluorescein derivative, chromoionophore VI and protamine within a bulk droptode system (A) Chemical structure of CH VI (B) Image of bulk droptode extraction between aqueous sample and readout phase after vigorous mixing and centrifugation.

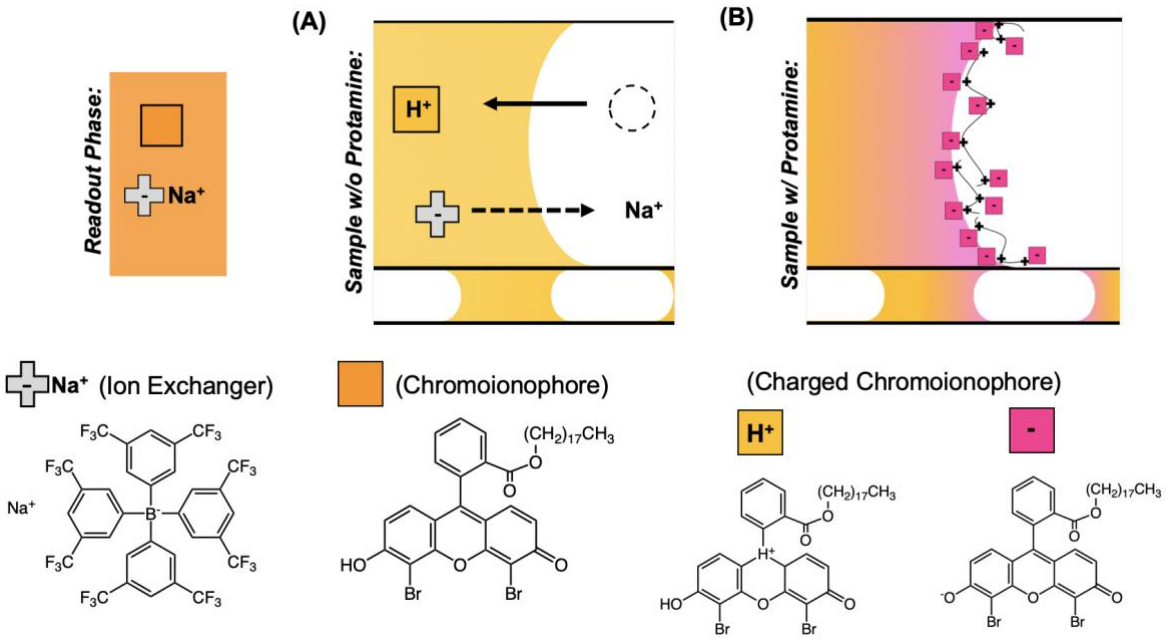

Figure 3.2. Schematic for protamine sensing with CH VI on a microfluidic droptode device (A) Proton dissociation from CH VI is suppressed as sodium ions migrate into the aqueous phase. Subsequently, CH VI is protonated via ion-exchange. (B) Protamine in sample complexes with deprotonated CH VI by electrostatic interaction.

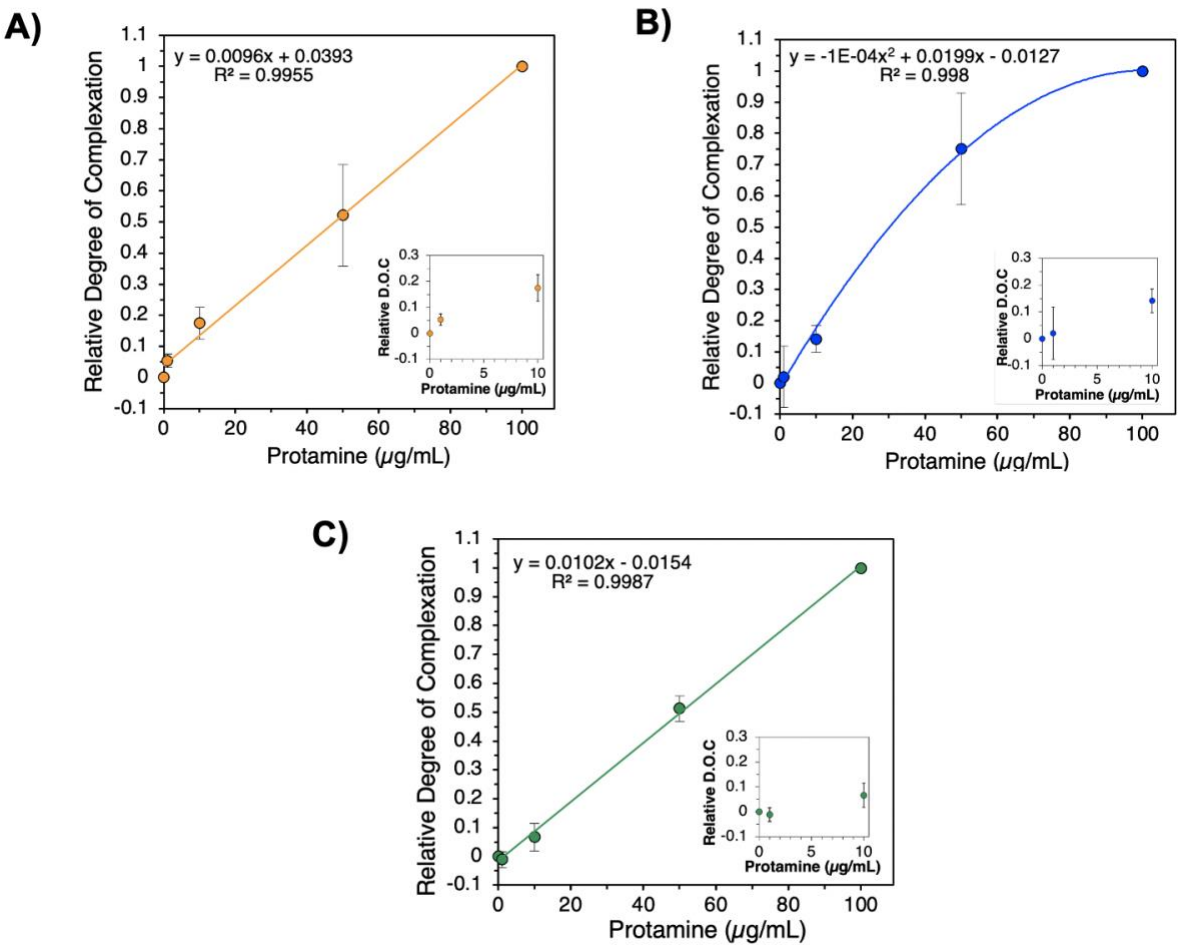

Figure 3.3. Bulk readout phase response towards various concentrations of protamine after vortex times of (A) 10 (B) 15 and (C) 30 seconds. Data points representative of average relative degree of complexation (D.O.C) ± standard deviation.

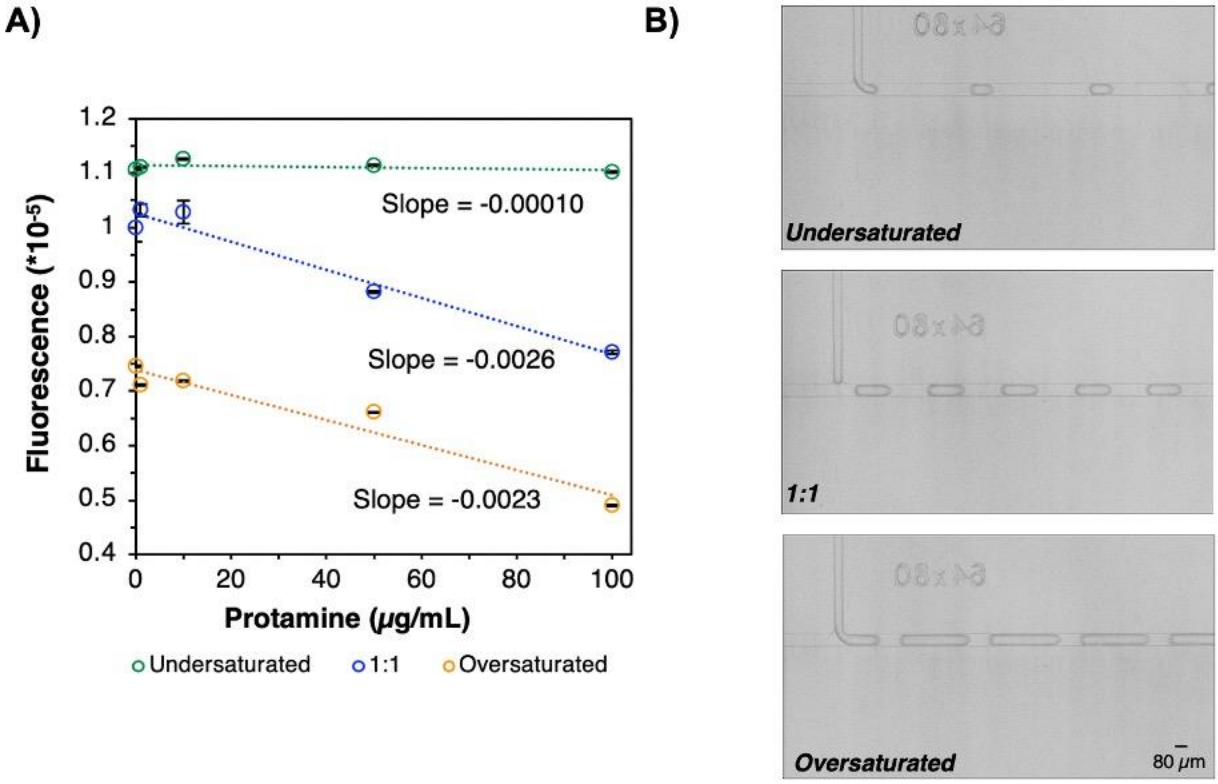

Figure 3.4. Segmented flow on a droplet microfluidic device at various droplet to readout segment ratios (A) The average fluorescence of protamine-sensitive readout segments interacting with aqueous droplets. Data points are representative of average readout segment fluorescence ± standard deviation. (B) Brightfield images of segmented flow at several droplet to readout segment ratios.

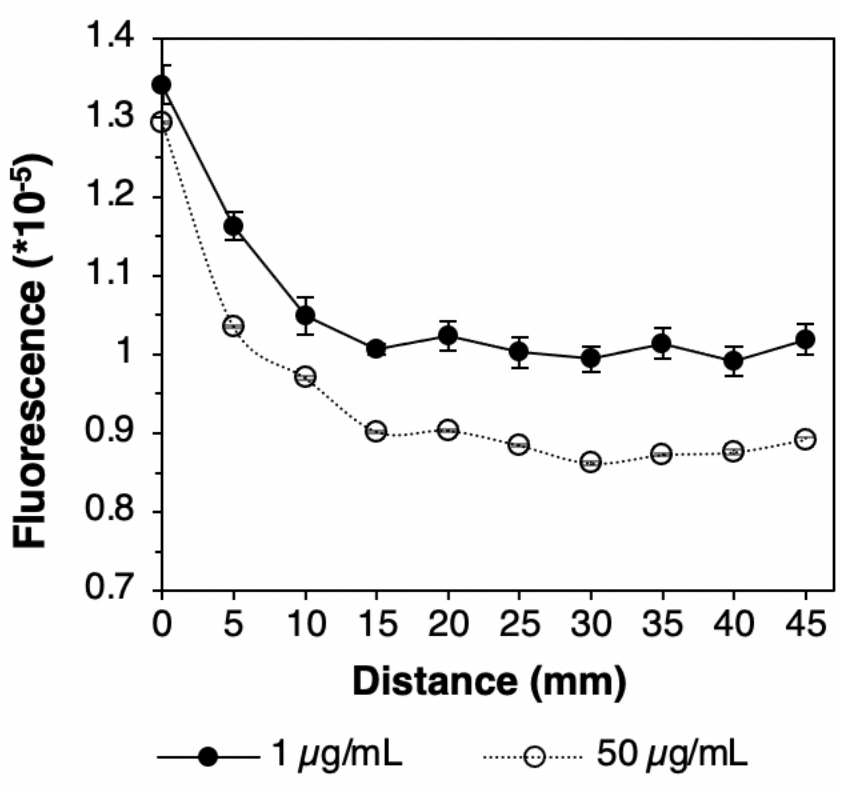

Figure 3.5. Average fluorescence of protamine-sensitive readout segments interacting with aqueous droplets at several distance points (mm) on a droplet microfluidic device. Data points are representative of average readout segment fluorescence ± standard deviation.

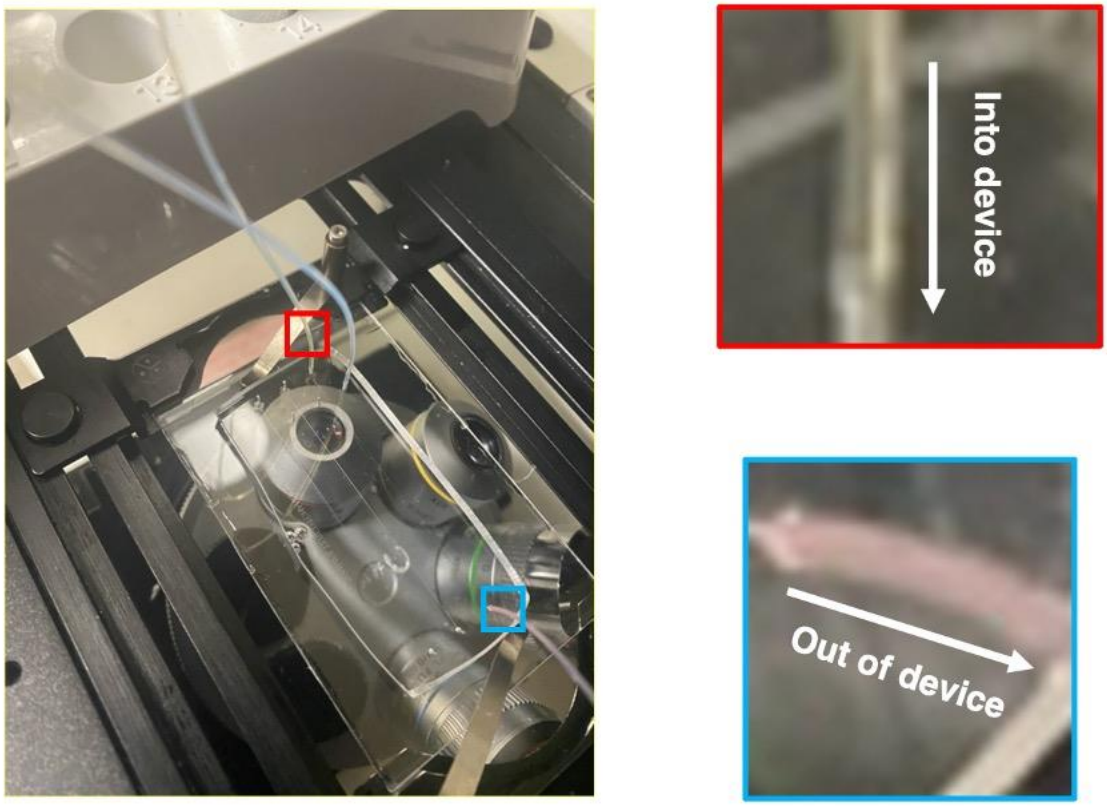

Figure 3.6. Interaction of protamine sample and readout phase on a droplet microfluidic device. Similar to bulk droptodes, the readout phase has an orange hue before entering the device. Upon reaction with protamine concentrated sample at the junction and traversing down the channel, readout segments exit the device with a pink-reddish hue.

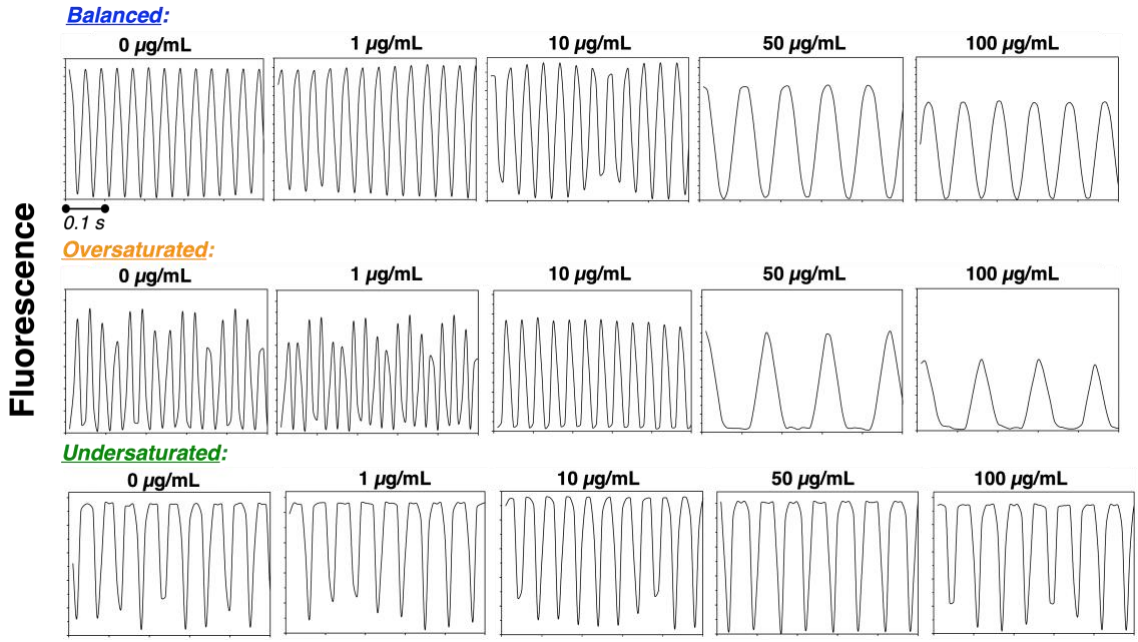

Figure 3.7. Fluorescence traces of segmented flow on a droplet microfluidic device for balanced, oversaturated, and undersaturated conditions. Fluctuations in signal at the base of peaks, considered as local maxima by the macro code were not included in average fluorescence intensity calculations. As these fluctuations were only observed within traces for oversaturating conditions it is likely that prevalent amounts of protamine-CH VI complexes are forming at the aqueous-organic interface in this case, leading to variations in fluorescence signal.

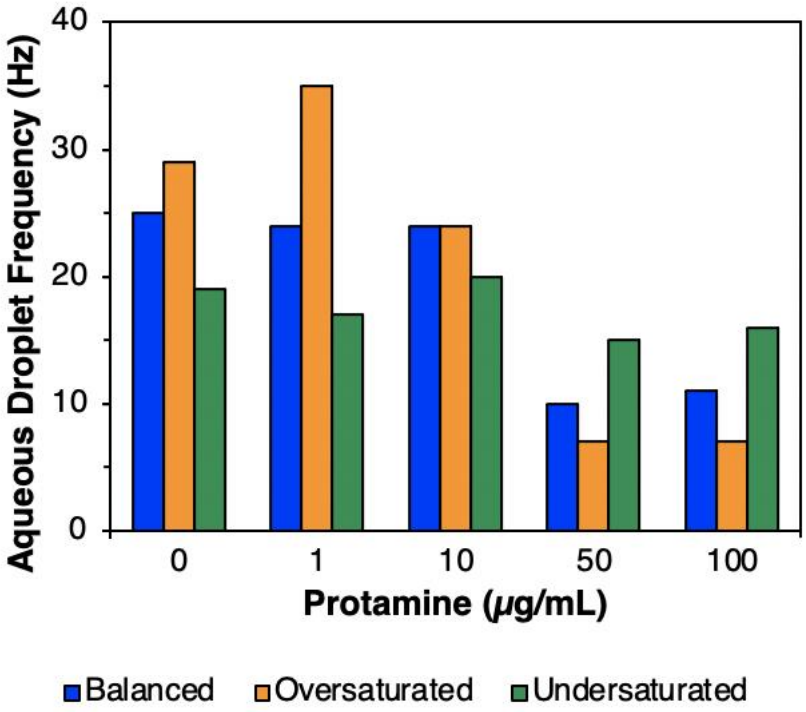

Figure 3.8. Effect of protamine concentration on droplet frequency (Hz) at various phase ratios. Aqueous droplet frequencies in balanced and oversaturated systems drastically decrease at protamine concentrations ≥50 μg/mL whereas undersaturated conditions remain relatively stable.

3.5 References

(1) Roach, P.; Trautmann, M.; Arora, V.; Sun, B.; Anderson, J. H. Improved Postprandial Blood Glucose Control and Reduced Nocturnal Hypoglycemia during Treatment with Two Novel Insulin Lispro-Protamine Formulations, Insulin Lispro Mix25 and Insulin Lispro Mix50. *Clin. Ther.* **1999**, *21* (3), 523–534. https://doi.org/10.1016/S0149-2918(00)88307-1.

(2) Nicolucci, A.; Ceriello, A.; Di Bartolo, P.; Corcos, A.; Orsini Federici, M. Rapid-Acting Insulin Analogues Versus Regular Human Insulin: A Meta-Analysis of Effects on Glycemic Control in Patients with Diabetes. *Diabetes Ther.* **2020**, *11* (3), 573–584. https://doi.org/10.1007/s13300-019-00732-w.

(3) Balhorn, R. The Protamine Family of Sperm Nuclear Proteins. *Genome Biol.* **2007**, *8* (9). https://doi.org/10.1186/gb-2007-8-9-227.

(4) Aoki, V. W.; Emery, B. R.; Liu, L.; Carrell, D. T. Protamine Levels Vary between Individual Sperm Cells of Infertile Human Males and Correlate with Viability and DNA Integrity. *J. Androl.* **2006**, *27* (6), 890–898. https://doi.org/10.2164/jandrol.106.000703.

(5) Pandey, S. P.; Jha, P.; Nadimetla, D. N.; Bhosale, S. V.; Singh, P. K. A Tetracationic Aggregation Induced Emission-Based Probe for Efficient and Improved Detection of Heparin. *Sensors Actuators B Chem.* **2022**, *353* (October 2021), 131016. https://doi.org/10.1016/j.snb.2021.131016.

(6) Culliford, A. T.; Gitel, S. N.; Starr, N.; Thomas, S. T.; Baumann, F. G.; Wessler, S.; Spencer, F. C. Lack of Correlation between Activated Clotting Time and Plasma Heparin during Cardiopulmonary Bypass. *Ann. Surg.* **1981**, *193* (1), 105–111. https://doi.org/10.1097/00000658-198101000-00017.

(7) Bates, S. M.; Weitz, J. I.; Johnston, M.; Hirsh, J.; Ginsberg, J. S. Use of a Fixed Activated Partial Thromboplastin Time Ratio to Establish a Therapeutic Range for Unfractionated Heparin. *Arch. Intern. Med.* **2001**, *161* (3), 385–391. https://doi.org/10.1001/archinte.161.3.385.

(8) Yun, J. H.; Meyerhoff, M. E.; Yang, V. C. Protamine-Sensitive Polymer Membrane Electrode: Characterization and Bioanalytical Applications. *Analytical Biochemistry*. 1995, pp 212–220. https://doi.org/10.1006/abio.1995.1032.

(9) Gadzekpo, V. P. Y.; Xiao, K. P.; Aoki, H.; Bühlmann, P.; Umezawa, Y. Voltammetric Detection of the Polycation Protamine by the Use of Electrodes Modified with Self-Assembled Monolayers of Thioctic Acid. *Anal. Chem.* **1999**, *71* (22), 5109–5115. https://doi.org/10.1021/ac990580m.

(10) Snycerski, A.; Dudkiewicz-Wilczynska, J.; Tautt, J. Determination of Protamine Sulphate in Drug Formulations Using High Performance Liuid Chromatography. *J. Pharm. Belg.* **1998**, *53* (3), 252.

(11) Srivatsa, K.; Gokhale, Y.; Chakrabarti, P. P.; Kulshrestha, A.; Vajpai, N. Simultaneous Characterization of Insulin HMWP and Protamine Sulphate in Complex Formulations through SEC-Coupled Mass Spectrometry. *J. Pharm. Biomed. Anal.* **2021**, *203*, 114188. https://doi.org/10.1016/j.jpba.2021.114188.

(12) Wang, X.; Mahoney, M.; Meyerhoff, M. E. Inkjet-Printed Paper-Based Colorimetric Polyion Sensor Using a Smartphone as a Detector. *Anal. Chem.* **2017**, *89* (22), 12334–12341. https://doi.org/10.1021/acs.analchem.7b03352.

(13) Kim, S. B.; Kang, T. Y.; Cho, H. C.; Choi, M. H.; Cha, G. S.; Nam, H. Determination of Protamine Using Microtiter Plate-Format Optodes. *Anal. Chim. Acta* **2001**, *439* (1), 47–53. https://doi.org/10.1016/S0003-2670(01)01003-0.

(14) Vidya, R.; Saji, A. Naked Eye Detection of Infertility Based on Sperm Protamine-Induced Aggregation of Heparin Gold Nanoparticles. *Anal. Bioanal. Chem.* **2018**, *410* (13), 3053–3058. https://doi.org/10.1007/s00216-018-1026-6.

(15) Wiriyachaiporn, N.; Srisurat, P.; Cherngsuwanwong, J.; Sangsing, N.; Chonirat, J.; Attavitaya, S.; Bamrungsap, S. A Colorimetric Sensor for Protamine Detection Based on the Self-Assembly of Gold Nanorods on Graphene Oxide. *New J. Chem.* **2019**, *43* (22), 8502–8507. https://doi.org/10.1039/c9nj00552h.

(16) Pandey, S. P.; Jha, P.; Singh, P. K. Aggregation Induced Emission of an Anionic Tetraphenylethene Derivative for Efficient Protamine Sensing. *J. Mol. Liq.* **2020**, *315*, 113625. https://doi.org/10.1016/j.molliq.2020.113625.

(17) Gao, Y.; Wei, K.; Li, J.; Li, Y.; Hu, J. A Facile Four-Armed AIE Fluorescent Sensor for Heparin and Protamine. *Sensors Actuators, B Chem.* **2018**, *277* (August), 408–414. https://doi.org/10.1016/j.snb.2018.09.054.

(18) Zhao, J.; Yi, Y.; Mi, N.; Yin, B.; Wei, M.; Chen, Q.; Li, H.; Zhang, Y.; Yao, S. Gold Nanoparticle Coupled with Fluorophore for Ultrasensitive Detection of Protamine and Heparin. *Talanta* **2013**, *116*, 951–957. https://doi.org/10.1016/j.talanta.2013.08.010.

(19) He, W.; Weng, W.; Sun, X.; Liu, B.; Shen, J. Novel Plasmon-Enhanced Fluorescence Sensing Platform Based on RGO/MoS2Films for Ultrasensitive Detection of Protamine and Heparin. *ACS Sustain. Chem. Eng.* **2020**, *8* (27), 9988–9997. https://doi.org/10.1021/acssuschemeng.0c00905.

(20) Wang, X.; Sun, M.; Ferguson, S. A.; Hoff, J. D.; Qin, Y.; Bailey, R. C.; Meyerhoff, M. E. Ionophore-Based Biphasic Chemical Sensing in Droplet Microfluidics. *Angew. Chemie - Int. Ed.* **2019**, *58* (24), 8092–8096. https://doi.org/10.1002/anie.201902960.

(21) Yeom, C. K.; Kim, H. K.; Rhim, J. W. Removal of Trace VOCs from Water through PDMS Membranes and Analysis of Their Permeation Behaviors. *J. Appl. Polym. Sci.* **1999**, *73* (4), 601–611.

(22) Liang, L.; Dickson, J. M.; Zhu, Z.; Jiang, J.; Brook, M. A. Removal of 1,2-Dichloroethane

from Aqueous Solutions with Novel Composite Polydimethylsiloxane Pervaporation Membranes. *J. Appl. Polym. Sci.* **2005**, *98* (4), 1477–1491. https://doi.org/10.1002/app.21752.

(23) Yeom, C. K.; Dickson, J. M.; Brook, M. A. A Characterization of PDMS Pervaporation Membranes for the Removal of Trace Organic from Water. *Korean J. Chem. Eng.* **1996**, *13* (5), 482–488. https://doi.org/10.1007/BF02705998.

(24) Lee, J. N.; Park, C.; Whitesides, G. M. Solvent Compatibility of Poly(Dimethylsiloxane)-Based Microfluidic Devices. *Anal. Chem.* **2003**, *75* (23), 6544–6554. https://doi.org/10.1021/ac0346712.

(25) Song, A.; Zhang, J.; Zhang, M.; Shen, T.; Tang, J. Spectral Properties and Structure of Fluorescein and Its Alkyl Derivatives in Micelles. *Colloids Surfaces A Physicochem. Eng. Asp.* **2000**, *167* (3), 253–262. https://doi.org/10.1016/S0927-7757(99)00313-1.

(26) Shchepinova, M. M.; Denisov, S. S.; Kotova, E. A.; Khailova, L. S.; Knorre, D. A.; Korshunova, G. A.; Tashlitsky, V. N.; Severin, F. F.; Antonenko, Y. N. Dodecyl and Octyl Esters of Fluorescein as Protonophores and Uncouplers of Oxidative Phosphorylation in Mitochondria at Submicromolar Concentrations. *Biochim. Biophys. Acta - Bioenerg.* **2014**, *1837* (1), 149–158. https://doi.org/10.1016/j.bbabio.2013.09.011.

(27) Panchompoo, J.; Aldous, L.; Baker, M.; Wallace, M. I.; Compton, R. G. One-Step Synthesis of Fluorescein Modified Nano-Carbon for Pd(Ii) Detection via Fluorescence Quenching. *Analyst* **2012**, *137* (9), 2054–2062. https://doi.org/10.1039/c2an16261j.

(28) Wang, E.; Wang, G.; Ma, L.; Stivanello, C. M.; Lam, S.; Patel, H. Optical Films for Protamine Detection with Lipophilic Dichlorofluorescein Derivatives. *Anal. Chim. Acta* **1996**, *334* (1–2), 139–147. https://doi.org/10.1016/S0003-2670(96)00299-1.

(29) Chen, Q.; Li, X.; Wang, R.; Zeng, F.; Zhai, J.; Xie, X. Rapid Equilibrated Colorimetric Detection of Protamine and Heparin: Recognition at the Nanoscale Liquid-Liquid Interface. *Anal. Chem.* **2019**, *91* (16), 10390–10394. https://doi.org/10.1021/acs.analchem.9b01654.

(30) Wetzler-Quevedo, S. P.; Meyerhoff, M. E.; Bailey, R. C. Characterization of the Impact of Mixing and Droplet Volumes on the Behavior of Microfluidic Ion-Selective Droptodes. *Analyst* **2021**, *146* (16), 5095–5101. https://doi.org/10.1039/d1an00733e.

(31) Doonan, S. R.; Bailey, R. C. K-Channel: A Multifunctional Architecture for Dynamically Reconfigurable Sample Processing in Droplet Microfluidics. *Anal. Chem.* **2017**, *89* (7), 4091–4099. https://doi.org/10.1021/acs.analchem.6b05041.

(32) Booksh, K. S.; Kowalski, B. R. Theory of Analytical Chemistry. *Anal. Chem.* **1994**, *66* (15), 782–791. https://doi.org/10.1021/ac00087a001.

(33) Wang, R.; Zhou, Y.; Ghalehjoughi, N. G.; Mawaldi, Y.; Wang, X. Ion-Induced Phase Transfer of Cationic Dyes for Fluorescence-Based Electrolyte Sensing in Droplet Micro Fl

Uidics. **2021**. https://doi.org/10.1021/acs.analchem.1c03394.

(34) Mary, P.; Studer, V.; Tabeling, P. Microfluidic Droplet-Based Liquid - Liquid Extraction. **2008**, *80* (8), 2680–2687.

Chapter 4 – Polyion-Sensitive Droptodes for Direct and Indirect Sensing of Polymeric Quaternary Ammonium Compounds

Acknowledgments

This work was done in collaboration with Ayush Chitrakar who completed experiments and data analysis for off-device PQ sensing experiments. Contributions to written portion of the manuscript made by Ayush include the introduction section and discussion of off-device experiments implemented for direct PQ sensing. My contributions consisted of project lead and design for all experiments, execution of and data analysis for on-device experiments, and manuscript writing.

Abstract

Polymeric quaternary ammonium compounds (PQs) are a unique group of cationic, synthetic polymers commonly used in a variety of cosmetic, recreational, medical, and industrial products. Based upon their frequent usage, the ability to measure PQ species accurately and reproducibly is of high interest, as their quantitative amount can be linked to a desired or adverse effect within a respective system. Chemically, various forms of PQ species exist, differing in structure, size, and charge density. This has inspired the development and application of several electrochemical and optical techniques as all-purpose analytical methods for PQ sensing. However, such methods require extended response times between the sample-sensor interface and are low in sample throughput. Polyion-sensitive, microfluidic droptodes – which implement a fluorescent chromoionophore and ion-exchanger in a hydrophobic "readout phase" – have successfully been demonstrated as a reagent-conservative, high-throughput method for the

detection of heparin (anticoagulant) and protamine (protein/heparin antagonist). We build upon the success of polyion-sensitive droptodes by applying them for the detection of PQ-2, PQ-6, and PQ-10 compounds. Bulk, off-device droptodes are used as a preliminary method for direct and indirect sensing, each having a unique response toward PQs. The bulk system serves as a guide for the development of our droplet microfluidic platform which demonstrates polyanion-sensitive, microfluidic droptodes as the preferred analytical method for indirect sensing of PQs.

4.1 Introduction

Polyions are polymers with several positive or negative charges along the length of the polymer chain. Polymeric quaternary ammonium compounds, also known as polyquaterniums (PQs), are a specific group of polyions whose positive charge is inherent from multiple organo-ammonium residues present within their chemical structure.[1] Their charge remains cationic independent from the pH of the background matrix[2] – a key component of their utility in several environmental, cosmetic, and biomedical applications. In the cosmetic industry, PQs are found in a range of products including lotions,[3] contact solutions,[4] and shampoos.[5] Within the environmental and industrial sectors PQs have also been used for water treatment[6] and paper making.[7] PQs are widely prevalent, with continued growth in application; therefore, the availability of methods to detect and quantify PQs are essential. Several methods for PQ detection have been presented,[8] yet PQs remain as challenging species to measure as they exist in several chemical forms[9] varying in charge density, molecular weight, and structure.

Polyion-sensitive ion-selective electrodes (ISEs) – electrochemical sensors coated with chemically responsive, polymeric membranes[10,11] – have been demonstrated as an alternate polyion sensing method. For PQ measurements in samples, this platform has been implemented through the use of a potentiometric titration with dextran sulfate and monitoring with a

polyanion-sensitive ISE.[12] The method was shown to be responsive toward varying levels of PQ-10; however, large volumes of sample (tens of mL) were required. Additionally, this was a single use system, limiting its sample throughput. A series of polyion-sensitive ISEs for PQ sensing followed suit, demonstrating direct and indirect quantitation of PQ-2, PQ-6, PQ-10, and poly(2-methacryloxyethyl trimethylammonium) chloride (PMETAC) in a variety of sample matrices.[13,14] However, these methods were plagued by similar limitations associated with the pioneering PQ-10 electrode system.[12] Polyion-sensitive ion-selective optodes (ISOs) were later developed for PQ sensing as an optical counterpart to polyion-sensitive ISEs.[15] This platform proved as a promising step toward the miniaturization of PQ detection systems, requiring only a cell phone camera as the detector for sample analysis. Yet, this method has limited response toward PQ species of low charge densities (~2 mEq/g) and is low in sample throughput, highlighting a need for further advancements.

Previous works within and outside[16] this dissertation have successfully implemented microfluidic droptodes for polyion sensing, indicating such technology as a promising candidate for advancement of PQ-sensitive optical sensors. For polyion-sensitive droptodes, lipophilic ion-exchanger and chromoionophore are concentrated in a water-immiscible oil, which in its entirety is sensitive to the target polyion of interest. Upon merging of the polyion-sensitive oil and aqueous sample at the junction of the droplet microfluidic device, each respective phase is segmented into immobilized, alternating aliquots (100s of pL). Micro-scale, biphasic extractions occur between multiply generated aqueous droplets and readout segments as they traverse down the microfluidic channel. The amount of polyions in aqueous droplets are directly related to the fluorescence of adjacent oil segments, which are monitored by a high-speed camera.[16] As tens of aqueous droplets (per readout segment) are generated per second, this method is high in sample

throughput and low in required sample and reagent volume. Notably, enhanced mass-charge transfer between segments intrinsically occurs due to increased mixing and surface area-to-volume ratios associated with small segment volumes.[17] Off-device liquid-liquid extractions, or bulk droptodes which require 100s of µL of each respective phase, function on a similar biphasic sensing principle as their microfluidic counterpart. Hence, these remain as useful tools for preliminary investigation of droptode platforms for chemical sensing. Herein, both bulk and microfluidic methods are used in conjunction to develop and demonstrate polyion-sensitive droptodes as a novel technique for the detection of PQ species.

4.2 Experimental Methods

4.2.1 Chemicals and Materials

Chromoionophore I (CH 1), poly[bis(2-chloroethyl) ether-alt-1,3-bis[3-(dimethylamino) propyl]urea] quaternized, solution (PQ-2), poly(diallyldimethylammonium chloride) solution (PQ-6), hydroxyethylcellulose ethoxylate, quaternized (PQ-10), sodium phosphate dibasic heptahydrate, sodium phosphate monobasic monohydrate, dioctyl sebacate (DOS), and heparin sodium salt from porcine intestinal mucosa were purchased from Sigma Aldrich (St. Louis, MO). Tridodecylmethylammonium chloride (TDMACl) was purchased from Polysciences, Inc. and sodium chloride from Fisher Scientific. Chromoionophore XI (CH XI) was obtained from Abcam. Dinonylnaphthalene sulfonic acid (50% active in 2-Butoxyethanol) was purchased as NACURE 1051 from King Industries (Norwalk, CT). Materials needed for pressure-driven, segmented flow on-device, were purchased as previously described.[18] Standard materials and reagents for soft and photo- lithography processes used for microfabrication were purchased as previously described.[19]

4.2.2 Droptode Experiments

All aqueous samples were dissolved in 10 mM phosphate buffered saline (PBS) buffer (pH 7.6 - 7.7) diluted from 100 mM PBS (pH 7.4). Respective PQ and heparin stock solutions were created separately at concentrations of 1000 µg/mL. For direct sensing experiments, PQ samples were created by dilution. For indirect sensing experiments, the sample consisted of one part PQ sample at respective concentration (µg/mL) and one part heparin stock (100 µg/mL). Polycation-sensitive readout phase consisted of 50 µM chromoionophore I and 50 µM DNNSH. Polyanion-sensitive readout phase consisted of 200 µM CH XI and 300 µM TDMACl. Reagent concentrations in each respective polyion-sensitive phase were made from sonicated 1000 µM stocks using DOS as a diluent.

For bulk, off-device droptode experiments, a 0.6 mL Eppendorf tube containing 200 µL of sample and 200 µL polyion-sensitive oil was vortexed for 10 seconds at 3000 rpm using a Fisher Scientific Digital Vortex Mixer. This process was repeated for all other samples which were centrifuged together for 10 seconds per sample set for phase separation. A Tecan Infinite F500 well plate reader was used to measure the fluorescence of respective 100 µL of polycation-sensitive oil or polyanion-sensitive oil, extracted from each respective Eppendorf tube.

For microfluidic droptode experiments, a T-junction device with a depth of 80 µm, aqueous channel width of 64 µm, and oil carrying channel width of 80 µm was used. Total distance between the T junction of the device and waste port was 35 mm. A nitrogen gas delivering regulator as previously described[18] connected to a OB1 MK3+ pressure controller (Elveflow) was used to deliver pressure to respective vials containing aqueous and oil phases. Aqueous droplet frequencies were maintained at 18 – 21 Hz. Light from a Prior Lumen 200 illumination system, filtered through a GFP filter cube ($\lambda_{excitation}$: 470/40 nm; $\lambda_{emission}$: 500 - 550

nm) housed within a Leica DMi8 microscope, was used to fluoresce chromoionophore XI. A VEO 640L high speed camera (Vision Research Inc.) was used to monitor and record videos of segmented flow at 100 frames per second (fps), 30 mm from the T-junction of the droplet microfluidic device. An Image J macro code was used to determine the fluorescence of a total of 100 frames of segmented flow for each PQ concentration per PQ species. Data points for each concentration were determined as an average fluorescence value from local maxima within collected traces.

4.3 Results and Discussion

4.3.1 Relative Fluorescence of Polyion-Sensitive Droptodes

To normalize for fluorescence across all experiments the following equation is used:

$$Relative\ Fluorescence\ (R.F.) = \frac{F - F_{min}}{F_{max} - F_{min}}$$

where F represents the fluorescence of the readout phase when interacting with PQ-concentrated sample. The fluorescence of the readout phase when interacting with 10 mM NaOH is represented by F_{min} for the polycation-sensitive readout phase and F_{max} for the polyanion-sensitive readout phase. For microfluidic droptode experiments, each readout segment is considered as an individual measurement per adjacent, aqueous sample. Error associated with the average fluorescence of microfluidic readout segments is then represented by the following:

$$\sigma_{R.F.} = \frac{\sigma_F - \sigma_{F_{min}}}{\sigma_{F_{max}} - \sigma_{F_{min}}} = \frac{\sigma_{F-F_{min}}}{\sigma_{F_{max}-F_{min}}}$$

4.3.2 Theory Behind Polycation Sensing via Polycation-Sensitive Droptodes

Direct sensing of polycations via polycation-sensitive ISOs incorporates a standard CH I and DNNSH format which has been employed in several polycation-sensitive ISO works to

date.[15,16,20] The functionality of this chemistry is reliant upon an acidic DNNSH molecule (pK_a ~ 1.9)[21] which immediately protonates CH I upon interaction in an organic sensing (readout) phase. When samples are concentrated with polycation, DNNSH serves as two-in-one ion-exchanger and ionophore-like agent which expulses cations into the aqueous phase and complexes with the target polycation extracted from the aqueous phase by electrostatic interaction (**Figure 4.1**). We expected this polycation-sensitive chemistry to react similarly toward several PQ species (**Figure 4.2**) which each possess cationic and sterically accessible organo-ammonium groups along the length of their structures.

For previous applications of polycation-sensitive, microfluidic droptodes,[16] DNNSH and CH I sensing reagents were dissolved in dichloroethane, an organic solvent incompatible with polydimethylsiloxane (PDMS). To prevent adverse effects from solvent interaction with the PDMS droplet microfluidic device such as channel swelling,[22] we replaced dichloroethane with dioctyl sebacate (DOS) as the solvent for polycation-sensitive reagents. Having concern of poor optical response toward high concentrations of densely charged PQs, concentrations of CH I and DNNSH were increased by a factor of 10× to enhance fluorescence signal.

4.3.3 Direct Sensing of PQs

Bulk response of the polycation-sensitive droptode did not produce a clear trend for any of the PQs tested. As direct sensing of PQs relies on biphasic transfer of polyions between phases it is likely that highly water soluble PQs[23] aren't fully extracting into the readout phase. Poor biphasic extraction is further evidenced by the large variations in error associated with measurements made for all the tested PQs **(Figure 4.3)**. Such could likely be due to weak interactions with DNNS- at the interface between the aqueous and readout segments. In this case, CH I remains primarily in its protonated state, limiting the change in fluorescent response of

droptodes between PQ samples of different concentrations. Considering the limitations of the pioneering polycation-sensitive droptodes[16] as detailed in this manuscript, an alternate chemical configuration of polyion-sensitive droptodes was pursued for improved consistency in responsiveness, dependent on PQ concentration (between measurements) and charge density (between each PQ species).

4.3.4 Theory Behind Polycation Sensing via Polyanion-Sensitive Droptodes

Works within this document have demonstrated polyanion-sensitive, microfluidic droptodes for direct sensing of polyanion species. In this case, a lipophilic anion exchanger (TDMACl) and a chromoionophore (CH XI) are used in the readout phase which fluorescently responds to varying concentrations of polyanions by the principle of electroneutrality. To this point, polyion-sensitive droptodes remain undemonstrated as a platform for indirect sensing of polyions. However, their usage may be beneficial in droptode systems where direct measurements are limited in analytical response and reproducibility as seen in **Figure 4.3**.

For indirect detection of polycations, there is a constant concentration of polyanion and varying concentration of polycation in each aqueous sample. Fluorescent response is then dependent on the amount of unbound or excess levels of polyanions extracted into the readout phase (**Figure 4.4**). For indirect sensing of PQ species we implement heparin **(Figure 4.5)** – a polyanion with the highest negative charge density amongst biological macromolecules[24] – as the background polyanion in the aqueous sample. In this system, we hypothesized improved measurements of PQ concentrations as analytical readout is now dependent on stable, biphasic extractions rather than weak interactions at the droplet-readout segment interface.

4.3.5 Indirect Sensing of PQs

Polyanion-sensitive bulk droptodes were found to have an improved response toward PQ species relative to their polycation-sensitive counterparts. A clear relationship exists between PQ charge density and slope response **(Figure 4.6)** demonstrating the feasibility of using polyanion-sensitive droptodes for polycation measurements. Having improved success with indirect sensing of PQs via bulk methods, consolidating this method onto a droplet microfluidic was pursued.

For indirect sensing of PQs on a droplet microfluidic device, analytical response of the polyanion-sensitive readout phase was drastically enhanced in comparison to bulk droptodes. For reference, the coefficient of variation (R^2) – which correlates the fluorescence response of readout phase and PQ concentration – was used as a linking factor to compare and contrast the response of bulk **(Figure 4.6)** and microfluidic droptode **(Figure 4.7)** systems. For PQ-2 and PQ-6 species, the R^2 value remained at ≥ 0.92 for both bulk and microfluidic systems, as low and high amounts of charge dense PQs are effectively neutralizing background heparin in solution. Additionally, the R^2 value decreases with PQ charge density, an occurrence accredited to the decreasing number of cationic sites in each structure **(Figure 4.2)** available to interact with the oppositely charged polyanion. An analytically acceptable coefficient of variation (≥ 0.95) is observed for all three of the PQ-species detected with the microfluidic droptode **(Figure 4.7)**. This can be tied to the enhanced mixing in small aqueous droplets (100s of pL) showcased in several droplet microfluidic applications.[25]

For bulk sensing, excess amounts of polyanion are likely limited in their ability to extract into the readout phase in presence of large polycation-polyanion complexes as evidenced by large variations in error associated with data points **(Figure 4.6)**. The augmented surface area-to-volume ratio associated with microfluidic droptodes allows for increased mass-charge transfer

between microscale compartments. This shows especially true for the droplet microfluidic calibration curve for the PQ-10 species, which yielded an improvement in the coefficient of variation by a factor of ~1.25 relative to its respective bulk curve. Overall, the coefficient of variation provides an explanation for observed differences in response of the polyanion-sensitive readout phase towards PQs in presence of background polyanion for both bulk and on-device methods. Within this dissertation, parameters such as sample volume (100s of μL vs 100s of pL) and biphasic reaction time (tens of seconds vs seconds) were discussed as influencing factors in the analytical response of bulk and microfluidic droptodes, as chemical interactions occur on scales varying in magnitude for each respective system. As PQ charge density has been demonstrated to have a more predictable effect on the response of the polyanion-sensitive readout phase in the droplet microfluidic system, microfluidic droptodes were examined as a stand-alone, analytical method.

Results from droplet microfluidic experiments demonstrate the practicality of using polyion-sensitive microfluidic droptodes as an alternate method for PQ sensing **(Figure 4.7)**. The high throughput nature of this method is advantageously presented as the average fluorescence response from nearly 20 PQ samples per data point that is captured in a 1.0 second video. Including the minimum and maximum points used as reference, a combined video time of only 8.0 seconds was needed to track fluorescence response from nearly 140 PQ samples within each calibration curve. This is a great improvement in sample-throughput relative to previously reported, polyion-sensitive ISOs[15] and ISEs[13,14] used for PQ sensing. For each data point, error does not exceed ±1% of the total range of relative fluorescence (y-axis) further demonstrating this sensor as a reproducible and reliable technique.

Lastly, the relationship between PQ charge density and droptode response is examined within the droplet microfluidic system. As shown in **Figures 4.7 and 4.8**, the slope response of microfluidic droptodes toward PQs is highly dependent on PQ charge density, despite the varying chemical structure of each PQ species **(Figure 4.2)**. Considering this highly correlative relationship, this method may find more use in application by measuring 'milliequivalents of PQ charge per milliliter of sample' as the independent variable. In this way, the amount of cationic charge in samples from PQ(s), associated with a specific effect in a given system, can be quantified based on the readout response. The limit of detection ($3.3\sigma_{y\text{-intercept}}/m$) calculated from a linear regression analysis of slope response and PQ charge density (**Figure 4.8)** indicates PQ species with densities as low as 0.75 mEq/g can be measured using polyion-sensitive, microfluidic droptodes. This stands as reference for the potential expansion of this system for measurement of additional PQs varying in charge density and structure.

4.4 Conclusions

In this work, polyion-sensitive droptodes have been demonstrated for the detection of polymeric quaternary ammonium compound species PQ-2, PQ-6, and PQ-10. However, analytically preferred direct PQ measurements made via polycation-sensitive droptodes were found to be limited in both response and reproducibility. Polyanion-sensitive droptodes were found to have an improved response towards PQ species, pushing past the limitations of their direct sensing counterpart. Furthermore, consolidating the indirect system onto a droplet microfluidic device increased sample-throughput and decreased required sample volumes relative to polyion-sensitive ISOs and ISEs. A highly correlative relationship between PQ charge density and slope response was revealed using the polyanion-sensitive microfluidic droptode platform, demonstrating the potential use of this method to detect a variety of different PQ

species. As polyion-sensitive droptodes are unable to characterize PQ structure, this method may find benefit from being combined with a secondary characterization technique to verify the chemical structure of PQ species being detected. This may be especially useful for PQ measurements in environmental and wastewater samples which contain a diverse array of chemical components.

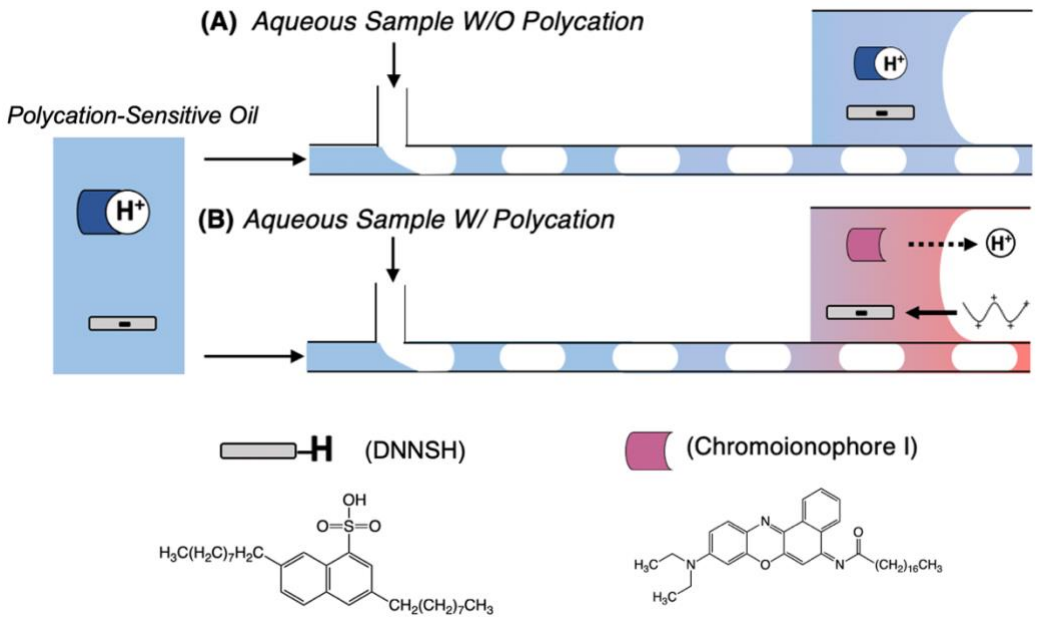

Figure 4.1. Schematic for direct sensing of polycations on a droplet microfluidic device. (A) when the sample does not contain polycation, chromoionophore I remains protonated. (B) when the sample contains target polyion, protons dissociate from charged chromoionophore I as a result of DNNS- electrostatically interacting with the polycation.

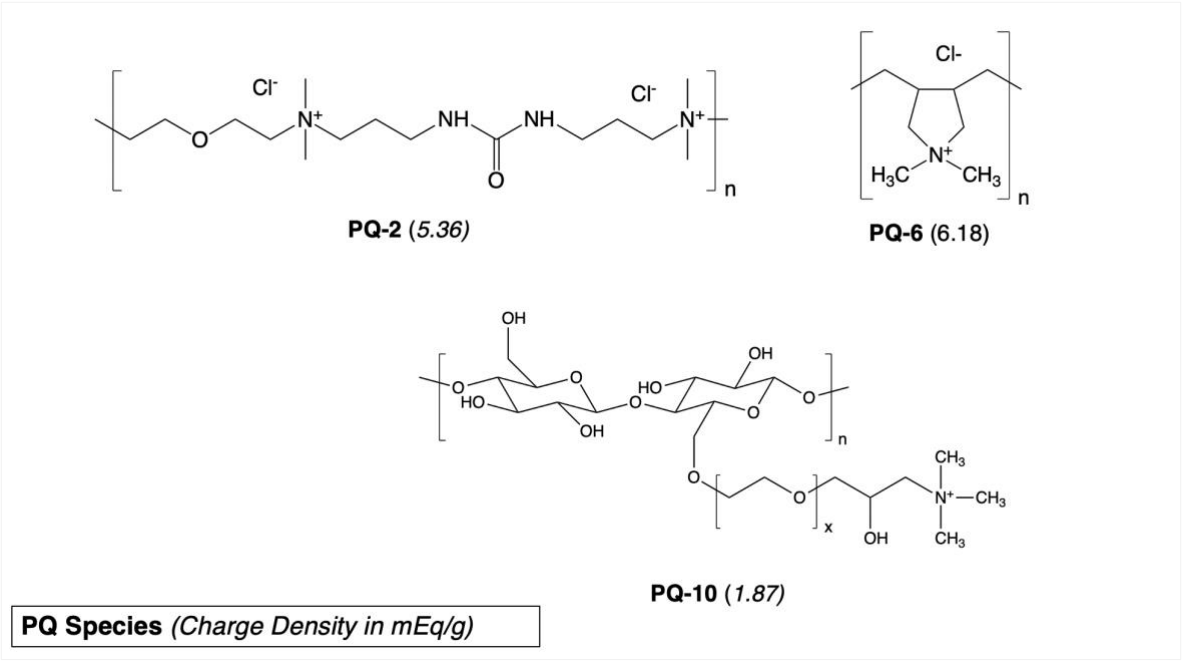

Figure 4.2. Chemical structures of polymeric quaternary ammonium compounds (PQs) detected in bulk and on-device droptode experiments. Charge density is the milliequivalents of charge associated with the primary monomeric unit of each PQ species.

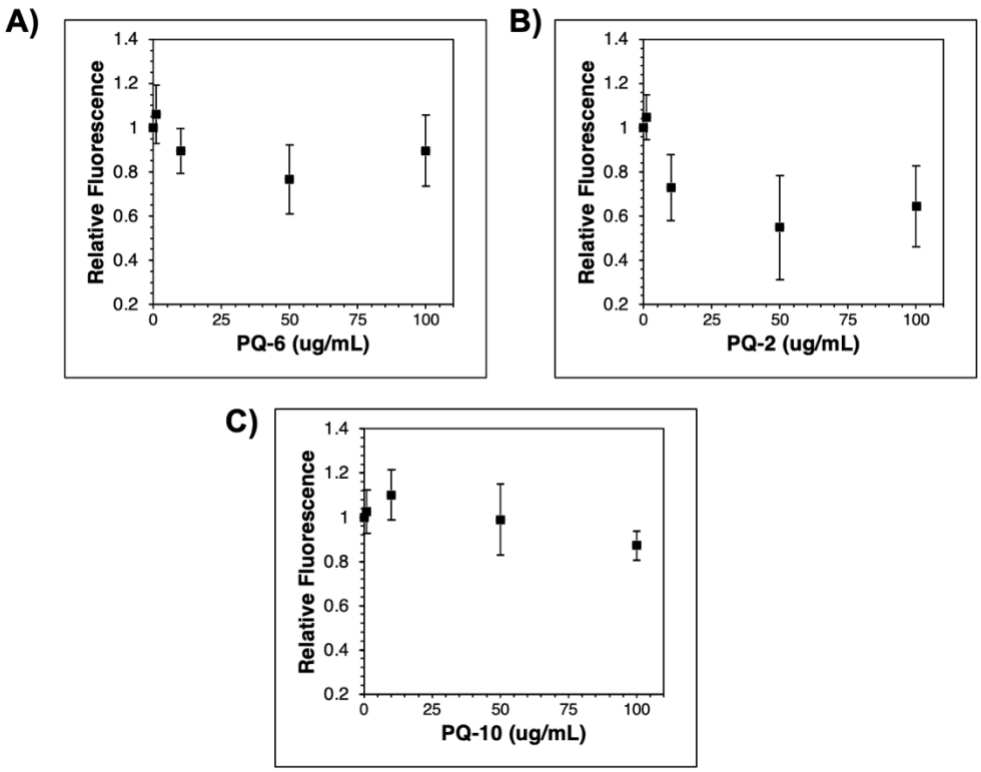

Figure 4.3. Bulk response of polycation-sensitive droptode toward (A) PQ-6 (B) PQ-2 and (C) PQ-10. Data points are representative of average relative fluorescence of the readout phase ± standard deviation for n ≥3 trials. Chromoionophore I in the readout phase was excited at a wavelength range of 607 – 617 nm. Fluorescence was measured at an emission wavelength range of 657.5 – 682.5 nm.

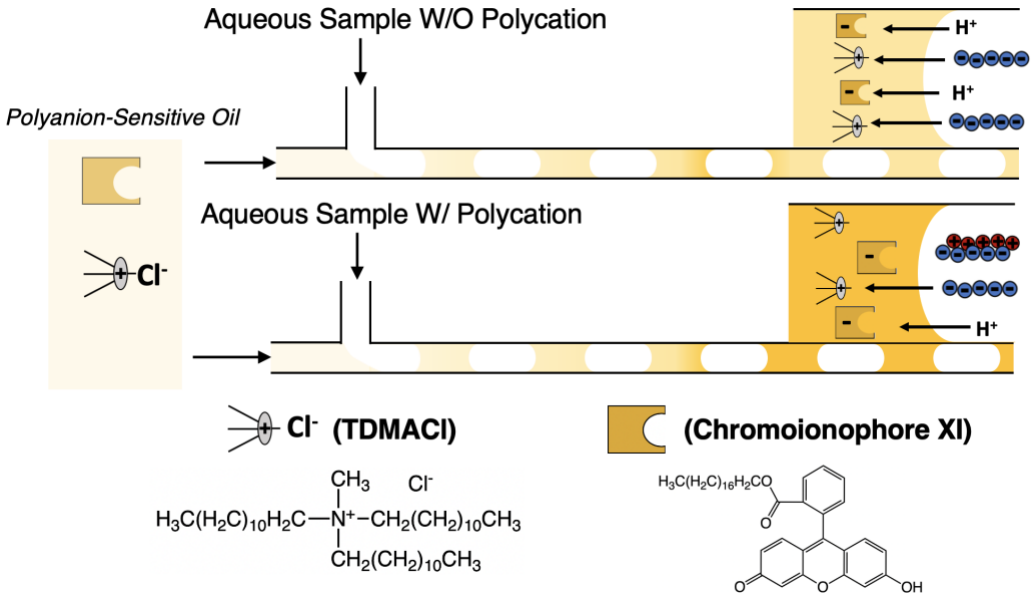

Figure 4.4. Schematic for indirect sensing of polycations on a droplet microfluidic device (A) when the sample does not have polycation, polyanions are extracted from the aqueous sample and electrostatically complex with $TDMA^+$ in the readout phase. The fluorescence signal of CH XI is suppressed as it is saturated with co-extracted protons. (B) When the sample is concentrated with polycations, corresponding amounts of polyanion are neutralized. Decreasing amounts of excess polyanion are proportional to increased amounts of highly fluorescent, deprotonated CH XI in the oil phase by principle of electroneutrality.

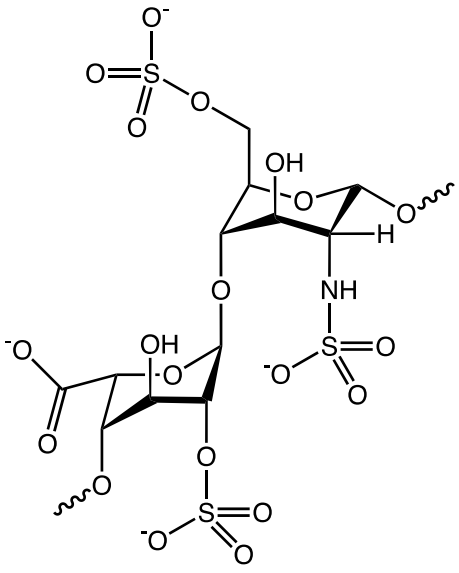

Figure 4.5. Chemical structure of heparin. This polyanion remains at a constant concentration in the background of the aqueous phase used in the indirect, polycation-sensitive droptode system.

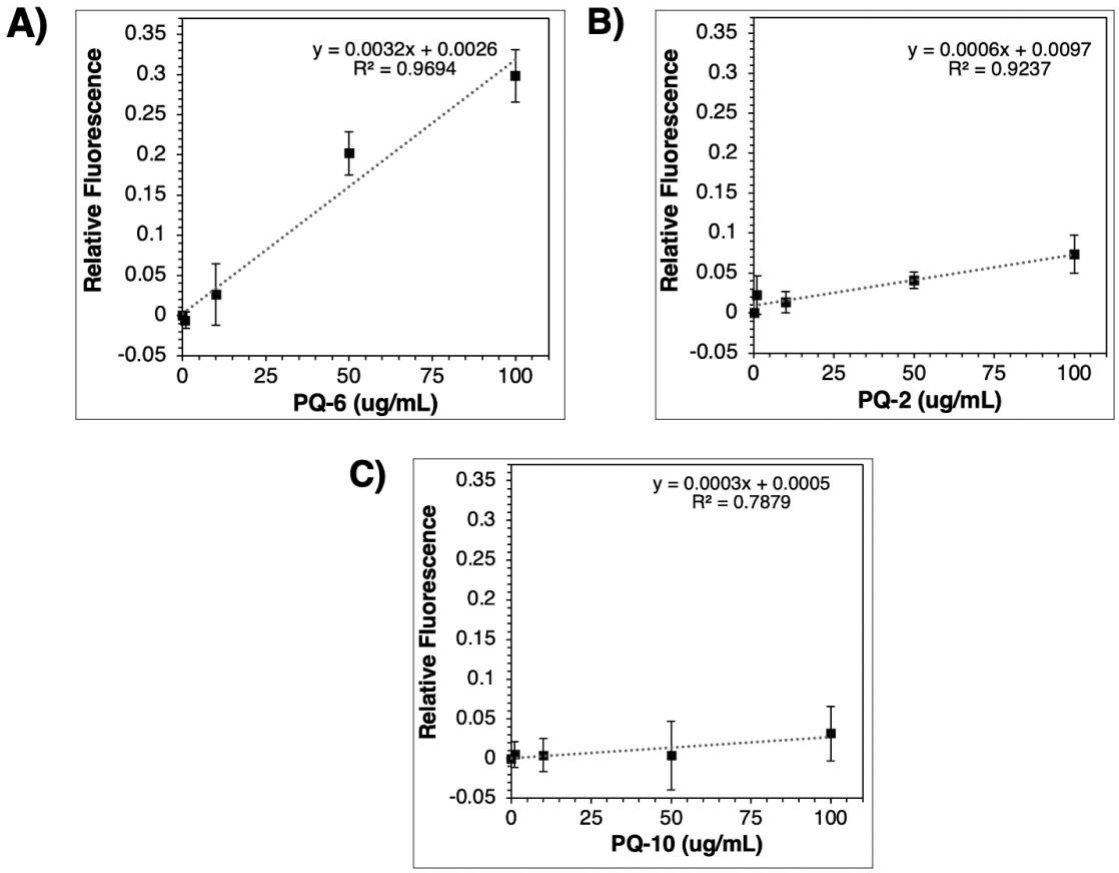

Figure 4.6. Bulk response of polyanion-sensitive readout phase toward various concentrations of (A) PQ-6 (B) PQ-2 and (C) PQ-10, with heparin as the background polyanion. Data points are representative of average relative fluorescence of the readout phase ± standard deviation for n=4 trials. Chromoionophore XI in the readout phase was excited at wavelength range of 475 – 495 nm. Fluorescence was measured at an emission wavelength range of 522.5 – 547.5 nm.

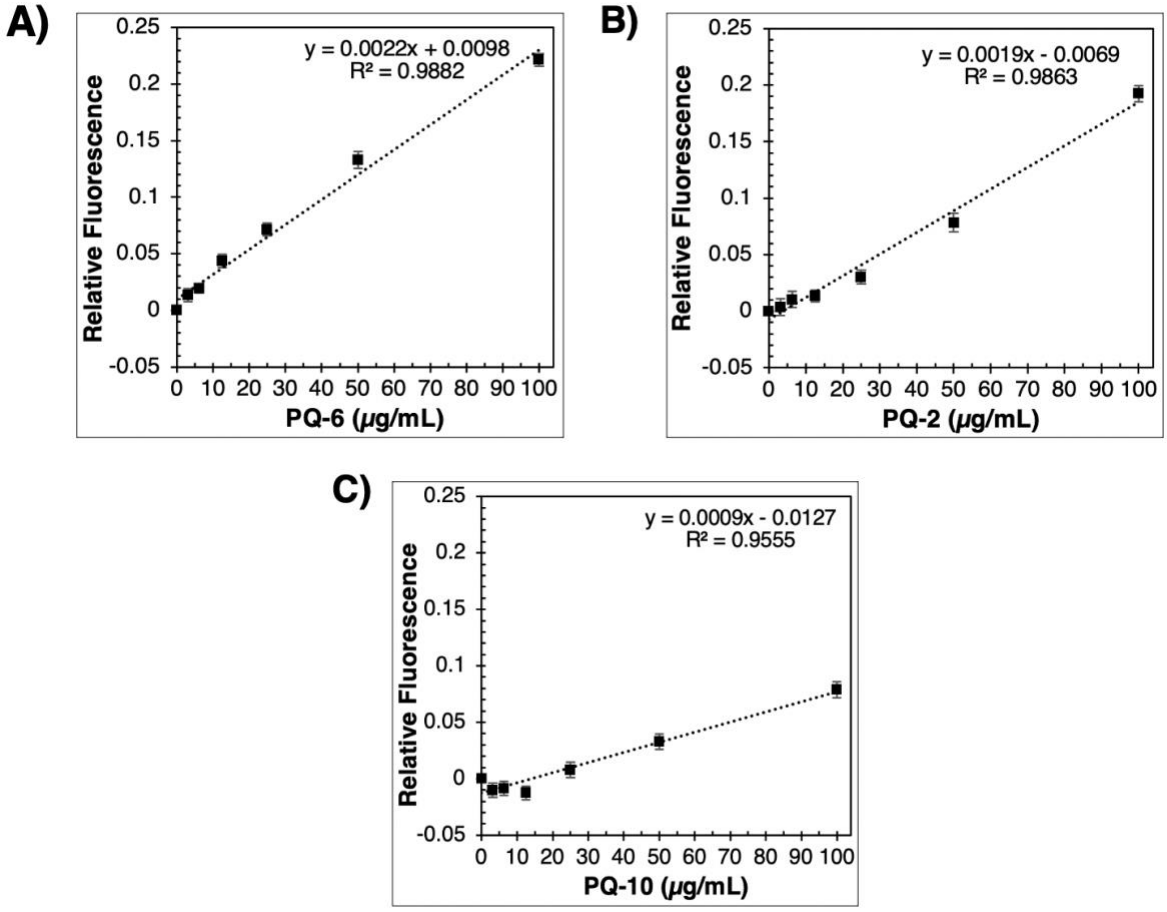

Figure 4.7. On-device response of polyanion-sensitive readout segments toward various concentrations of (A) PQ-6 (B) PQ-2 and (C) PQ-10, with heparin as the background polyanion. Data points are representative of average fluorescence of readout segments ± standard deviation for n≥18 PQ samples.

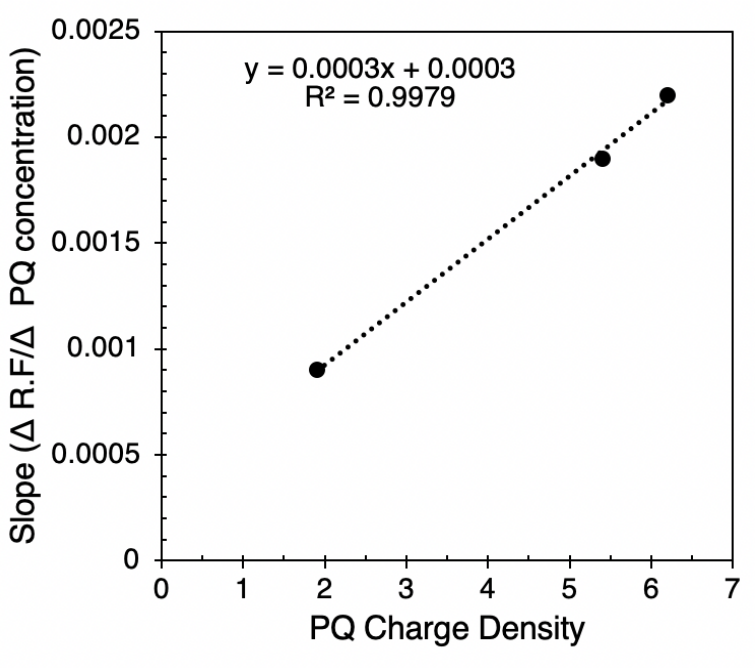

Figure 4.8. Slope (m) response of polyanion-sensitive, microfluidic droptode toward several PQs in background of heparin plotted against PQ charge density. The limit of detection ($3.3\sigma_{y\text{-intercept}}/m$) or average minimum PQ charge density which can be detected by the polyanion-sensitive, microfluidic droptode was calculated to be 0.75 mEq/g. Standard deviation of the y-intercept of the regression line is represented by $\sigma_{y\text{-intercept}}$.

4.5 References

(1) Ferguson, S. A.; Meyerhoff, M. E. Characterization and Quantification of Polyquaterniums via Single-Use Polymer Membrane-Based Polyion-Sensitive Electrodes. *ACS Sensors* **2017**, *2* (2), 268–273. https://doi.org/10.1021/acssensors.6b00787.

(2) Cumming, J.; Hawker, D.; Chapman, H.; Nugent, K. The Fate of Polymeric Quaternary Ammonium Salts from Cosmetics in Wastewater Treatment Plants. *Water. Air. Soil Pollut.* **2011**, *216* (1–4), 441–450. https://doi.org/10.1007/s11270-010-0543-5.

(3) Ponizovsky, A.; Schaefer, E.; Stanton, K.; Heisler, R. Adsorption Isotherms of Polyquaternium-10 Polymers by Activated Sludge Solids. *Chemosphere* **2022**, *307* (P2), 135891. https://doi.org/10.1016/j.chemosphere.2022.135891.

(4) Bradley, C. S.; Sicks, L. A.; Pucker, A. D. Common Ophthalmic Preservatives in Soft Contact Lens Care Products: Benefits, Complications, and a Comparison to Non-Preserved Solutions. *Clin. Optom.* **2021**, *13*, 271–285. https://doi.org/10.2147/OPTO.S235679.

(5) Nazir, H.; Zhang, W.; Liu, Y.; Chen, X.; Wang, L.; Naseer, M. M.; Ma, G. Silicone Oil Emulsions: Strategies to Improve Their Stability and Applications in Hair Care Products. *Int. J. Cosmet. Sci.* **2014**, *36* (2), 124–133. https://doi.org/10.1111/ics.12104.

(6) Hamad, M. J. A.; Chirwa, E. M. N. Forward Osmosis for Water Recovery Using Polyelectrolyte PolyDADMAC and DADMAC Draw Solutions as a Low Pressure Energy Saving Process. *Desalination* **2019**, *453* (May 2018), 89–101. https://doi.org/10.1016/j.desal.2018.11.016.

(7) Yang, H.; Deng, Y. Preparation and Physical Properties of Superhydrophobic Papers. *J. Colloid Interface Sci.* **2008**, *325* (2), 588–593. https://doi.org/10.1016/j.jcis.2008.06.034.

(8) Cumming, J. L.; Hawker, D. W.; Matthews, C.; Chapman, H. F.; Nugent, K. Analysis of Polymeric Quaternary Ammonium Salts as Found in Cosmetics by Metachromatic Polyelectrolyte Titration. *Toxicol. Environ. Chem.* **2010**, *92* (9), 1595–1608. https://doi.org/10.1080/02772248.2010.482062.

(9) Iwata, H.; Shimada, K. *Formula Ingredients and Production in Cosmetics*; 2013; Vol. 53.

(10) Yang, V. C.; Ma, S. C.; Meyerhoff, M. E. A Novel Electrochemical Heparin Sensor. *Proceedings of the Controlled Release Society*. 1994, pp 274–275.

(11) Yun, J. H.; Meyerhoff, M. E.; Yang, V. C. Protamine-Sensitive Polymer Membrane Electrode: Characterization and Bioanalytical Applications. *Analytical Biochemistry*. 1995, pp 212–220. https://doi.org/10.1006/abio.1995.1032.

(12) Ferguson, S. A.; Wang, X.; Meyerhoff, M. E. Detecting Levels of Polyquaternium-10 (PQ-10): Via Potentiometric Titration with Dextran Sulphate and Monitoring the

Equivalence Point with a Polymeric Membrane-Based Polyion Sensor. *Anal. Methods* **2016**, *8* (29), 5806–5811. https://doi.org/10.1039/c6ay01748g.

(13) Ferguson, S. A.; Meyerhoff, M. E. Characterization and Quantification of Polyquaterniums via Single-Use Polymer Membrane-Based Polyion-Sensitive Electrodes. *ACS Sensors* **2017**, *2* (2), 268–273. https://doi.org/10.1021/acssensors.6b00787.

(14) Ferguson, S. A.; Meyerhoff, M. E. Manual and Flow-Injection Detection/Quantification of Polyquaterniums via Fully Reversible Polyion-Sensitive Polymeric Membrane-Based Ion-Selective Electrodes. *ACS Sensors* **2017**, *2* (10), 1505–1511. https://doi.org/10.1021/acssensors.7b00527.

(15) Ferguson, S. A.; Wang, X.; Mahoney, M.; Meyerhoff, M. E. Detection and Quantification of Polyquaterniums via Polyion- Sensitive Ion-Selective Optodes Inkjet Printed on Cellulose Paper. *Anal. Sci.* **2018**, *34* (1), 45–50. https://doi.org/10.2116/analsci.34.45.

(16) Wang, X.; Sun, M.; Ferguson, S. A.; Hoff, J. D.; Qin, Y.; Bailey, R. C.; Meyerhoff, M. E. Ionophore-Based Biphasic Chemical Sensing in Droplet Microfluidics. *Angew. Chemie - Int. Ed.* **2019**, *58* (24), 8092–8096. https://doi.org/10.1002/anie.201902960.

(17) Xiao, Z.; Niu, M.; Zhang, B. Droplet Microfluidics Based Microseparation Systems. *J. Sep. Sci.* **2012**, *35* (10–11), 1284–1293. https://doi.org/10.1002/jssc.201200115.

(18) Doonan, S. R.; Bailey, R. C. K-Channel: A Multifunctional Architecture for Dynamically Reconfigurable Sample Processing in Droplet Microfluidics. *Anal. Chem.* **2017**, *89* (7), 4091–4099. https://doi.org/10.1021/acs.analchem.6b05041.

(19) Wetzler-Quevedo, S. P.; Meyerhoff, M. E.; Bailey, R. C. Characterization of the Impact of Mixing and Droplet Volumes on the Behavior of Microfluidic Ion-Selective Droptodes. *Analyst* **2021**, *146* (16), 5095–5101. https://doi.org/10.1039/d1an00733e.

(20) Wang, X.; Mahoney, M.; Meyerhoff, M. E. Inkjet-Printed Paper-Based Colorimetric Polyion Sensor Using a Smartphone as a Detector. *Anal. Chem.* **2017**, *89* (22), 12334–12341. https://doi.org/10.1021/acs.analchem.7b03352.

(21) Ershad, M.; Almeida, M. I. G. S.; Spassov, T. G.; Cattrall, R. W.; Kolev, S. D. Polymer Inclusion Membranes (PIMs) Containing Purified Dinonylnaphthalene Sulfonic Acid (DNNS): Performance and Selectivity. *Sep. Purif. Technol.* **2018**, *195* (December 2017), 446–452. https://doi.org/10.1016/j.seppur.2017.12.037.

(22) Yeom, C. K.; Dickson, J. M.; Brook, M. A. A Characterization of PDMS Pervaporation Membranes for the Removal of Trace Organic from Water. *Korean J. Chem. Eng.* **1996**, *13* (5), 482–488. https://doi.org/10.1007/BF02705998.

(23) Zeng, J.; Sun, X.; Zheng, L.; He, Q.; Li, S. Recovery of Tungsten (VI) from Aqueous Solutions by Complexation- Ultrafiltration Process with the Help of Polyquaternium. *Chinese J. Chem. Eng.* **2012**, *20* (5), 831–836. https://doi.org/10.1016/S1004-9541(12)60406-6.

(24) Gao, Y.; Wei, K.; Li, J.; Li, Y.; Hu, J. A Facile Four-Armed AIE Fluorescent Sensor for Heparin and Protamine. *Sensors Actuators, B Chem.* **2018**, *277* (August), 408–414. https://doi.org/10.1016/j.snb.2018.09.054.

(25) Teh, S. Y.; Lin, R.; Hung, L. H.; Lee, A. P. Droplet Microfluidics. *Lab Chip* **2008**, *8* (2), 198–220. https://doi.org/10.1039/b715524g.

Chapter 5 – Advancement of Microfluidic Droptodes for Multiplex Sensing of Electrolytes

Acknowledgments

Dr. Shannon Wetzler-Quevedo is acknowledged for optimizing ionophore, ion-exchanger, and chromoionophore stoichiometries for physiologically relevant sensitivity of potassium and sodium selective readout phases. My contributions to the project consisted of conceptualizing and designing the described multiplex device, executing bulk and on-device experiments, and all described data analysis and writing.

Abstract

Several works have demonstrated ionophore-based droplet microfluidics, or "microfluidic droptodes", for single-plex detection of polycations, polyanions, and atomically charged electrolytes in a diverse array of samples. Multiplex sensing of such targets via microfluidic droptodes is of high interest as it would allow for efficient collection of multi-analyte profiles in a single sample using a high throughput method. In traditional droptode experiments, a T-junction microfluidic device is used for target analyte sensing but is limited in its application as it only has a single port of entry for the analyte-selective oil. Detection of multiple analytes with our current design requires manual changing of the analyte-selective oil phase per target and device purging of residual oil between measurements – additional steps which decrease the automated nature of microfluidic droptode systems. Hence, we have developed an alternate droplet microfluidic device design for spatial multiplexing of various analytes on a single device. Given the highly selective nature of ionophores relative to the

complexing agents used for polyion sensing, sodium (Na^+) and potassium (K^+) ions are measured as targets of interest in these initial studies. Herein, a novel method for spatial multiplexing of analytes in droptode systems without adverse effects on measurement throughput is demonstrated and established.

5.1 Introduction

Electrolytes—atomic or molecular species which carry a net electrical charge—are fundamental units of reactivity in biochemical systems. In mammalian physiology, electrolytes regulate many important processes, including maintenance of cell membrane polarity, and nerve and muscle function, among others.[1] Under healthy bodily function, electrolytes are found at tightly regulated concentration ranges that can vary by environments within cellular compartments or systemically.[2–5] However, abnormally high (e.g. hyper-) or low (e.g. hypo-) levels often underscore abnormal physiology that can be linked to disease states **(Table 5.1)**.[6–8] Techniques capable of accurately monitoring electrolytes in different types of biological matrices are essential to ensure clinicians make accurate diagnoses and subsequently initiate appropriate treatment.

Blood gas electrolyte analyzers are used in clinical settings for accurate and reliable electrolyte measurements. These instruments measure multiple electrolyte concentrations in whole blood, serum, and plasma.[9] Despite their frequent usage, this electrode based technique is susceptible to limitations of traditional ion-selective electrodes, including protein buildup[10], adherence of clots[11] at the membrane surface, and deterioration of the electrode's polymeric film from sample leaching.[12] Furthermore, cartridge-based analyzers are subject to interferences from lipophilic, per fluorinated chemicals often found in emulsion-based quality control materials.[13]

Alternatively, ion-selective optodes (ISOs) have emerged contiguously to their electrochemical counterparts. Classical ISOs consist of a polymeric film containing poly(vinyl chloride), dioctyl sebacate plasticizer, ionophore (i.e. ion receptor), and chromoionophore, whose optical properties change as a result of ion partitioning into the film.[12] Adaptations of ISOs include incorporation of ion-selective chemistries into several formats including microtiter plate wells[14], emulsified nanospheres[15], fabrics[16] and cellulose papers[17]. Despite their continued development, ISOs are prone to deterioration of sensing substrate and signal interference from non-transparent matrices, such as serum and whole blood. Droplet microfluidics has been explored as an alternative sensing platform for electrolyte sensing using classical ion-selective reagents without the common interferences associated with traditional ISOs. As background, this method involves the generation of aqueous droplets segmented by a water immiscible "oil" on microfluidic channels tens of hundreds of micrometers. Each aqueous droplet (100s of pL) can be considered as an individual aliquot allowing for tens to thousands of samples to be analyzed per second (Hz).[18]

Using potassium as model ion, ionophore based droplet microfluidics or "microfluidic droptodes" were successfully implemented for electrolyte detection in buffer and whole blood.[19] For generation of segmented flow, a T-junction device connected to a syringe pump was used to generate alternating aliquots (800 pL) of dioctyl sebacate concentrated with lipophilic sensing components – potassium ionophore, sodium ion-exchanger, and chromoionophore – per aqueous droplet. As samples with low amounts of potassium interact with potassium-selective readout segments, the chromoionophore is protonated as a result of sodium and proton exchange between phases. Increases in potassium concentrations induce ion-exchange between hydrophilic sodium

ions – expulsed into the aqueous droplet – and ionophore-bound potassium ions, leaving the chromoionophore in a deprotonated state.

To improve on the success of single ion-selective droptodes, the development of multiplexed electrolyte sensing methods is of high interest. As a number of ionophores, ion-exchangers, and chromoionophores are soluble in dioctyl sebacate[20,21], this organic "readout" phase can easily be configured for selective detection of a variety of electrolytes. However, by principle of electroneutrality, fluorescence response from target analyte is correspondent to a single set of chromoionophore, ionophore, and ion-exchanger concentrated in the readout phase. Considering that multiple sets of sensing reagents dissolved in a single amount of dioctyl sebacate would not generate a functional response toward multi-ion solutions, the standard T junction microfluidic device design used for measurements is limited in application as it requires respective ion-selective oil phases to be manually changed per target analyte. This creates additional steps needed for measurements as residual ion-selective oil must be purged from connected tubing, through the microfluidic device, and out of the waste port before the subsequent ion-selective oil can be introduced to the oil port.

To develop a multiplex droptode detection platform, we utilize the ease of designing and fabricating microfluidic devices via standard lithography methods[22,23] that allows for an infinite number of designs to be prototyped and tailored for applications of interest. We designed and implemented a droplet microfluidic "H-channel" device consisting of a single sample port and multiple oil carrying channels to increase the plexity of microfluidic droptode devices. This unique design allows for a single sample to be split into separate streams directed towards spatially separated channels which each carry an ion-selective oil. As a model system for electrolyte detection in multi-ion solutions, we initially focused on spatial multiplexed detection

of Na^+ and K^+ ions, as they are similar in size and identical in charge. Herein, we demonstrate an H-channel device for the simultaneous detection of Na^+ and K^+ ions in individual samples, advancing the capabilities of multi-target sensing in droptode systems.

5.2 Experimental Methods

5.2.1 Chemicals and Materials

Chromoionophore I (CH I), sodium tetrakis[3,5-bis(trifluoromethyl)phenyl]borate (NaTFPB), Potassium tetrakis[3,5-bis(trifluoromethyl)phenyl]borate (KTFPB), sodium Ionophore X, potassium Ionophore II, and dioctyl sebacate (DOS) were all purchased from Sigma Aldrich. Biopsy punches (0.75 mm) were purchased from World Precision Instruments Inc. and 30-gauge PTFE tubing from Cole-Parmer. Potassium sulfate, sulfuric acid, potassium chloride, and sodium chloride were purchased from Fisher Scientific.

5.2.2 Multiplex Device Fabrication

Devices were made using a combination of photolithography and soft lithography with standard materials as previously described.[24] Inlet and outlets of the fabricated H-channel device were punched using 0.75 mm biopsy punch and bound to glass slides using either oxygen plasma or PDMS-PDMS bonding. All channels were 80 µm in depth and 80 µm in width, except for the aqueous channel, which was only 64 µm in width at intersecting junctions.

5.2.3 Droptode Experiments

All aqueous samples were dissolved in Tris-H_2SO_4 buffer at near neutral pH (7.2 - 7.4). Tris-H_2SO_4 concentration in buffer was diluted from 100 to 10 mM for all multiplex experiments to reduce interference from sulfate ions. Sodium ion-selective readout phase consisted of 100 µM

chromoionophore I, 200 μM KTFPB, and 400 μM sodium ionophore X. Potassium ion-selective oil consisted of 100 μM Chromoionophore I, 200 μM NaTFPB, and 300 μM Potassium ionophore II. Reagent concentrations in each respective ion-selective phase were made from sonicated 1000 μM stocks using DOS as a diluent. Samples from initial bulk and on-device were diluted tenfold from a 1 M K^+, 1 M Na^+ stock.

For bulk droptode experiments (i.e., liquid-liquid extractions), a 600 μL Eppendorf tube containing 200 μL each of sample and ion-selective oil was vortexed for 10 seconds at 3000 rpm (unless otherwise noted) using a Fisher Scientific Digital Vortex Mixer. This process was repeated for all other samples which were centrifuged together for 10 seconds to separate the phases out. A Tecan Infinite® F500 well plate reader ($\lambda_{excitation}$ =607 - 617 nm, $\lambda_{emission}$ = 657.5 – 682.5 nm) was used to measure the fluorescence from 100 μL of reacted, ion-selective oil, extracted from each respective Eppendorf tube.

For final multiplexing measurements on-device, samples were ten-fold diluted from a 1 M Na^+, 0.1 M K^+ solution created from a 2 M Na^+, 1 M K^+ stock solution. In this case, each sample was concentrated with sodium ions a magnitude higher than potassium ions. A home-built pressure system as previously described[25] was used to generate segmented flow on device. Pressures were maintained around 80 kPa to generate aqueous droplets. A VEO 640L high speed camera (Vision Research Inc.) attached to a DMi8 light microscope (Leica Microsystems) was used to image and record videos of generated segments. Fluorescence measurements of readout segments were taken 4.5 cm from the T-junction at both detection points in which the device was exposed to light source (Lumen 200, Prior Scientific) filtered through a 49006 – ET – Cy5 filter cube set (Chroma Technology).

5.2.4 Data Analysis for Droptodes

For droplet microfluidic experiments, videos of generated segments in bright and dark field modes were collected at 100 frames per second. Fluorescence intensity of generated segments at the distal end of the device was quantified using an Image J (NIH) macro code. Data points were obtained as an average fluorescence intensity of local maxima within collected traces which correspond to fluorescent readout segments. To normalize for fluorescence across experiments, the following equation was used:

$$Relative\ Fluorescence = 1 - \frac{F_{max} - F_{sample}}{F_{max} - F_{min}}$$

F_{sample} represents the fluorescence of the readout phase interacting with sample, whereas F_{max} and F_{min} are representative of readout phase interacting with the least and most concentrated electrolyte solutions, respectively. For on-device experiments error associated with the average fluorescence of multiply generated microfluidic droptodes (per second) was represented by the following equation:

$$\sigma = \frac{Variation\ in\ Readout\ Segment\ Fluorescence\ \ Intensity\ (\pm)}{F_{max} - F_{min}}$$

5.3 Results and Discussion

5.3.1 Off-Device Response of Ion-Selective Droptodes in Multiplex Systems

Using bulk liquid-liquid extractions as proof-of-concept, ion-selective oil phases were found to have unique responses toward samples containing both sodium and potassium relative to samples containing individual ions. For the K^+-selective oil, substantial response within the sensing region of interest (i.e., 0.1 – 10 mM) was observed in both systems (**Figures 5.1b, 5.1c**), indicating potassium can be detected in the presence of sodium with minimal interference. In the case of the Na^+-selective oil phase, effects from potassium ions in the sample background are

more evident as the linear response shifts from over three orders of magnitude (1 – 100 mM) in the single-plex system (**Figure 5.1a**) to two orders of magnitude (1 – 10 mM) in the multiplex system (**Figure 5.1c**). Though the potassium ionophore appears to be more selective in multiplex systems, it should be noted that 3x reaction times (i.e., vortex times) were required to induce colorimetric responses of sensing phases interacting with multi-ion samples (**Figure 5.2**). This indicates interference from non-target ions and that both ion-selective oils need extra time to distinguish between monovalent K^+ and Na^+ in solution, despite selectivity of their respective ionophores. Such was taken into consideration in the development of microfluidic experiments.

5.3.2 Development of a Droplet Microfluidic Device for Multiplex Sensing

Having success with demonstrating selectivity of each ionophore toward target cation in the presence of background cation using bulk droptodes, this workflow was next consolidated onto a 'H-Channel' microfluidic chip. The main feature of this microfluidic design is a single sample-carrying channel that perpendicularly intersects at a 90º angle with two oil-carrying channels **(Figure 5.3)**. This latitudinal spacer allows for the two different oil phases to remain independent of one another as it splits the aqueous sample stream to separate junctions. Other additional features were incorporated into the H-channel device to reduce sources of random error within measurements and improve efficiency of experiments.

Filter structures within the oil and aqueous ports were included in the device design to prevent device clogging from dust and fibers (i.e., tens of microns) often found in unfiltered solutions. Distance between the droplet junction and detection point was increased by a factor of 1.5 relative to the standard T-junction design,[19] allowing more time for ionophores to distinguish between various ions in solution, an issue first observed in off-device (i.e., bulk) experiments. Lastly, the large distance between lanes A and B (~7.5 mm) prevents optical crosstalk from

fluorescent chromoionophores, allowing for multiple chemical measurements to be made on a single microfluidic chip (**Figure 5.4**).

5.3.3 Implementation of the Multiplex Device for Ion Sensing

Using samples containing equal concentrations of sodium and potassium, the H-Channel device was successfully implemented for calibration of electrolyte concentrations over four orders of magnitude. The K^+-selective oil calibrated readily within the 0.1 to 10 mM range (**Figure 5.5**), which extensively covers reported K^+ concentrations found in serum.[26] Additionally, the Na^+-selective phase was found to be very responsive in the 1 – 100 mM range, which spans across a region that includes hyper- levels of background potassium ions[27] in solution. To improve the response of ion-selective oil phases, samples were created at concentrations in which sodium ions are a magnitude higher than potassium ions. In this way, samples more closely resembled the ratio of sodium to potassium[28] found in biological media. Each ion-selective oil calibrated well within physiological concentration ranges as error associated with each measurement did not exceed ±2% of the dynamic range **(Figure 5.6)**. Fluorescence traces further demonstrate the responsiveness of each ion-selective oil as the height of peaks (local maxima) decrease with increasing amounts of ions.

As the H-Channel was only implemented for measurement of sodium and potassium, incorporation of ion-selective chemistries for calcium and chloride on the microfluidic device are of high interest as such concentrations are commonly included in traditional electrolyte panels. The multiplex device can then be used for electrolyte measurements in serum as a step toward point-of-care analysis. Though, for four-plex sensing of the entire electrolyte panel (K^+, Cl^-, Ca^{2+}, and Na^+), the current device design would require connected oil phases to be manually changed for every two target electrolyte concentrations. Device designs capable of distributing a

single sample to four separate lanes as shown in **Figure 5.7** and **Figure 5.8** may be considered for further advancement of branched droplet microfluidic devices.

5.4 Conclusion

A microfluidic droptode device capable of spatially multiplexing Na^+ and K^+ electrolytes has been developed and implemented for the first time. Bulk droptodes demonstrate the feasibility of measuring a target cation in the presence of an equal amount of like charge ion in solution, chemically validating the selectivity of ionophores. Furthermore, features of the H-channel microfluidic device allow for multiple ion-selective chemistries to be consolidated onto a single device. Cross contamination of oil phases is easily avoided for on-device experiments as respective phases are physically separated from the other. In this way, ion-selective oil phases no longer require reconfiguration for multiple electrolyte measurements on-device, a great improvement from the previously developed single ion droptodes. Overall, the demonstrated utility of the H-channel microfluidic device provides a segue toward chemical sensing of macromolecular targets or polyions (e.g., heparin, proteins) which have only been detected using standard T-junction devices to this point.

Electrolyte	Imbalance	Signs and symptoms
Sodium	Hyponatremia	Nausea, vomiting, headache
	Hypernatremia	Increased thirst, fatigue
Potassium	Hypokalemia	Constipation, weakness, lethargy
	Hyperkalemia	Muscle weakness, flaccid paralysis
Chloride	Hyperchloremia	Reduced renal blood flow, excess morbidity and mortality (in critically ill patients)
Calcium	Hypocalcemia	Light-headedness, irritability, seizures, hyperventilation
	Hypercalcemia	Kidney stones, nausea, vomiting

Table 5.1. Signs and symptoms associated with electrolyte imbalance

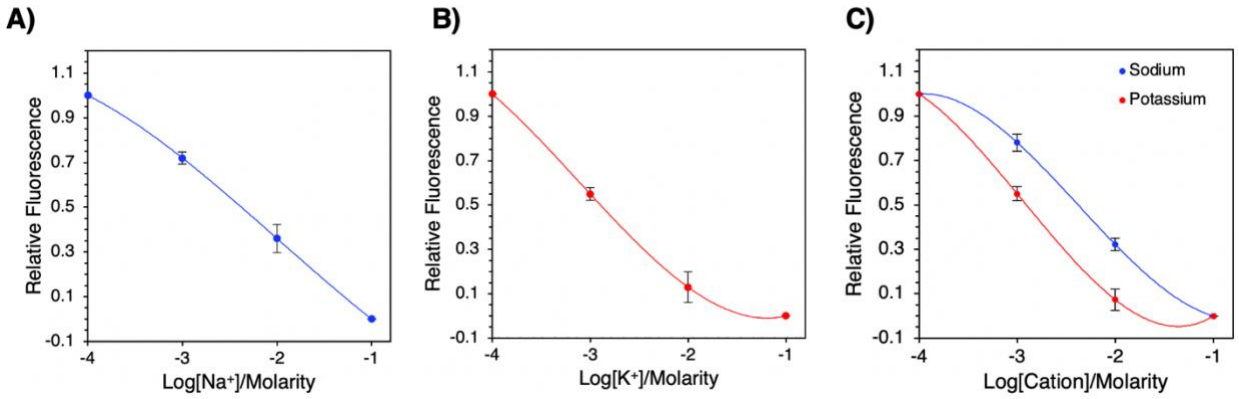

Figure 5.1. Bulk response of ion-selective oil phases toward single and multi-ion concentrated samples. Response of (A) sodium-selective oil phase toward samples with Na^+, (B) potassium-selective oil phase toward samples with K^+, (C) separate ion-selective oil phases toward samples with equal concentrations of Na^+ and K^+. Data points are representative of average fluorescence of the readout phase ± standard deviation for $n \geq 3$ trials.

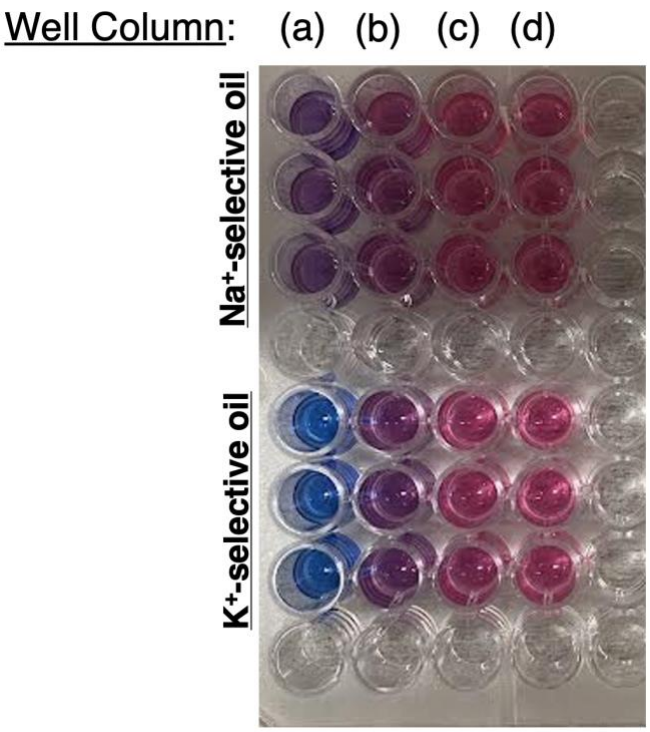

Figure 5.2. Well plate image of ion-selective oil from bulk droptode after reaction with multi-ion solution. Extracted ion-selective oil phase (100 uL) after 30 second vortex with aqueous sample concentrated with (A**)** 0.1 mM K^+ and 0.1 mM Na^+ (B) 1 mM K^+ and 1 mM Na^+ (C) 10 mM K^+ and 10 mM Na^+ (D) 100 mM K^+ and 100 mM Na^+. Each row is representative of a single trial for each ion-selective oil phase (n=3).

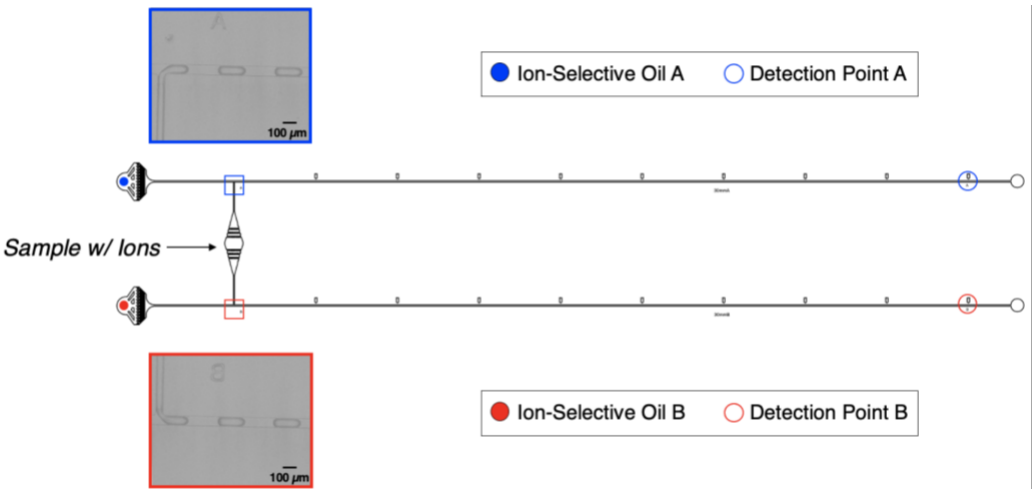

Figure 5.3. Schematic of H-Channel device. Sample containing the ions of interest enters the microfluidic device through a single port and splits into two streams flowing in opposite directions. Upon intersection with the ion-selective oil at each T-junction, sample streams are segmented into aqueous droplets which travel toward respective detection points.

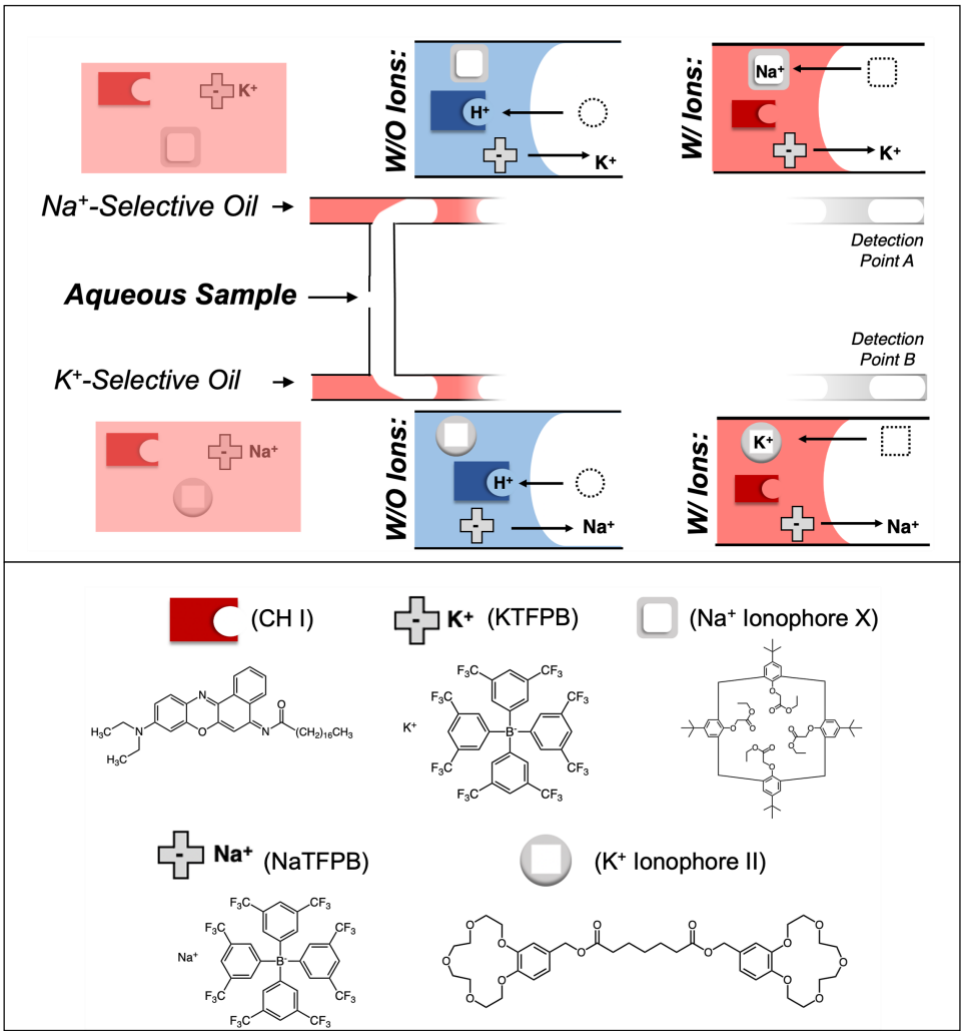

Figure 5.4. Schematic for chemical sensing of Na^+ and K^+ ions on an H-Channel device. For samples without ions, the chromoionophore is protonated as a result of ion exchange with respective cation exchangers in each readout phase. When the sample is concentrated with ions, chromoionophore remains deprotonated as a result of ion-exchange between the target analyte and cation exchanger. For the overall system, a decrease in fluorescence, or change in color of readout segments from blue to red occurs with an increase in concentration of ions in the sample.

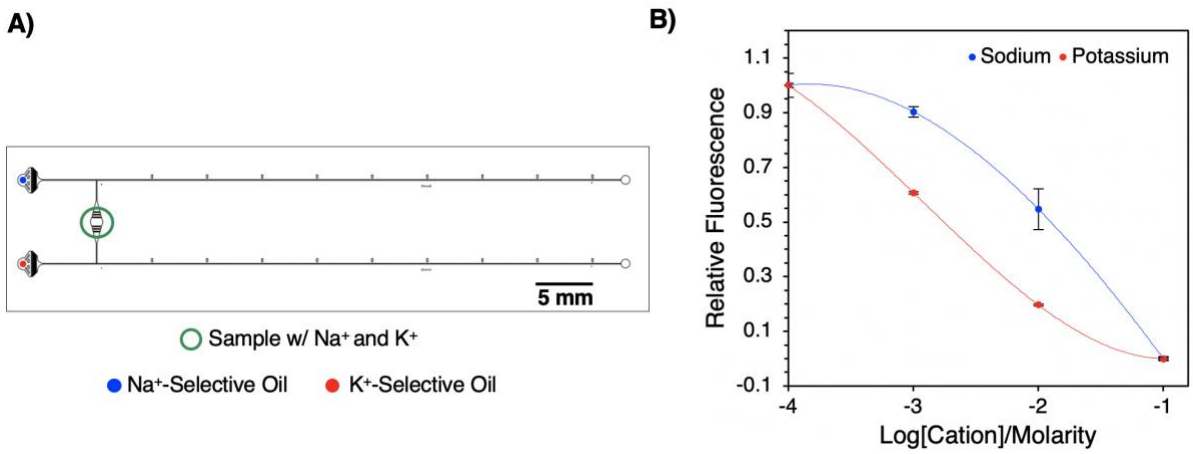

Figure 5.5. Multiplexed detection scheme of Na^+ and K^+. (A) H-channel schematic for Na^+ and K^+ sensing. (B) Response curve of ion-selective oil phases toward aqueous sample containing equal concentrations of Na^+ and K^+. Data points are representative of average relative fluorescence of readout segments ± standard deviation. Segmented flow was imaged at 10× objective.

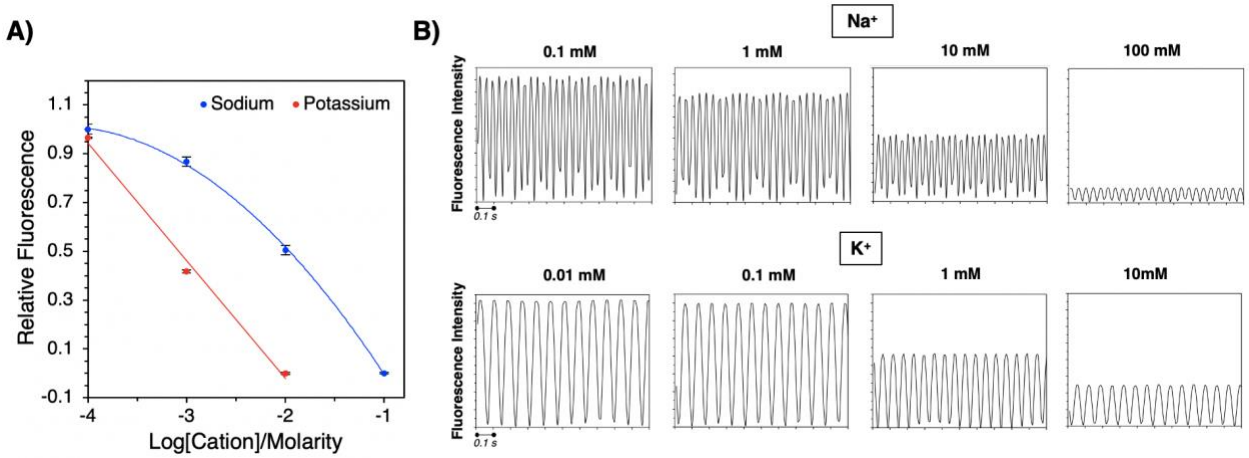

Figure 5.6. Multiplex sensing of Na^+ and K^+ in presence of near physiological levels of background ion (A) Response curve of ion-selective oil phases toward aqueous sample containing Na^+ and K^+. Data points are representative of average relative fluorescence intensity of readout segments ± standard deviation. (B) Fluorescence traces from segmented flow imaged at 5× objective.

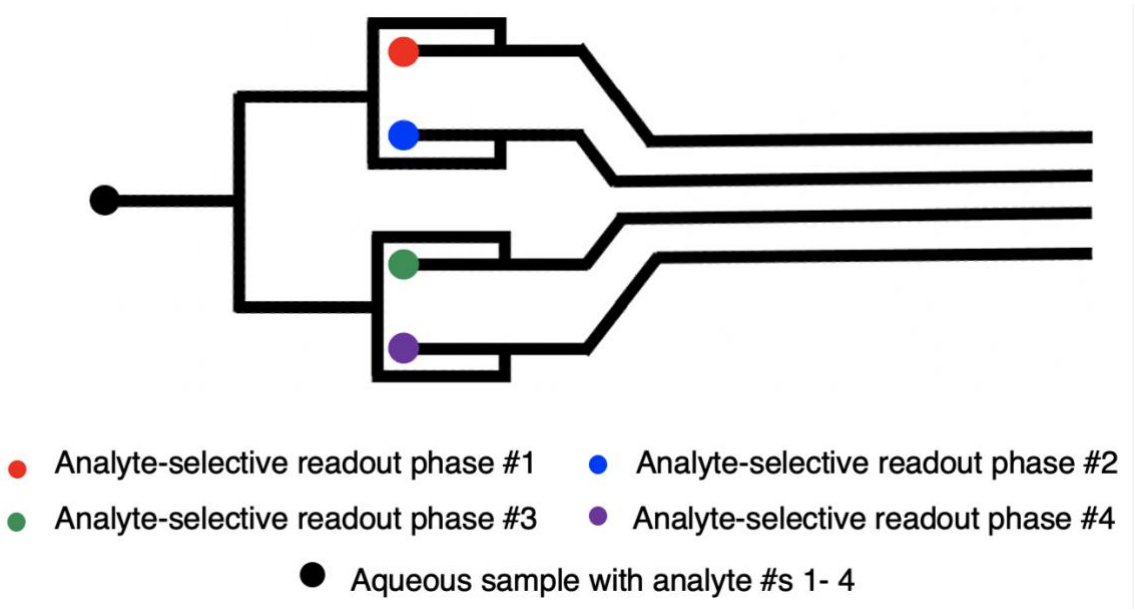

Figure 5.7. Droplet Microfluidic Multiplex Design #1. Schematic of droplet microfluidic, multiplex design number one. The aqueous sample channel splits into four sub channels, which each perpendicularly intersect with the respective oil carrying channel. Upon merging of aqueous and readout phases, channels carrying segmented flow can be viewed within a single image at the distal end of the device.

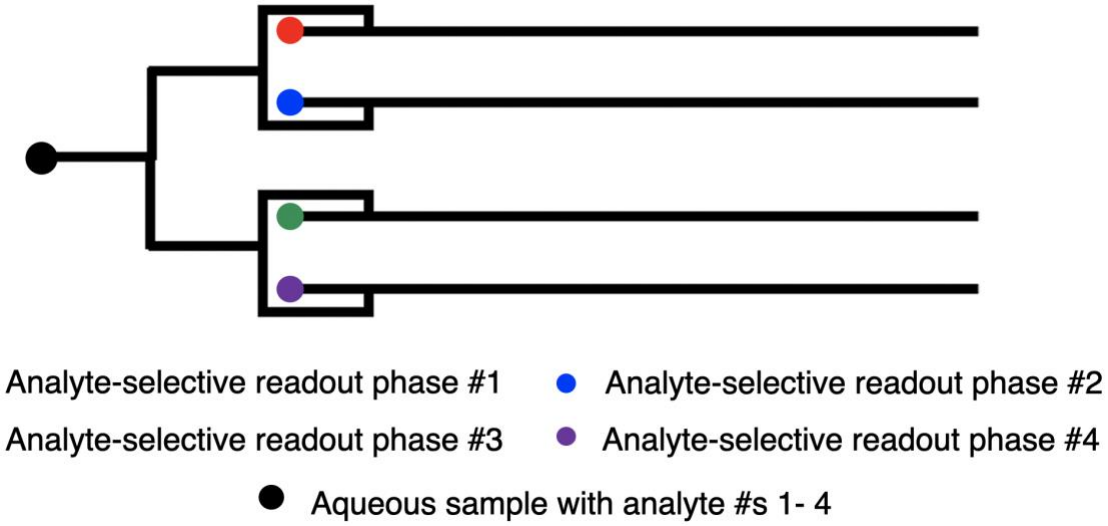

Figure 5.8. Droplet Microfluidic Multiplex Design #2. Schematic of droplet microfluidic, multiplex design number two. The aqueous sample channel splits into four sub channels which merge with respective oil carrying channels. Lanes carrying segmented flow are further distanced to reduce optical crosstalk from fluorescent chromoionophore in adjacent lanes.

5.5 References

(1) Navarro, M. P.; Vaquero, M. P. Potassium: Physiology. *Encycl. Food Heal.* **2015**, *80*, 432–438. https://doi.org/10.1016/B978-0-12-384947-2.00554-7.

(2) Rude, R. K. Physiology of Magnesium Metabolism and the Important Role of Magnesium in Potassium Deficiency. *Am. J. Cardiol.* **1989**, *63* (14). https://doi.org/10.1016/0002-9149(89)90216-6.

(3) Jones, J. W.; Sebastian, A.; Hulter, H. N.; Schambelan, M.; Sutton, J. M.; Biglieri, E. G. Systemic and Renal Acid-Base Effects of Chronic Dietary Potassium Depletion in Humans. *Kidney Int.* **1982**, *21* (2), 402–410. https://doi.org/10.1038/ki.1982.36.

(4) Budak, Y. U.; Huysal, K.; Polat, M. Use of a Blood Gas Analyzer and a Laboratory Autoanalyzer in Routine Practice to Measure Electrolytes in Intensive Care Unit Patients. *BMC Anesthesiol.* **2012**, *12*. https://doi.org/10.1186/1471-2253-12-17.

(5) Brett, C.; Charr, D. Fluids, Electrolytes, and Nutrition. *Greg. Pediatr. Anesth. Fifth Ed.* **2011**, *4* (6), 205–223. https://doi.org/10.1002/9781444345186.ch10.

(6) Kadri, A. General Characteristics of Patients with Electrolyte Imbalance Admitted to Emergency Department. *World J. Emerg. Med.* **2013**, *4* (2), 113. https://doi.org/10.5847/wjem.j.issn.1920-8642.2013.02.005.

(7) Rhoda, K. M.; Porter, M. J.; Quintini, C. Fluid and Electrolyte Management: Putting a Plan in Motion. *J. Parenter. Enter. Nutr.* **2011**, *35* (6), 675–685. https://doi.org/10.1177/0148607111421913.

(8) Nagami, G. T. Hipercloremia: Por Qué y Cómo. *Nefrologia* **2016**, *36* (4), 347–353. https://doi.org/10.1016/j.nefro.2016.04.001.

(9) Young, C. C. Evolution of Blood Chemistry Analyzers Based on Ion Selective Electrodes. *J. Chem. Educ.* **1997**, *74* (2), 177–182. https://doi.org/10.1021/ed074p177.

(10) Dybko, A. Errors in Chemical Sensor Measurements. *Sensors* **2001**, *1* (1), 29–37. https://doi.org/10.3390/s10100029.

(11) Dimeski, G.; Badrick, T.; John, A. S. Ion Selective Electrodes (ISEs) and Interferences-A Review. *Clin. Chim. Acta* **2010**, *411* (5–6), 309–317. https://doi.org/10.1016/j.cca.2009.12.005.

(12) Bakker, E.; Bühlmann, P.; Pretsch, E. Carrier-Based Ion-Selective Electrodes and Bulk Optodes. 1. General Characteristics. *Chem. Rev.* **1997**, *97* (8), 3083–3132. https://doi.org/10.1021/cr940394a.

(13) Dukić, L.; Kopčinović, L. M.; Dorotić, A.; Baršić, I. Blood Gas Testing and Related Measurements: National Recommendations on Behalf of the Croatian Society of Medical

Biochemistry and Laboratory Medicine. *Biochem. Medica* **2016**, *26* (3), 318–336. https://doi.org/10.11613/BM.2016.036.

(14) Kim, S. B.; Cho, H. C.; Cha, G. S.; Nam, H. Microtiter Plate-Format Optode. **1998**, *70* (22), 4860–4863.

(15) Xie, X.; Zhai, J.; Bakker, E. PH Independent Nano-Optode Sensors Based on Exhaustive Ion-Selective Nanospheres. *Anal. Chem.* **2014**, *86* (6), 2853–2856. https://doi.org/10.1021/ac403996s.

(16) Brady, B.; Wang, R.; Cheong, R.; Wang, X. Digital Printing of Selective and Reversible Ion Optodes on Fabrics: Toward Smart Clothes for Epidermal Chemical Sensing. *Analyst* **2021**. https://doi.org/10.1039/d1an01349a.

(17) Wang, X.; Zhang, Q.; Nam, C.; Hickner, M.; Mahoney, M.; Meyerhoff, M. E. An Ionophore-Based Anion-Selective Optode Printed on Cellulose Paper. *Angew. Chemie - Int. Ed.* **2017**, *56* (39), 11826–11830. https://doi.org/10.1002/anie.201706147.

(18) Teh, S. Y.; Lin, R.; Hung, L. H.; Lee, A. P. Droplet Microfluidics. *Lab Chip* **2008**, *8* (2), 198–220. https://doi.org/10.1039/b715524g.

(19) Wang, X.; Sun, M.; Ferguson, S. A.; Hoff, J. D.; Qin, Y.; Bailey, R. C.; Meyerhoff, M. E. Ionophore-Based Biphasic Chemical Sensing in Droplet Microfluidics. *Angew. Chemie - Int. Ed.* **2019**, *58* (24), 8092–8096. https://doi.org/10.1002/anie.201902960.

(20) Wang, R.; Zhou, Y.; Ghanbari Ghalehjoughi, N.; Mawaldi, Y.; Wang, X. Ion-Induced Phase Transfer of Cationic Dyes for Fluorescence-Based Electrolyte Sensing in Droplet Microfluidics. *Anal. Chem.* **2021**. https://doi.org/10.1021/acs.analchem.1c03394.

(21) Kim, P.; Kwon, K. W.; Park, M. C.; Lee, S. H.; Kim, S. M.; Suh, K. Y. Soft Lithography for Microfluidics: A Review. *Biochip J.* **2008**, *2* (1), 1–11.

(22) Tan, Y. C.; Fisher, J. S.; Lee, A. I.; Cristini, V.; Lee, A. P. Design of Microfluidic Channel Geometries for the Control of Droplet Volume, Chemical Concentration, and Sorting. *Lab Chip* **2004**, *4* (4), 292–298. https://doi.org/10.1039/b403280m.

(23) Wetzler-Quevedo, S. P.; Meyerhoff, M. E.; Bailey, R. C. Characterization of the Impact of Mixing and Droplet Volumes on the Behavior of Microfluidic Ion-Selective Droptodes. *Analyst* **2021**, *146* (16), 5095–5101. https://doi.org/10.1039/d1an00733e.

(24) Doonan, S. R.; Bailey, R. C. K-Channel: A Multifunctional Architecture for Dynamically Reconfigurable Sample Processing in Droplet Microfluidics. *Anal. Chem.* **2017**, *89* (7), 4091–4099. https://doi.org/10.1021/acs.analchem.6b05041.

(25) Macdonald, J. E.; Struthers, A. D. What Is the Optimal Serum Potassium Level in Cardiovascular Patients? *J. Am. Coll. Cardiol.* **2004**, *43* (2), 155–161. https://doi.org/10.1016/j.jacc.2003.06.021.

(26) Hunter, R. W.; Bailey, M. A. Hyperkalemia: Pathophysiology, Risk Factors and Consequences. *Nephrol. Dial. Transplant.* **2019**, *34*, III2–III11. https://doi.org/10.1093/ndt/gfz206.

(27) Lolekha, P. H.; Vanavanan, S.; Teerakarnjana, N.; Chaichanajarernkul, U.; Lolekha, S. Reference Ranges of Electrolyte and Anion Gap in Venous Whole Blood and Plasma of Healthy School Children [2]. *Clin. Chim. Acta* **2003**, *331* (1–2), 167–169. https://doi.org/10.1016/S0009-8981(03)00116-5.

Chapter 6 – Conclusions and Suggested Future Directions

6.1 Dissertation Summary and Conclusion

Polyion-sensitive microfluidic droptodes – a subcategory of ionophore-based, droplet microfluidics – have been demonstrated within this dissertation as a novel method for polyion sensing. Fluorescence measurements are made in readout (oil) segments concentrated with lipophilic chromoionophore and ionic complexing agent, adjacent to sample-containing droplets. This platform advances the utility of fluorescent-based, droplet microfluidics which often use fluorescence signal from water-soluble reagents encapsulated within aqueous droplets as the analytical readout.[1] In this way, the functionality of the water immiscible oil is extended beyond usage as a standard carrier phase[2] for segmenting of aqueous flow. Relative to standard analytical techniques used for macromolecular sensing, droptodes now exist as an alternate method with reduced sample volumes, analysis times, and reagent amounts. Furthermore, target polyion measurements are made without background interference from the sample matrix color, a common interferent of optical platforms.[3] Herein a summary of works within this dissertation is presented, in addition to suggested future work for advancement of polyion-sensitive, microfluidic droptodes as a standard analytical technique.

6.1.1 Microfluidic Droptodes for Polyion Sensing

Ionophore-based droplet microfluidics, later coined as microfluidic droptodes, were first introduced as a technology for biphasic sensing of electrolytes (K^+, Na^+, and Cl^-) and polycationic protamine.[4] Chapter 2 further advances microfluidic droptodes through the development and application of the first polyanion-sensitive, microfluidic droptode. Using anticoagulative heparin as a model polyanion, CH XI and TDMACl-concentrated readout segments were found to be responsive toward an extensive range of heparin concentrations (USP

'units' per mL) within and outside of clinically relevant ranges. Readout segments also exhibited the highest response toward heparin relative to other negatively charged polyions and compounds, a result attributed from heparin's high degree of sulfation and charge density. The application of polyanion-sensitive droptodes for heparin measurements in individual, human citrated plasma samples further demonstrated their potential for use in clinical settings as an alternate method to unstandardized clotting assays.[5] The invention of polyanion-sensitive droptodes motivated the optimization of experimental parameters employed in polycation-sensitive droptodes.

Protamine, the only FDA-approved heparin-antagonist to date,[6] served as the target polycation of interest for experiments in Chapter 3. Within this chapter, chromoionophore VI, a lipophilic fluorescein derivative, was used to fluorescently quantitate the effects of changing aqueous droplet size volumes, segment spacing, and biphasic reaction time on the response of polycation-sensitive droptodes. Varying the magnitudes of such was found to have a measurable impact on the response of polycation-sensitive droptodes and these parameters must carefully be considered based on the target range of interest for polycation measurements. Bulk droptodes, which rely on the same biphasic principle as microfluidic droptodes but on a larger scale (100s of µL vs 100s of pL), were also introduced in this chapter as an off-device method to test the functionality of new sensing chemistries.

In Chapter 4, polyion-sensitive droptodes were used for direct and indirect sensing of polymeric quaternary ammonium compounds (PQs) PQ-2, PQ-6, and PQ-10. Polycation-sensitive droptodes were found to have a limited response toward PQs likely due to poor mass-charge transfer attributed from the high solubility of PQs in aqueous samples. Polyanion-sensitive droptodes, used for indirect sensing, were found to have an appreciable response

toward each of the three PQ species when a constant concentration of heparin was used in background of the aqueous samples. Works within this chapter were the first application of polyion-sensitive droptodes for the detection of non-biomedical polyions demonstrating their potential usage in industrial and/or cosmetic settings.

6.1.2 Microfluidic Droptodes for Multiplex Sensing

Chapter 5 further demonstrated microfluidic droptodes, previously limited to single analyte detection, for multiplex sensing. For proof-of-concept, electrolytes were pursued as initial targets considering the high degree of selectivity of the ionophores used in their respective, single-plex droptode systems. An "H-channel" microfluidic device design, developed in-house, was employed for measurement of two separate target cations (Na^+, K^+), concentrated in single samples. Having success with the H-channel, this droplet microfluidic device remains as a potential platform for multiplex sensing of the various polyions detected within dissertation.

6.2 Future Directions and Preliminary Results

6.2.1 Optimization of Polyion-Sensitive Droptodes for Measurement of Additional Polyions

Polyion-sensitive droptodes have been employed for the detection of polyanions (heparin, chondroitin sulfate) and polycations (protamine, polyquaternium compounds). Polycation-sensitive droptodes (Chapters 3 and 4) may find use in other applications, though sensing reagents employed in their associated readout phases have been shown to be limited in chemical interaction with the target polycation. For further advancement of polycation-sensitive droptodes, parameters such as sensing reagent concentration in the readout phase and the type of organic solvent used to dissolve sensing reagents should be thoroughly investigated.

In traditional liquid-liquid (i.e., aqueous-organic) extractions, the type of organic solvent used is key, as it influences extraction efficiency and selectivity toward the target analyte.[7] Based on the biphasic sensing principle of droptode systems presented within this dissertation, it is likely that the response of polycation-sensitive droptodes would be similarly impacted by this parameter. Therefore, the effects of changing the organic solvent of polycation-sensitive droptodes used to dissolve lipophilic sensing components should be explored. The concentration of chromoionophore and ion-exchanger used in the readout phase has also been shown to have a drastic impact on the response of polyanion-sensitive droptodes (Chapter 2), and hence should be explored in polycation-sensitive droptode systems as well. With the described conditions taken into consideration, polycation-sensitive, microfluidic droptodes may be applied for measurement of other natural and synthetic polycations including biologically relevant proteins, chitosan, and polyethyleneimine.

Alternatively, polyanion-sensitive droptodes, used for both direct and indirect polyion sensing, remain as a more polished version of their polycation-sensitive counterpart. Though indirect sensing is appreciable, target polyanions for direct-sensing applications are exclusively discussed for practicality. In previous works, polyanion-sensitive ISEs have been demonstrated to be responsive toward phosphate-rich polyanions.[8] This response is attributed to cooperative ion pairing with $TDMA^+$ sites and negatively charged phosphate groups along the length of the polyanion. Given that polyanion-sensitive microfluidic droptodes implement a TDMACl-based chemistry, they may serve as a useful analytical technique for measurement of polyanionic species high in phosphate content such as polyphosphates[9–11] and nucleic acids.[12]

Carrageenan– a sulfated polyanion commonly used as a thickening agent in food products[13] – is an additional target of interest for our polyanion-sensitive droptode system.

Polyanion-sensitive droptodes exist as a potential method to measure polyion concentrations in food and drink products which often contain optically interfering dyes (i.e., food coloring).[14] Lastly, polyanion-sensitive droptodes should demonstrate an appreciable response toward chondroitin sulfates which exist in various other chemical forms[15] beyond the porcine-derived species detected within Chapter 2. In this way, sulfate content of chondroitin sulfates may be quantified based on the fluorescent response from polyanion-sensitive droptodes calibrated by chondroitin sulfate standards.

6.2.2 Analysis of Mixing Behaviors and Chemical Equilibrium in Readout Segments

Mixing behaviors within segments generated on droplet microfluidic devices is an important characteristic which can be linked to chemical equilibrium and/or dispersion of reagent(s) in aqueous droplets.[16] Understanding these behaviors is especially important for our microfluidic droptode system as chemical transfer occurs between aqueous droplets and oil segments which traverse tens of millimeters (mm) on-device before measurements are made. Yet, droplet microfluidic studies which analyze mass-charge transport of chemical reagents between aqueous droplets and oil segments at various distances on microfluidic channels are limited. Hence, a preliminary study was conducted to both qualitatively and quantitatively characterize such using a chromoionophore as a fluorescent tracker.

For this study, measurements were made on a flow-focusing device using standard fluorescence monitoring and data analysis as described in experimental chapters 2 – 5. Fluorescence intensity of segments was an average of local maxima representative of signal either from aqueous droplets or readout segments, dependent on the partitioning behavior of chromoionophore molecules. The readout phase consisted of 400 µM chromoionophore XI (CH XI) and 600 µM TDMACl in dioctyl sebacate, and the aqueous phase consisted of 10 mM

sodium hydroxide (pH 12). In this way, the amount of fluorescence in segments depended upon the degree of proton dissociation from CH XI molecules.[17] **Figure 6.1** demonstrates that the fluorescence of segments increases as their distance traveled on-device increases. Notably, the magnitude of fluorescence in segments only changes by a factor of ~1.2 at the 45 mm distance point relative to 30 mm distance point at which measurements are made in standard droptode applications.[4] Though, at the further distance, variation associated with average fluorescence decreases by ~30% indicating that chemical equilibrium is being approached. This is further evidenced in **Figure 6.2b**, a first derivative plot representative of rate of change in segment fluorescence at each distance point on the device. In this case, the rate of change is ~500 fluorescence units/mm (RFU/mm) at the 0 mm distance, ~2500 RFU/mm at the 20 mm distance, and ~500 RFU/mm at the 40 mm distance.

Qualitatively, images of segmented flow in **Figure 6.3** show how the dispersion of CH XI molecules changes at different distances on-device. At the 0 mm distance point, CH XI is primarily concentrated in the aqueous droplets yet is homogeneously distributed in oil segments which have traversed to the final distance point (45 mm). Furthermore, fluorescence traces (**Figure 6.3**) associated with measurements made at respective distance points provide further insight on how the morphology of generated peaks are reflective of the dispersion of the analyte (protons) and chemical reagents between segments. Overall, this preliminary data demonstrates an alternate method to track analyte and reagent partitioning behaviors in droptode systems. In future works, these studies should be applied for analysis in other droptode systems to better understand how mass charge transfer and chemical equilibrium between segments are affected by the size and structure of the analyte and sensing reagents.

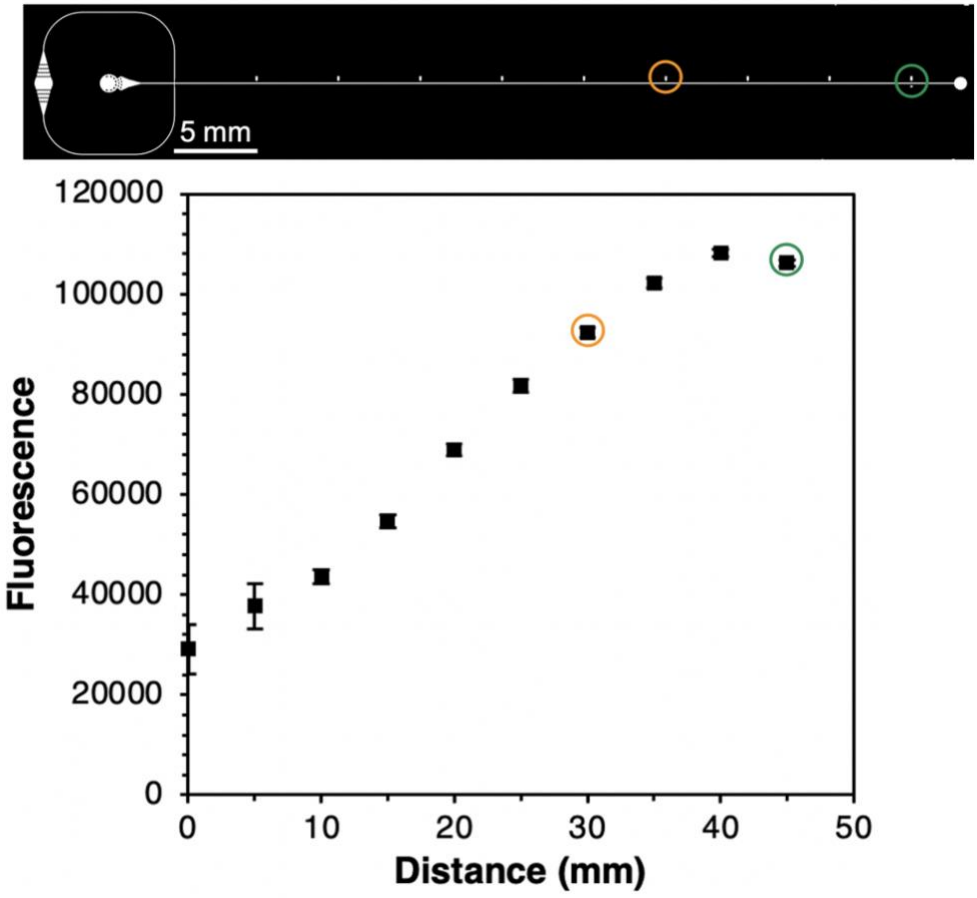

Figure 6.1. Overview of the distance study using a flow-focusing, droplet microfluidic device. Data points are representative of average fluorescence of segments at several incremental distances ± standard deviation. Aqueous droplet frequencies were maintained at 9 – 10 Hz. The 30 mm (orange) and 45 mm (green) points on the flow-focusing device are marked for comparison of standard and extended distances at which measurements are made.

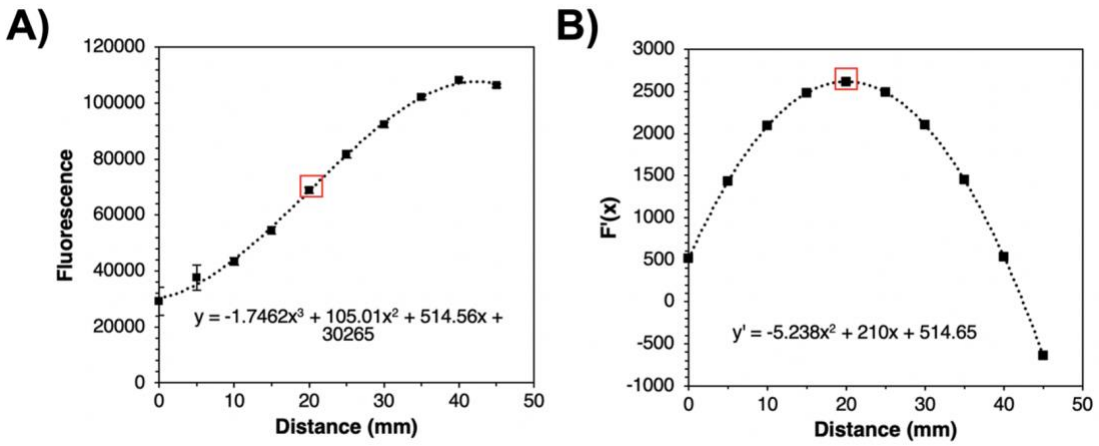

Figure 6.2. Comparison of segment fluorescence and rate of change in segment fluorescence at several distances on-device. (A) Plot of segment fluorescence at incremental distances fitted to a cubic polynomial function. (B) Rate of change in fluorescence at incremental distances plotted from the first derivative equation of the cubic polynomial function. The inflection point within each fitted curve is marked with a red square.

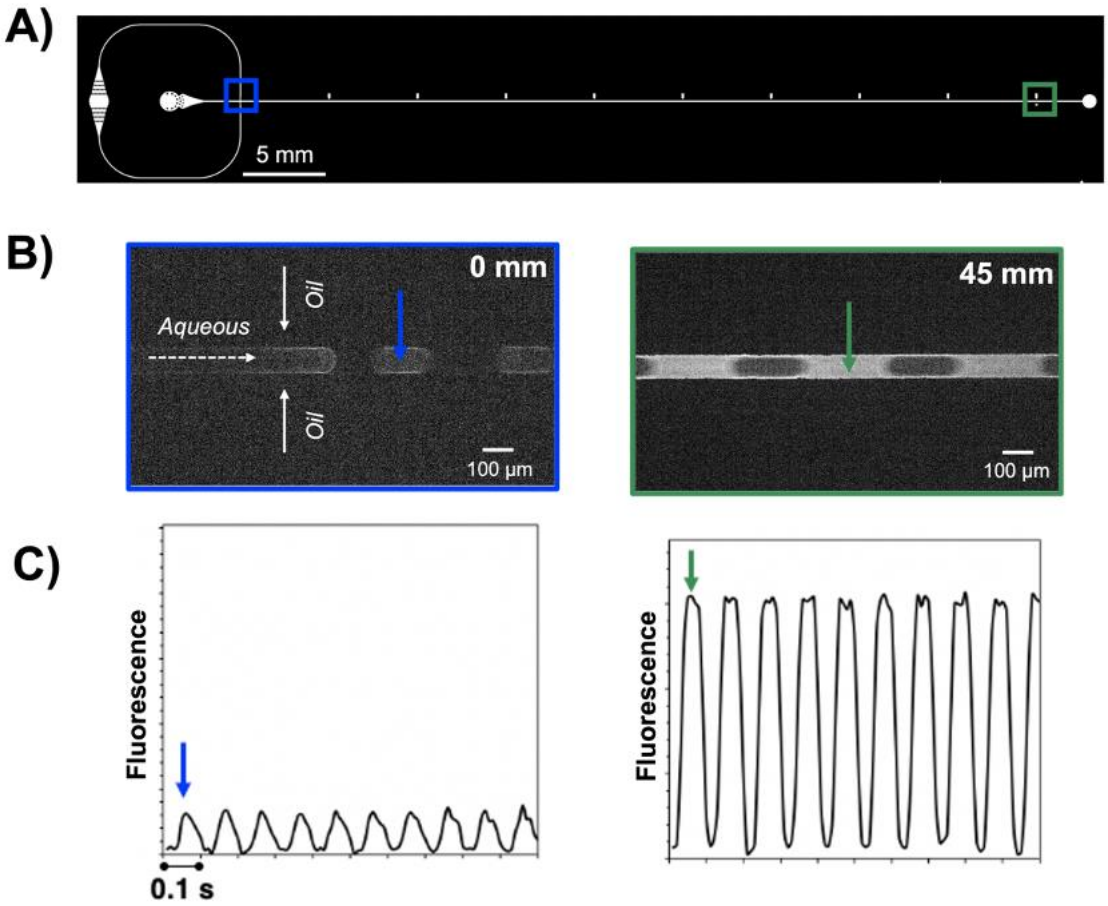

Figure 6.3. Qualitative study of segment fluorescence at incremental distances on a flow-focusing device. (A) Flow-focusing device marked at the droplet junction, or 0 mm (blue) and 45 mm (green) distances. (B) Darkfield images of segmented flow at marked distances. (C) Fluorescence traces of segmented flow at 0 and 45 mm, respectively. Arrows point to either the aqueous (blue) or oil (green) phase which the peaks in fluorescence traces correspond to. Local maxima at the base of peaks were included in average fluorescence calculations to account for uneven distribution of chromoionophore XI molecules at the aqueous droplet-oil segment interface.

6.3 References

(1) Huebner, A.; Srisa-Art, M.; Holt, D.; Abell, C.; Hollfelder, F.; DeMello, A. J.; Edel, J. B. Quantitative Detection of Protein Expression in Single Cells Using Droplet Microfluidics. *Chem. Commun.* **2007**, *2* (12), 1218–1220. https://doi.org/10.1039/b618570c.

(2) Baroud, C. N.; Gallaire, F.; Dangla, R. Dynamics of Microfluidic Droplets. *Lab Chip* **2010**, *10* (16), 2032–2045. https://doi.org/10.1039/c001191f.

(3) Wang, X.; Mahoney, M.; Meyerhoff, M. E. Inkjet-Printed Paper-Based Colorimetric Polyion Sensor Using a Smartphone as a Detector. *Anal. Chem.* **2017**, *89* (22), 12334–12341. https://doi.org/10.1021/acs.analchem.7b03352.

(4) Wang, X.; Sun, M.; Ferguson, S. A.; Hoff, J. D.; Qin, Y.; Bailey, R. C.; Meyerhoff, M. E. Ionophore-Based Biphasic Chemical Sensing in Droplet Microfluidics. *Angew. Chemie - Int. Ed.* **2019**, *58* (24), 8092–8096. https://doi.org/10.1002/anie.201902960.

(5) Culliford, A. T.; Gitel, S. N.; Starr, N.; Thomas, S. T.; Baumann, F. G.; Wessler, S.; Spencer, F. C. Lack of Correlation between Activated Clotting Time and Plasma Heparin during Cardiopulmonary Bypass. *Ann. Surg.* **1981**, *193* (1), 105–111. https://doi.org/10.1097/00000658-198101000-00017.

(6) Pandey, S. P.; Jha, P.; Nadimetla, D. N.; Bhosale, S. V.; Singh, P. K. A Tetracationic Aggregation Induced Emission-Based Probe for Efficient and Improved Detection of Heparin. *Sensors Actuators B Chem.* **2022**, *353* (October 2021), 131016. https://doi.org/10.1016/j.snb.2021.131016.

(7) Ha, S. H.; Mai, N. L.; Koo, Y. M. Butanol Recovery from Aqueous Solution into Ionic Liquids by Liquid-Liquid Extraction. *Process Biochem.* **2010**, *45* (12), 1899–1903. https://doi.org/10.1016/j.procbio.2010.03.030.

(8) Esson, J. M.; Meyerhoff, M. E. Polyion-Sensitive Membrane Electrodes for Detecting Phosphate-Rich Biological Polyanions. *Electroanalysis* **1997**, *9* (17), 1325–1330. https://doi.org/10.1002/elan.1140091705.

(9) Roewe, J.; Stavrides, G.; Strueve, M.; Sharma, A.; Marini, F.; Mann, A.; Smith, S. A.; Kaya, Z.; Strobl, B.; Mueller, M.; et al. Bacterial Polyphosphates Interfere with the Innate Host Defense to Infection. *Nat. Commun.* **2020**, *11* (1), 1–12. https://doi.org/10.1038/s41467-020-17639-x.

(10) Rashchi, F.; Finch, J. A. Polyphosphates: A Review. Their Chemistry and Application with Particular Reference to Mineral Processing. *Miner. Eng.* **2000**, *13* (10), 1019–1035. https://doi.org/10.1016/S0892-6875(00)00087-X.

(11) Kulakovskaya, T. V.; Vagabov, V. M.; Kulaev, I. S. Inorganic Polyphosphate in Industry, Agriculture and Medicine: Modern State and Outlook. *Process Biochem.* **2012**, *47* (1), 1–10. https://doi.org/10.1016/j.procbio.2011.10.028.

(12) Šponer, J.; Mládek, A.; Šponer, J. E.; Svozil, D.; Zgarbová, M.; Banáš, P.; Jurečka, P.; Otyepka, M. The DNA and RNA Sugar-Phosphate Backbone Emerges as the Key Player. An Overview of Quantum-Chemical, Structural Biology and Simulation Studies. *Phys. Chem. Chem. Phys.* **2012**, *14* (44), 15257–15277. https://doi.org/10.1039/c2cp41987d.

(13) Hassan, S. S. M.; Meyerhoff, M. E.; Badr, I. H. A.; Abd-Rabboh, H. S. M. Determination of Carrageenan in Food Products Using Potentiometric Polyion Sensors. *Electroanalysis* **2002**, *14* (6), 439–444. https://doi.org/10.1002/1521-4109(200203)14:6<439::AID-ELAN439>3.0.CO;2-L.

(14) De Andrade, F. I.; Florindo Guedes, M. I.; Pinto Vieira, Í. G.; Pereira Mendes, F. N.; Salmito Rodrigues, P. A.; Costa Maia, C. S.; Marques Ávila, M. M.; De Matos Ribeiro, L. Determination of Synthetic Food Dyes in Commercial Soft Drinks by TLC and Ion-Pair HPLC. *Food Chem.* **2014**, *157*, 193–198. https://doi.org/10.1016/j.foodchem.2014.01.100.

(15) Buzzega, D.; Maccari, F.; Volpi, N. Determination of Molecular Mass Values of Chondroitin Sulfates by Fluorophore-Assisted Carbohydrate Electrophoresis (FACE). *J. Pharm. Biomed. Anal.* **2010**, *51* (4), 969–972. https://doi.org/10.1016/j.jpba.2009.10.015.

(16) Tice, J. D.; Song, H.; Lyon, A. D.; Ismagilov, R. F. Formation of Droplets and Mixing in Multiphase Microfluidics at Low Values of the Reynolds and the Capillary Numbers. *Langmuir* **2003**, *19* (22), 9127–9133. https://doi.org/10.1021/la030090w.

(17) Panchompoo, J.; Aldous, L.; Baker, M.; Wallace, M. I.; Compton, R. G. One-Step Synthesis of Fluorescein Modified Nano-Carbon for Pd(Ii) Detection via Fluorescence Quenching. *Analyst* **2012**, *137* (9), 2054–2062. https://doi.org/10.1039/c2an16261j.